UNIL | Université de Lausanne

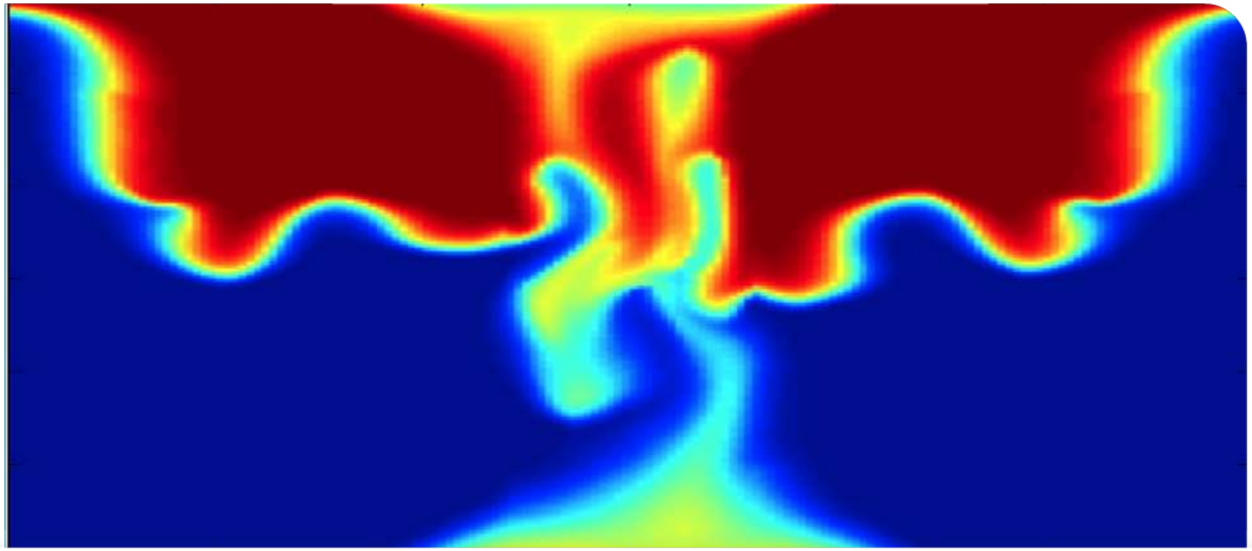

eVita Winter School: Multiscale problems
Geilo, Norway, January 23-28, 2011

Multiscale Finite-Volume methods for subsurface flow

Ivan Lunati

Institute of Geophysics, University of Lausanne, Switzerland

| le savoir vivant |

 Wednesday, January 26, 2011

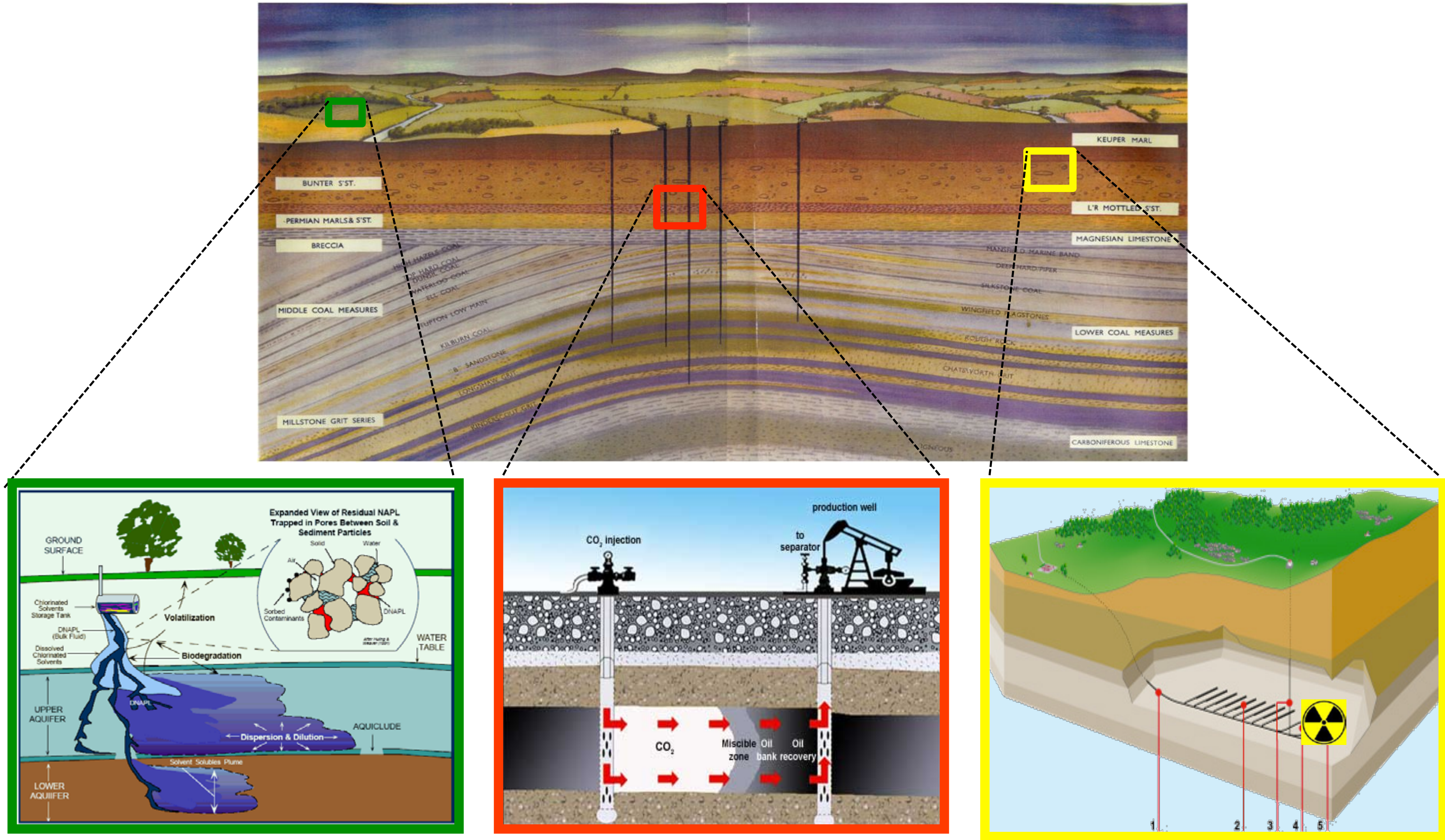

Water resources protection and remediation, hazardous waste disposal, geological sequestration of greenhouse gasses, geothermal energy, hydrocarbon recovery…

regional scale
(aquifer or
reservoir)
~ 1 km – 100 km

10 orders of magnitude / hor. Dim.
~ 10^{27} or more pores per reservoir

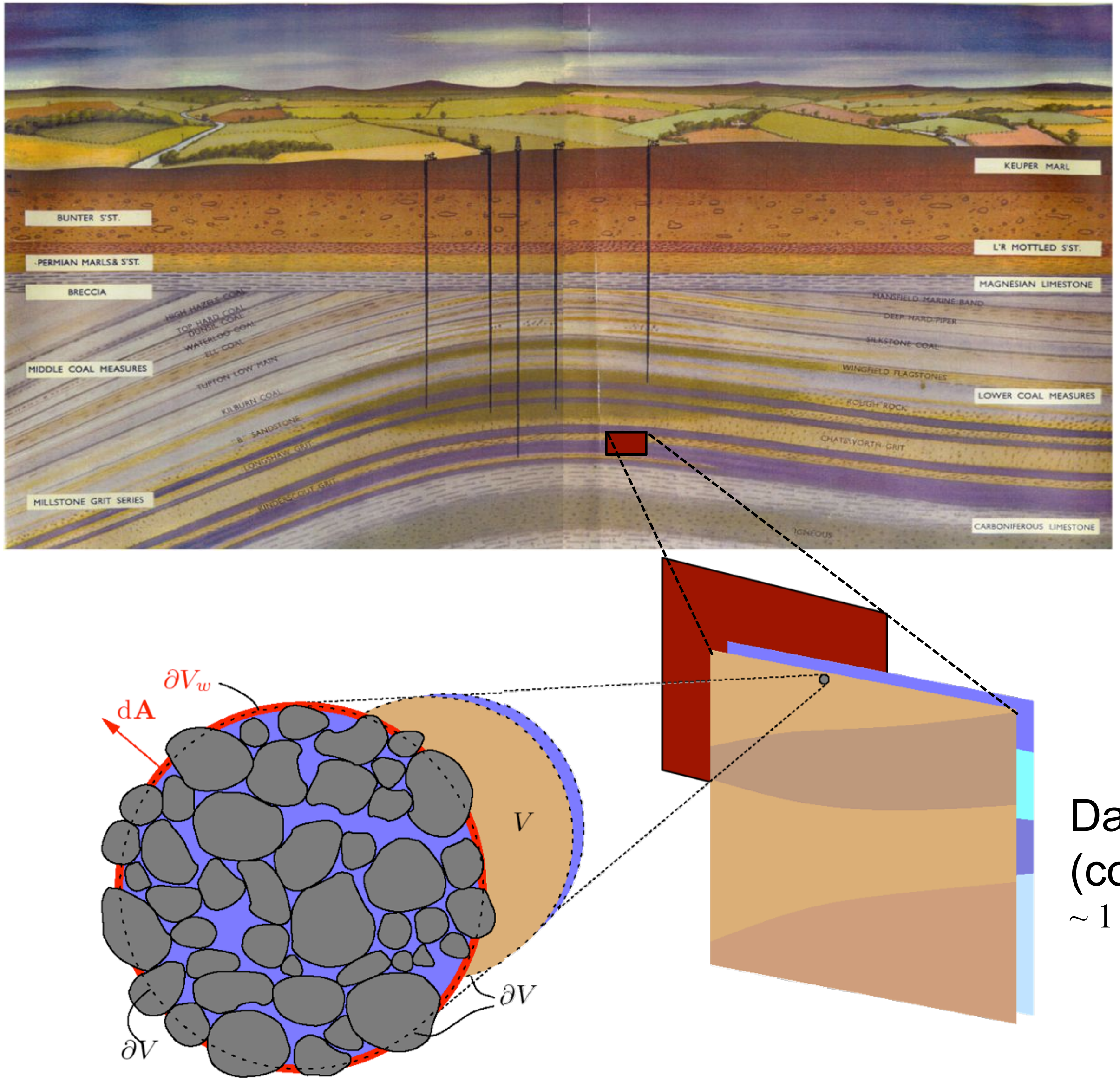

5 orders of magnitude / hor. dim.
or 10^{13} unknowns

Darcy scale
(continuum scale)
~ 1 m – 10 m

pore scale
< 10 μm – 1 cm

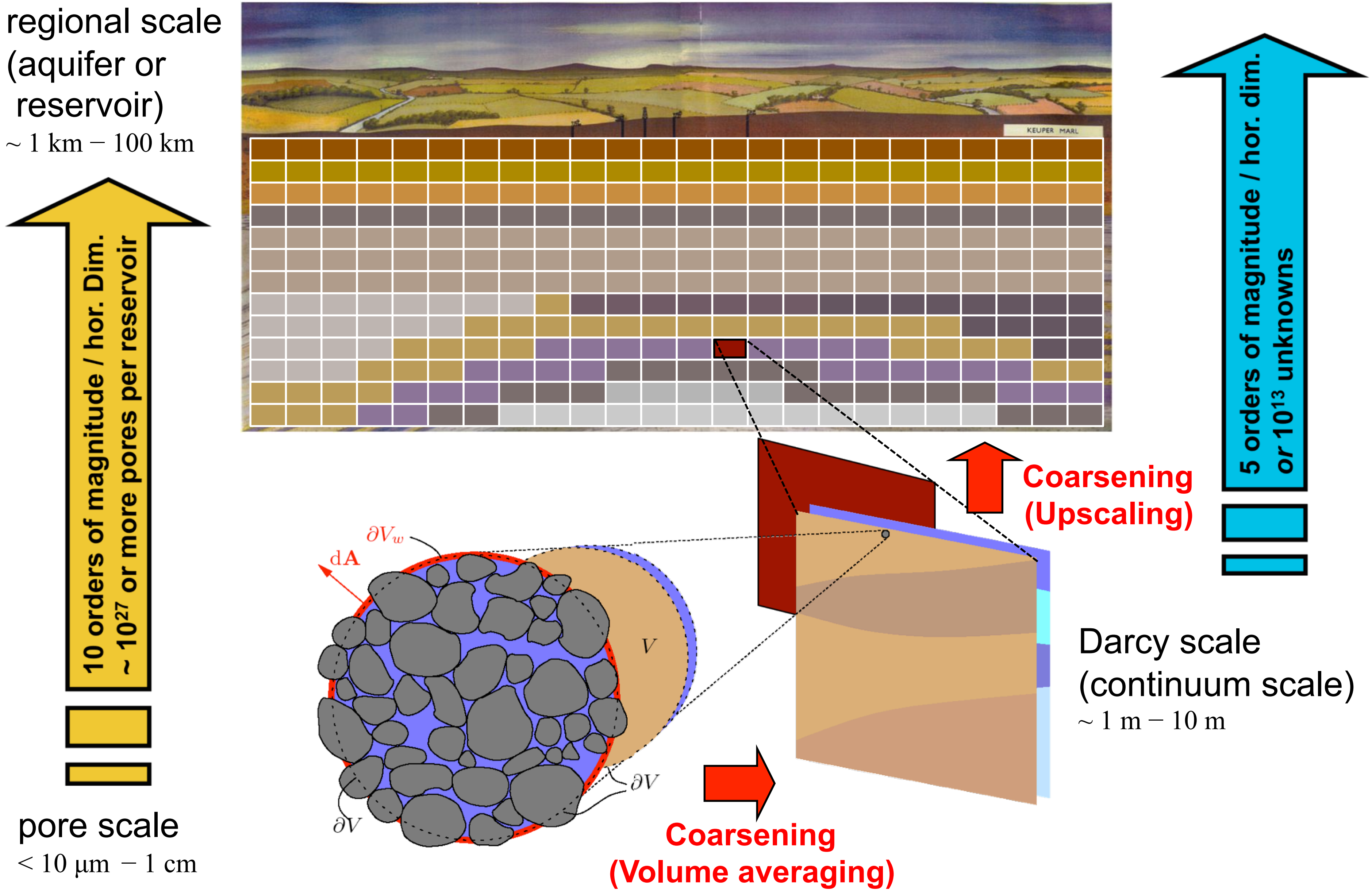

regional scale
(aquifer or
reservoir)
~ 1 km – 100 km
10 orders of magnitude / hor. Dim.
~ 10^{27} or more pores per reservoir
pore scale
< 10 µm – 1 cm
KEUPER MARL
∂V_w
dA
V
∂V
∂V
Coarsening
(Volume averaging)
Coarsening
(Upscaling)
5 orders of magnitude / hor. dim.
or 10^{13} unknowns
Darcy scale
(continuum scale)
~ 1 m – 10 m

Dynamic contact angle

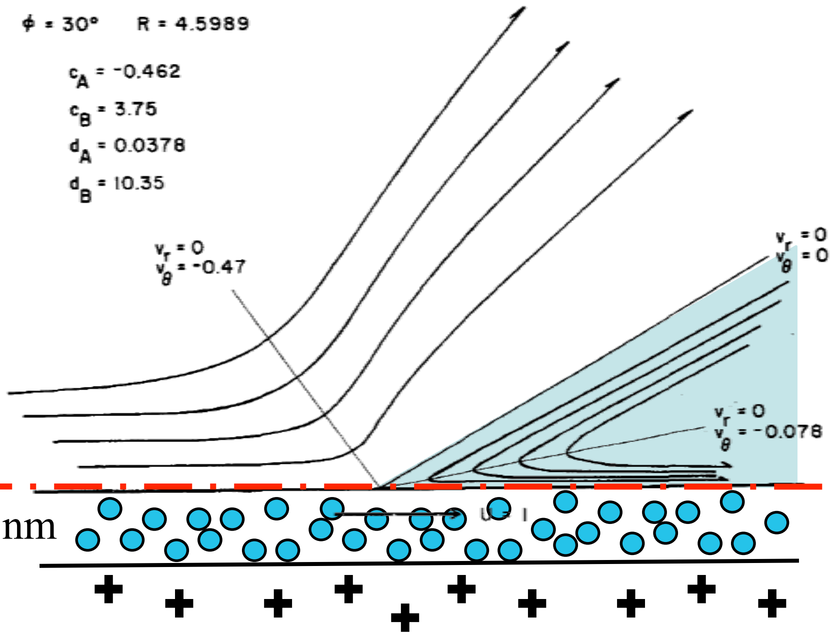

~ 1-0.1 nm

$$f_w \sim \mathrm{Ca} \int_{\ell}^{L} \frac{1}{h} dh = \mathrm{Ca} \ln(L/\ell)$$

Hydrodynamic theory

$$p_c = \Delta p = \gamma \kappa$$

Molecular theory

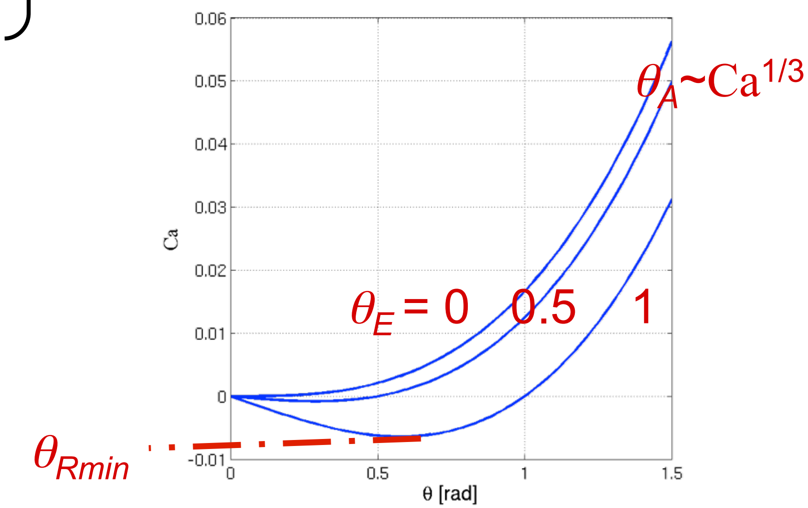

- cut off at molecular length scale
  - hydrodynamic description brakes down
  - avoids infinite friction
- dynamic contact angle, θ_A or θ_R
  - balance btw. viscous and capillary forces
    - e.g. *de Gennes, 1986*

Outline

- Darcy-scale description of subsurface flow
  - Darcy, REV, balance equation
  - Flow and transport
  - Numerical discretization
- From Darcy-scale to reservoir scale
  - Upscaling vs. Multiscale (Up-/Down-scaling)
- The Multiscale Finite-Volume method
  - Conceptual
  - Basis functions, “correction function”
  - Matrix formulation
- Iterative Multiscale FV method
  - Improved localization
- Adaptivity
  - Coupling flow and transport
  - Adaptive up-/downscaling
  - Adaptive improvement of boundary conditions

- Pore-scale simulations

Representative Elementary Volume (REV)

- Porosity, ϕ

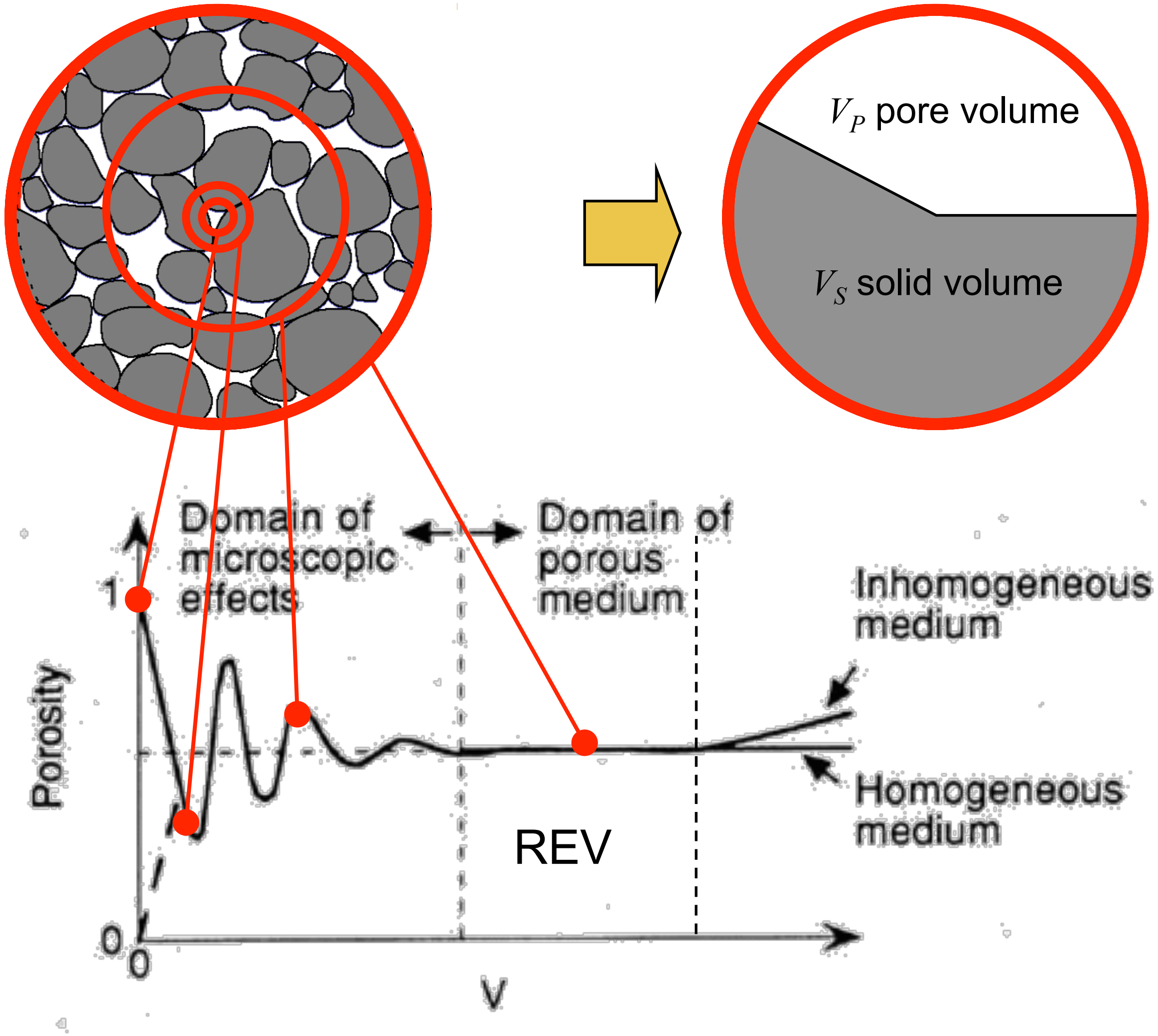

$$\phi = \frac{V_p}{V_p + V_s}$$

Adapted from Bear 1972

Average flow rate

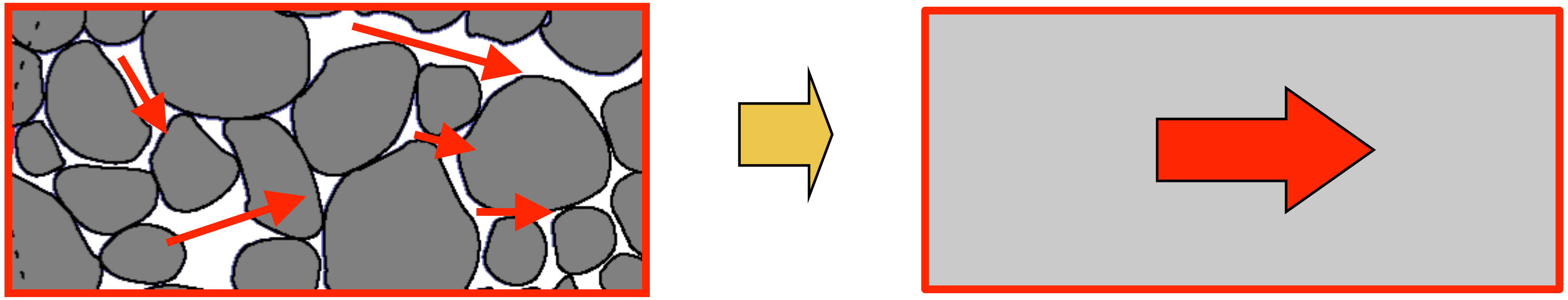

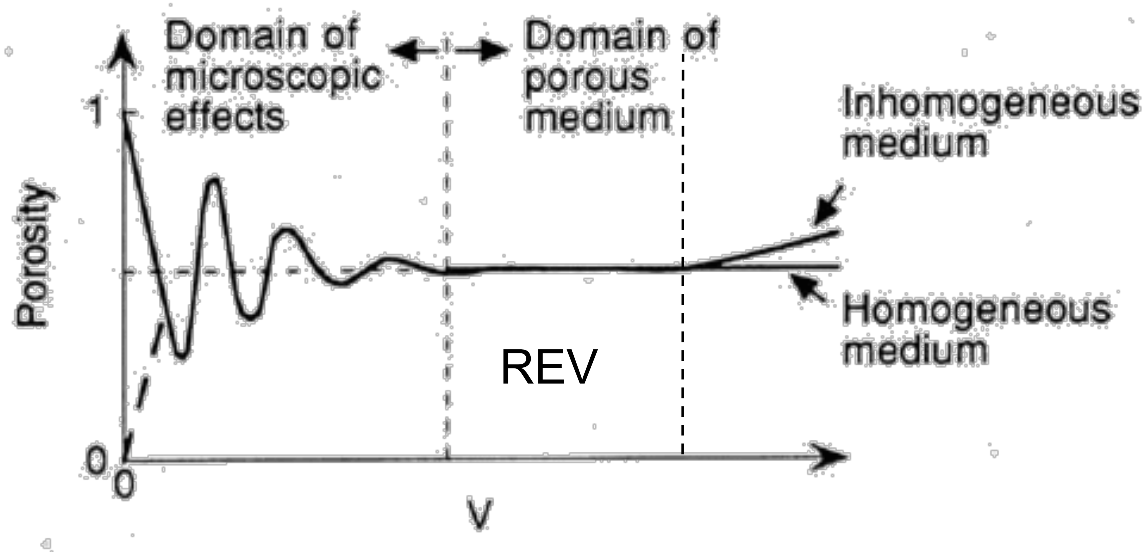

Adapted from Bear 1972

Darcy's law

- Flux linearly proportional to pressure gradient
- One of the empirical linear laws of the 19th century
  - Fourier's law (heat) [1822], Ohm's law (electric current) [1827], Fick's law (concentration) [1855]

- $u = \dfrac{Q}{A}$ specific flux (or Darcy «velocity»)

$$\boldsymbol{u} = -\frac{\mathbf{k}}{\mu}(\nabla p - \rho \boldsymbol{g})$$

$\boldsymbol{u}$	Darcy velocity	[m]
$\mathbf{k}$	permeability tensor	[m^2]
p	pressure	[Pa]
ρ	density	[kg/m^3]
μ	viscosity	[Pa s]
$\boldsymbol{g}$	gravity accelration	[m/s^2]
Q	flow rate	[m^3/s]
A	section	[m^2]

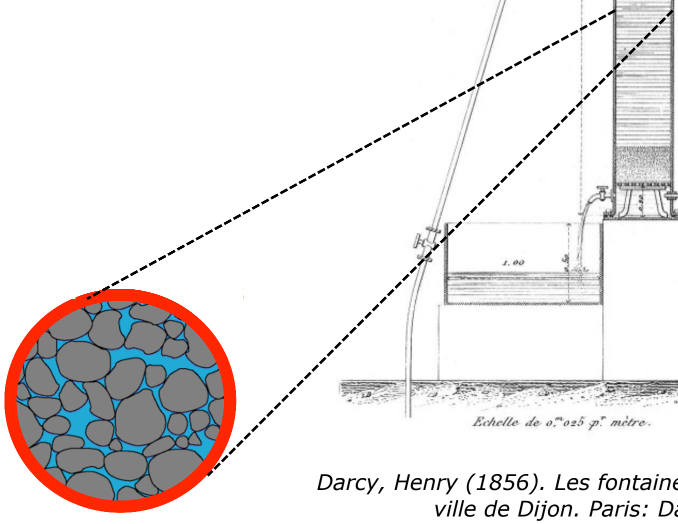

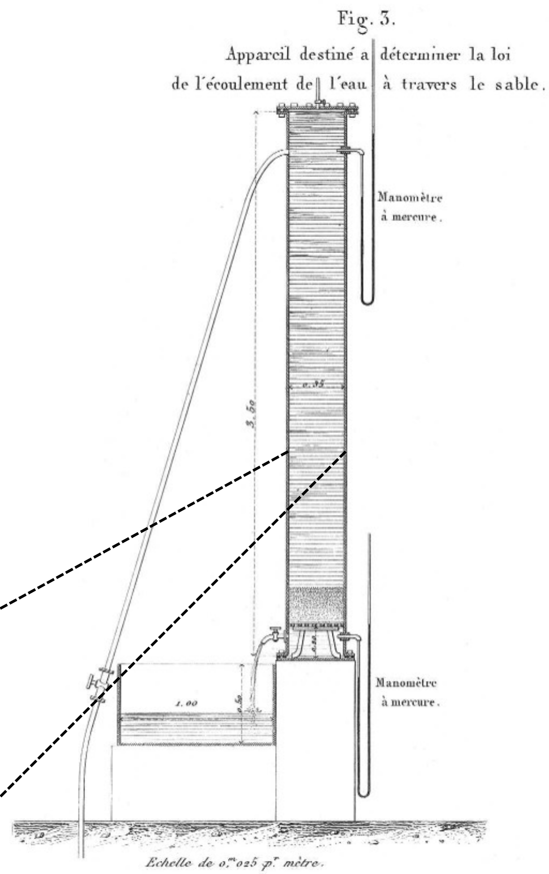

Darcy, Henry (1856). Les fontaines publiques de la ville de Dijon. Paris: Dalmont.

Mechanical energy

$$E = pV + mgz + \cancel{\frac{mv^2}{2}}$$

Small in porous media

Bernoulli (inviscid flow)

$$\frac{\Delta E}{V} = 0$$

Darcy (over damped)

$$\frac{\Delta E}{V} \sim L \cdot \frac{\mu}{k} v$$ Viscous loss

Hydraulic head (mechanical energy per unit weight)

$$h = \frac{E}{mg} = \frac{\rho V g}{mg}(h - z) + z \quad \Rightarrow \quad \boldsymbol{u} = -K \nabla h$$

<u>Groundwater potential (mechanical energy per unit volume)</u>

$$\varphi = \frac{E}{V} = p + \rho g z \quad \Rightarrow \quad \boldsymbol{u} = -\frac{k}{\mu}(\nabla p - \rho \boldsymbol{g})$$

Relationships: $h = \frac{p}{\rho g} + z = \frac{\varphi}{\rho g}$ $\quad K = k \frac{g}{\mu / \rho}$

Kinematic viscosity [m^2/s]
A fluid property

permeability [m^2]: a medium property

Balance equation (with internal sources)

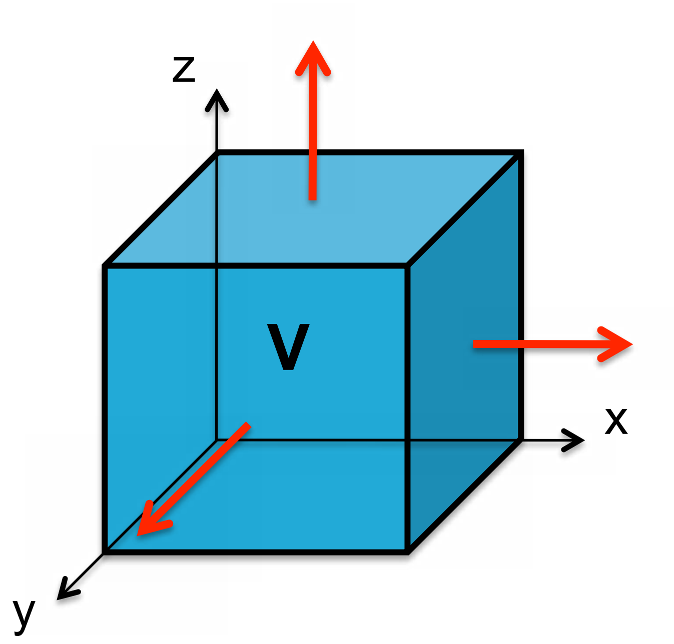

Control Volume, V
Control surface, S=∂V

Change in the volume
=
Flux across the surface
+
Sources in the volume

$$\frac{d}{dt}M_V = F_S + Q_V$$

$$\begin{aligned}\int_V \frac{\partial}{\partial t} m \, d\omega &= -\oint_S \boldsymbol{j}\cdot\boldsymbol{ds} + \int_V q \, d\omega \\ &= \int_V (-\nabla\cdot\boldsymbol{j} + q) \, d\omega\end{aligned}$$

Balance equation
in differential form

$$\frac{\partial}{\partial t} m + \nabla\cdot\boldsymbol{j} = q$$

System of equations

- Flow and (ideal tracer) transport: linear flow

$$\begin{cases} \beta \dfrac{\partial p}{\partial t} - \nabla \cdot \left[\dfrac{k}{\mu} \left(\nabla p - \rho \boldsymbol{g} \right) \right] = w \\ \boldsymbol{u} = -\dfrac{k}{\mu} \left(\nabla p - \rho \boldsymbol{g} \right) \\ \dfrac{\partial}{\partial t} (\phi c) + \nabla \cdot \left[c \boldsymbol{u} - \left(\mathbf{D}_d + D_m^* \right) \nabla c \right] = q_c \end{cases}$$

& B.C.

- Further complications: nonlinear flow
  - Density driven $\rho = \rho(c)$ $[\text{ possibly } \mu = \mu(c)\ ]$
  - Reactive transport $\phi = \phi(c)$
  - Multiphase flow $k = k(c)$ $p = p^* + p_c(c)$ $[\ D = D(k, p_c) = D(c)\ ]$

    $c \longrightarrow S$ Saturation (pore-volume fraction occupied by the phase)

Weighted residual method

discrete variable m_i

interpolator $\varphi_i(\boldsymbol{x})$

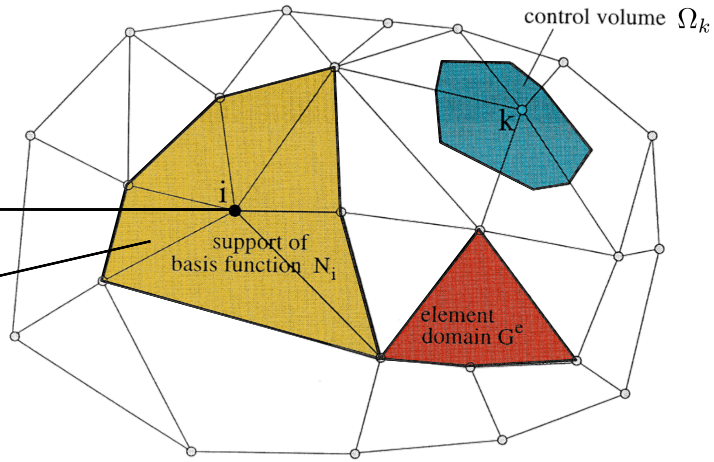

Balance equation in differential form

$$\epsilon(m) := \frac{\partial m}{\partial t} + \nabla \cdot \boldsymbol{f}(m) - q(m) = 0$$

Approximation on the discrete grid

$$m(\boldsymbol{x}) = \sum_i^N \varphi_i(\boldsymbol{x}) m_i$$

$$\int_\Omega w_j(\boldsymbol{x}) \epsilon(m(\boldsymbol{x})) d\boldsymbol{x} = 0, \qquad j = 1, 2, ..., N$$

Weighting functions

Finite Element (Standard Galerkin) $w_j(\boldsymbol{x}) = \varphi_j(\boldsymbol{x})$

Finite Volume $w_j(\boldsymbol{x}) = \chi_{\Omega_j}(\boldsymbol{x}) = \begin{cases} 1 & \text{if } \boldsymbol{x} \in \Omega_j \\ 0 & \text{otherwise} \end{cases}$

Weighted residual method: Finite-Volume

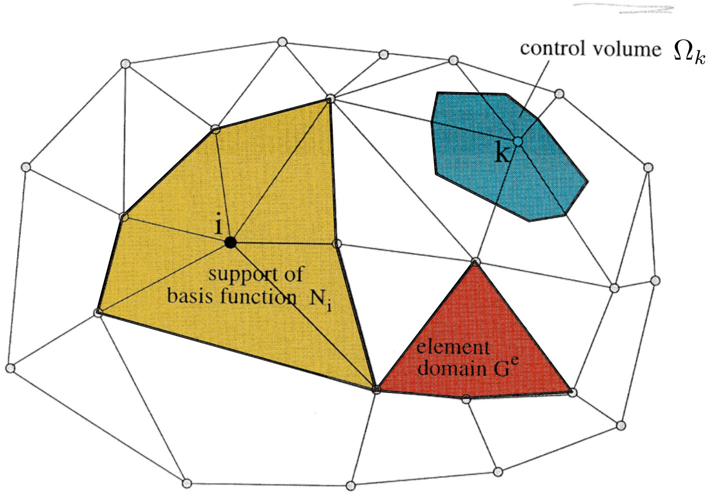

$$\frac{d}{dt}\int_{\Omega_j} m(\boldsymbol{x})d\boldsymbol{x} + \oint_{\partial\Omega_j} \boldsymbol{f}(m(\boldsymbol{x}))\cdot\boldsymbol{n}d\boldsymbol{x} - \int_{\Omega_j} q(m(\boldsymbol{x}))d\boldsymbol{x} = 0 \qquad j = 1, 2, ..., N$$

$$V_{ij} = \int_{\Omega_j} \varphi_i(\boldsymbol{x})d\boldsymbol{x} \qquad A_{ij} = \oint_{\partial\Omega_j} \boldsymbol{f}(\varphi_i(\boldsymbol{x}))\cdot\boldsymbol{n}d\boldsymbol{x} \qquad Q_{ij} = \int_{\Omega_j} q(\varphi_i(\boldsymbol{x}))d\boldsymbol{x}$$

$$\sum_i V_{ij}\frac{d}{dt}m_i + \sum_i A_{ij}m_i - \sum_i Q_{ij}m_i = 0, \quad j = 1, 2, ..., N$$

Finite-volume discretization of the balance equation

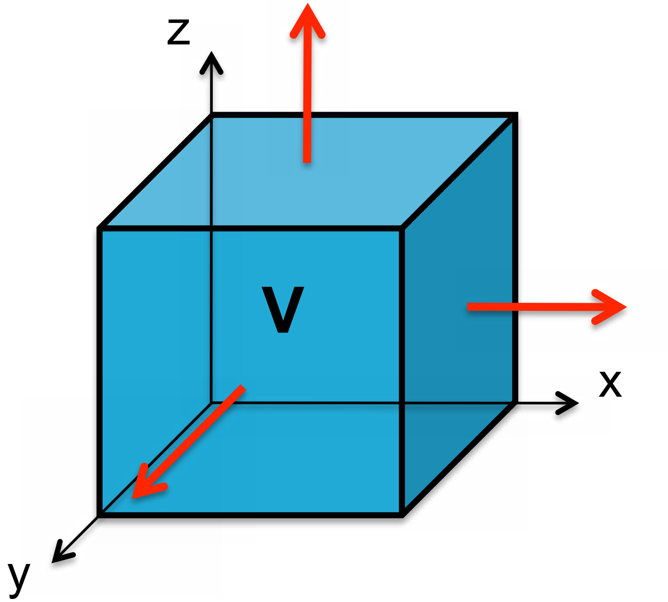

Change in the volume
=
Flux across the surface
+
Sources in the volume

$$\frac{d}{dt}M_V = F_S + Q_V$$

$$V_C\frac{d}{dt}m_C + F_{CN} + F_{CE} + F_{CS} + F_{CW} + F_{CU} + F_{CB} = Q_C$$

Finite Volume: spatial discretization

$$\frac{\partial m}{\partial t} + \nabla \cdot \boldsymbol{f}(m) = q(m)$$

Balance equation with source term

$$\int_\Omega \frac{\partial m}{\partial t} d\omega + \int_\Omega \nabla \cdot \boldsymbol{f}(m) d\omega = \frac{d}{dt}\int_\Omega m \; d\omega + \oint_{\partial\Omega} \boldsymbol{f}(m) \cdot \boldsymbol{n} \; da = \int_\Omega q(m) d\omega$$

$$\frac{d}{dt}\int_\Omega m \; d\omega = V_C \frac{d}{dt} m_C$$

$$\oint_{\partial\Omega} \boldsymbol{f}(m) \cdot \boldsymbol{n} \; da = F_{CN} + F_{CE} + F_{CS} + F_{CW}$$

$$\int_\Omega q(m) \; d\omega = V_C q(m_C)$$

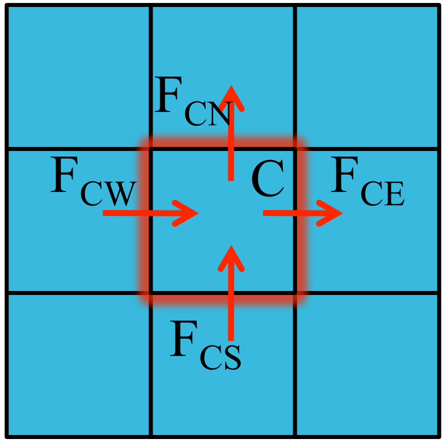

$$V_C \frac{d}{dt} m_C + F_{CN} + F_{CE} + F_{CS} + F_{CW} = V_C q(m_C)$$

Finite Volume: five-point stencil

$$\boldsymbol{f}(m) = -D\nabla m$$

e.g.: linear diffusive flux

$$F_{NC} = \int_{\partial\Omega_{NC}} -D\nabla m \cdot \boldsymbol{n}\; da \approx -A_N [D]_{NC} \frac{m_N - m_C}{x_N - x_C} = T_{NC}(m_N - m_C)$$

$$\begin{aligned} -\oint_{\partial\Omega} D\nabla m \cdot \boldsymbol{n}\; da \quad &\approx \quad T_{CN} m_N \\ &+ \quad T_{CW} m_W \\ &- \quad (T_{CN} + T_{CW} + T_{CS} + T_{CE})\, m_C \\ &+ \quad T_{CE} m_E \\ &+ \quad T_{CS} m_S \end{aligned}$$

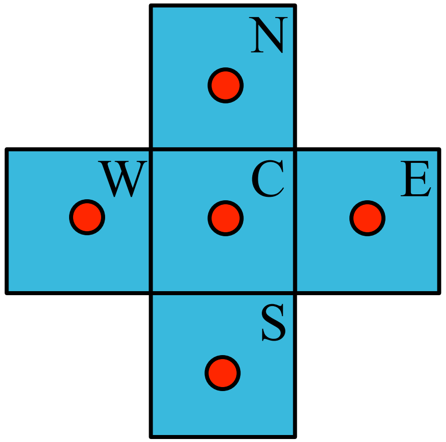

Finite Volume: five-point stencil

$$\boldsymbol{f}(m) = -D\nabla m$$ e.g.: linear diffusive flux

$$F_{NC} = \int_{\partial\Omega_{NC}} -D\nabla m \cdot \boldsymbol{n}\; da \approx -A_N[D]_{NC}\frac{m_N - m_C}{x_N - x_C} = T_{NC}(m_N - m_C)$$

$$\begin{array}{cc} & \\ \Omega_C \leftarrow & \\ & \\ & \\ \mathbf{T}\boldsymbol{m} & = \end{array} \begin{bmatrix} \cdots & & & & & & & & \\ \cdots & & & & & & & & \\ \cdots & T_{CN} & \cdots & T_{CW} & -\sum_I T_{CI} & T_{CE} & \cdots & T_{CS} & \cdots \\ \cdots & & & & & & & & \\ \cdots & & & & & & & & \\ \cdots & & & & & & & & \\ \cdots & & & & & & & & \\ \cdots & & & & & & & & \\ \cdots & & & & & & & & \\ \cdots & & & & & & & & \end{bmatrix} \begin{bmatrix} \cdots \\ \cdots \\ m_N \\ \cdots \\ m_W \\ m_C \\ m_E \\ \cdots \\ m_S \\ \cdots \end{bmatrix}$$

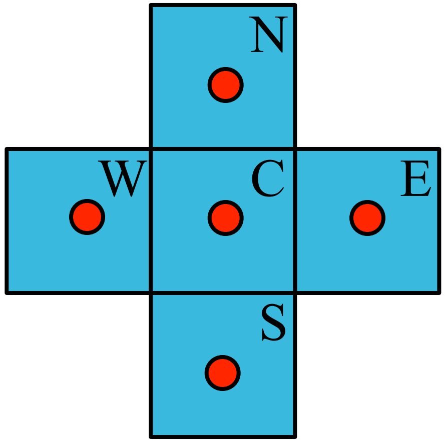

Finite Volume: five-point stencil

- The coefficient matrix is penta-diagonal (5pt stencil!)
  - Only the element on 5 diagonals can be nonzero
  - = non zero diagonals
  - N-pt stencil => N-diagonal

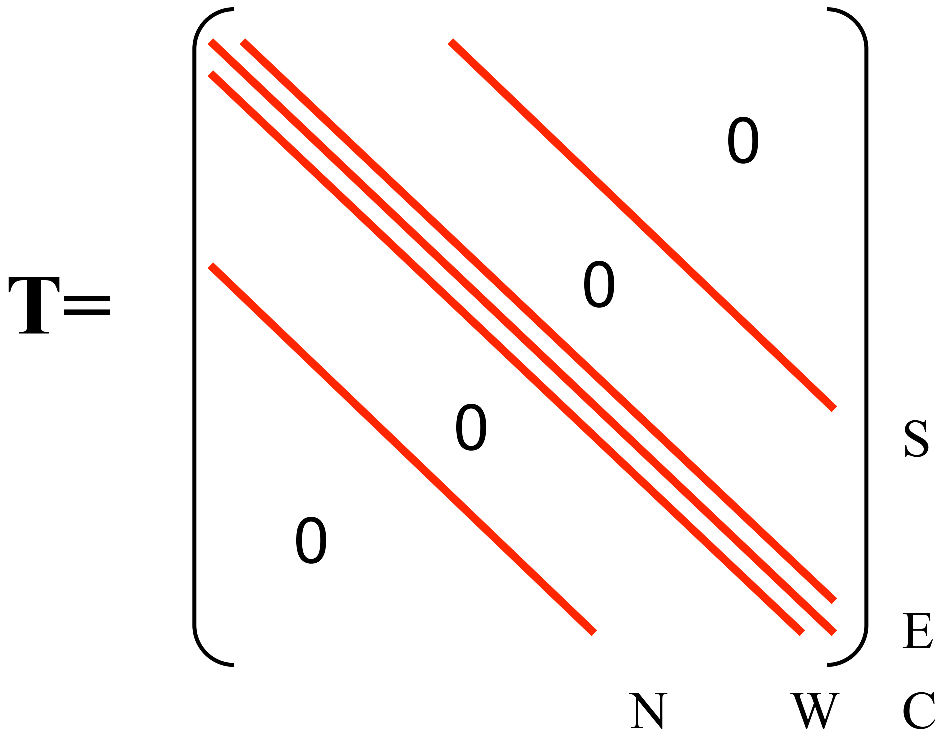

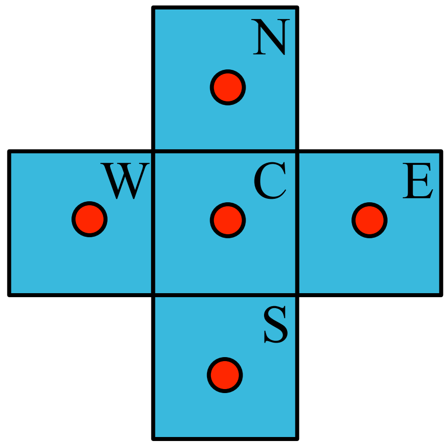

Finite Volume: nine-point stencil (2D)

- The coefficient matrix is ennea-diagonal (9pt stencil!)
  - Only the element on 9 diagonals can be nonzero
  - = non zero diagonals
  - N-pt stencil => N-diagonal

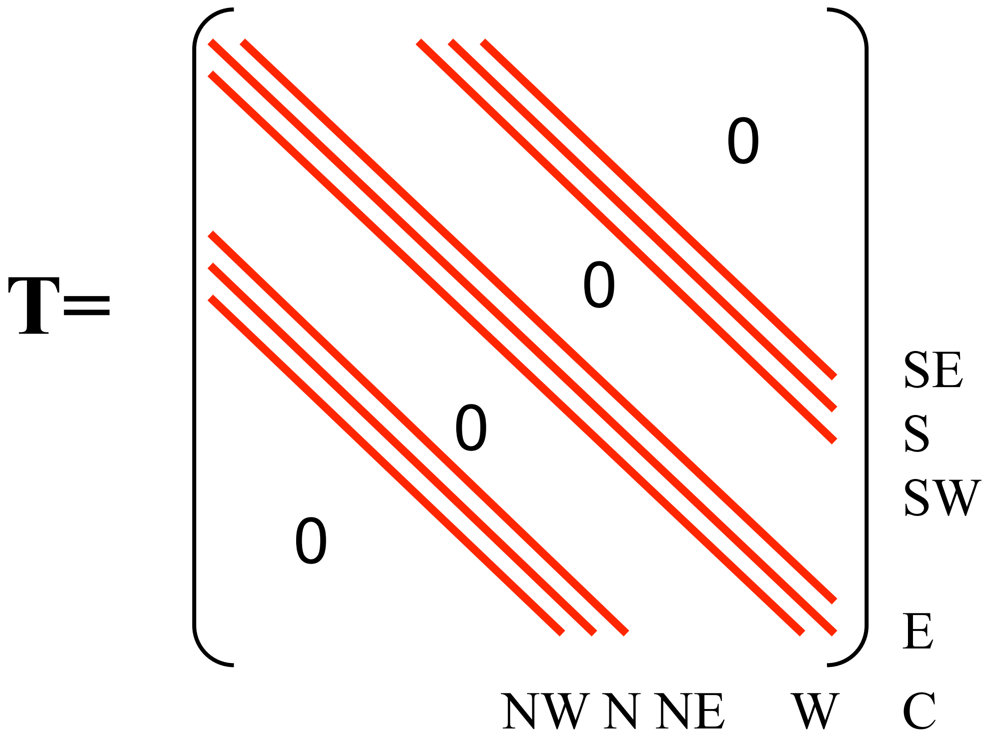

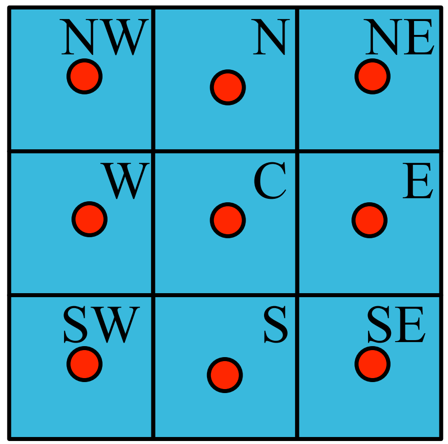

One, two, three dimensions

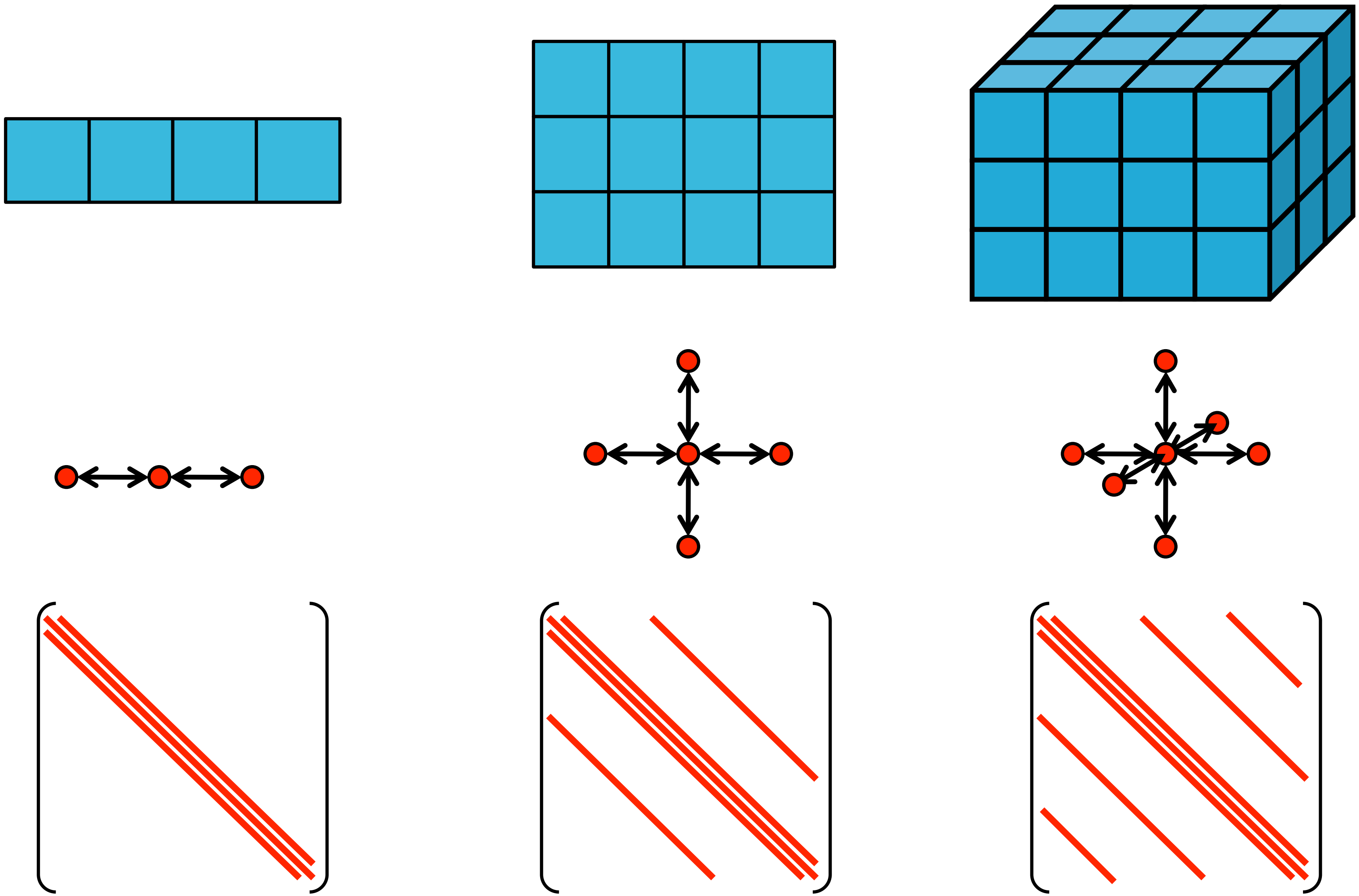

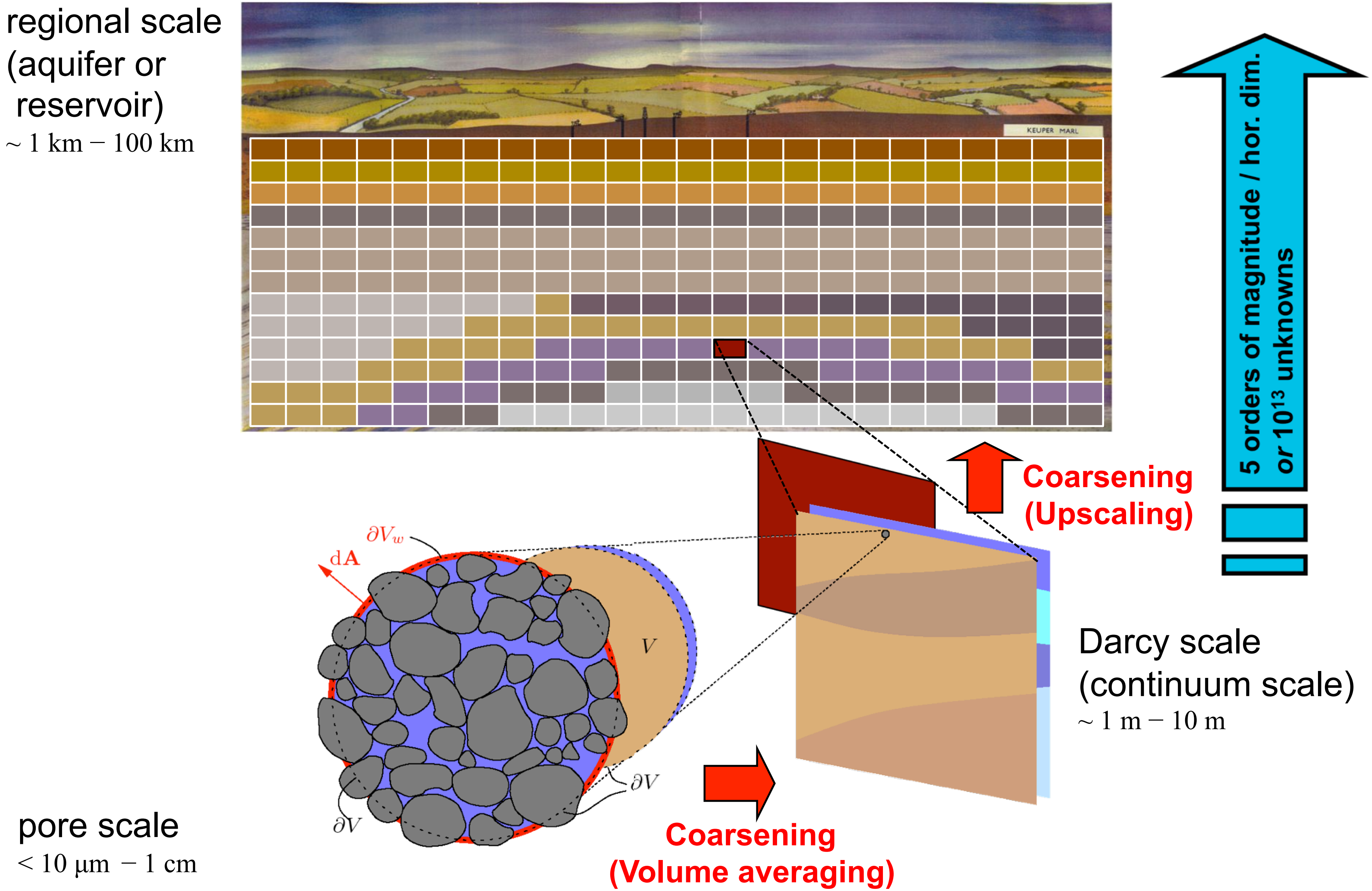
regional scale
(aquifer or
reservoir)
~ 1 km – 100 km
KEUPER MARL
5 orders of magnitude / hor. dim.
or 10^{13} unknowns
Coarsening
(Upscaling)
Darcy scale
(continuum scale)
~ 1 m – 10 m
∂V_w
$\mathrm{d}\mathbf{A}$
V
∂V
∂V
Coarsening
(Volume averaging)
pore scale
< 10 μm – 1 cm

The upscaling (coarsening) approach

Heterogeneous permeability

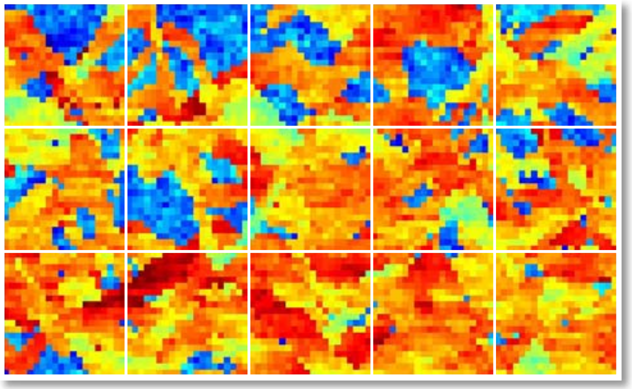

Saturation field

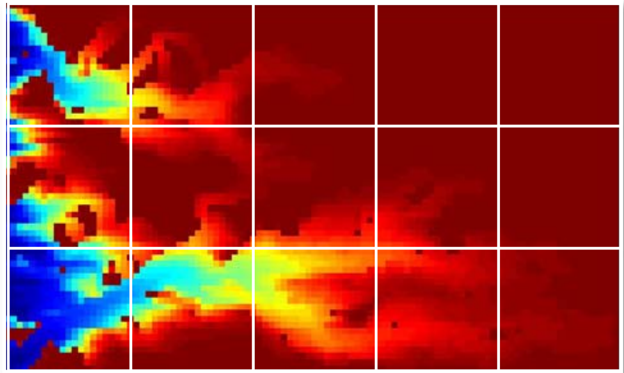

Global problem (coarse-grained)

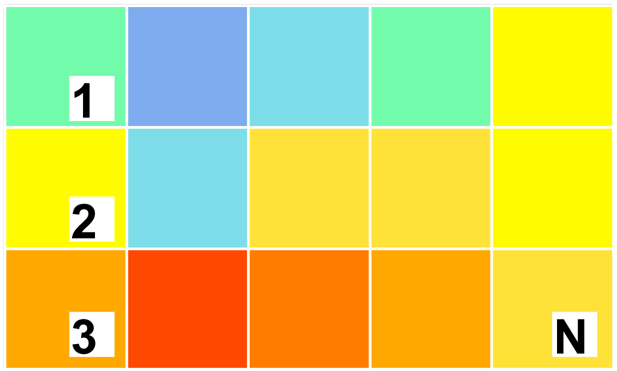

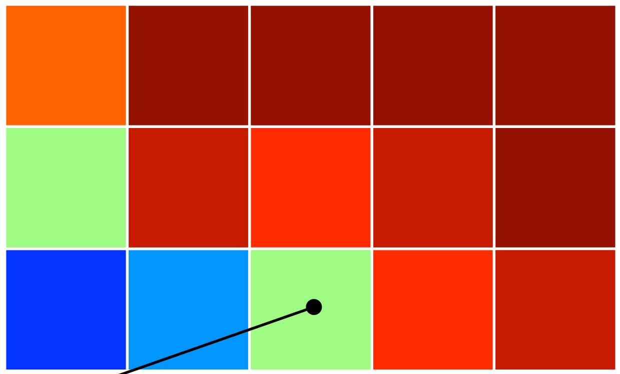

Unphysical "mixing":
Higher solution or reaction rate,
instability damping, etc.

The Multiscale approach

Heterogeneous permeability

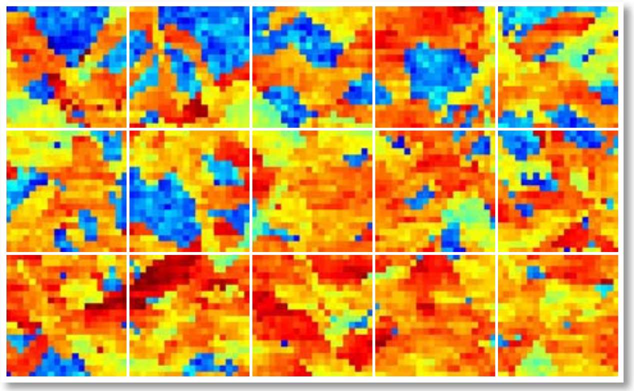

Saturation field

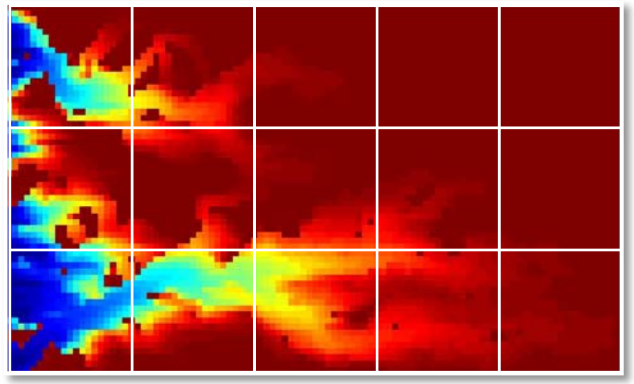

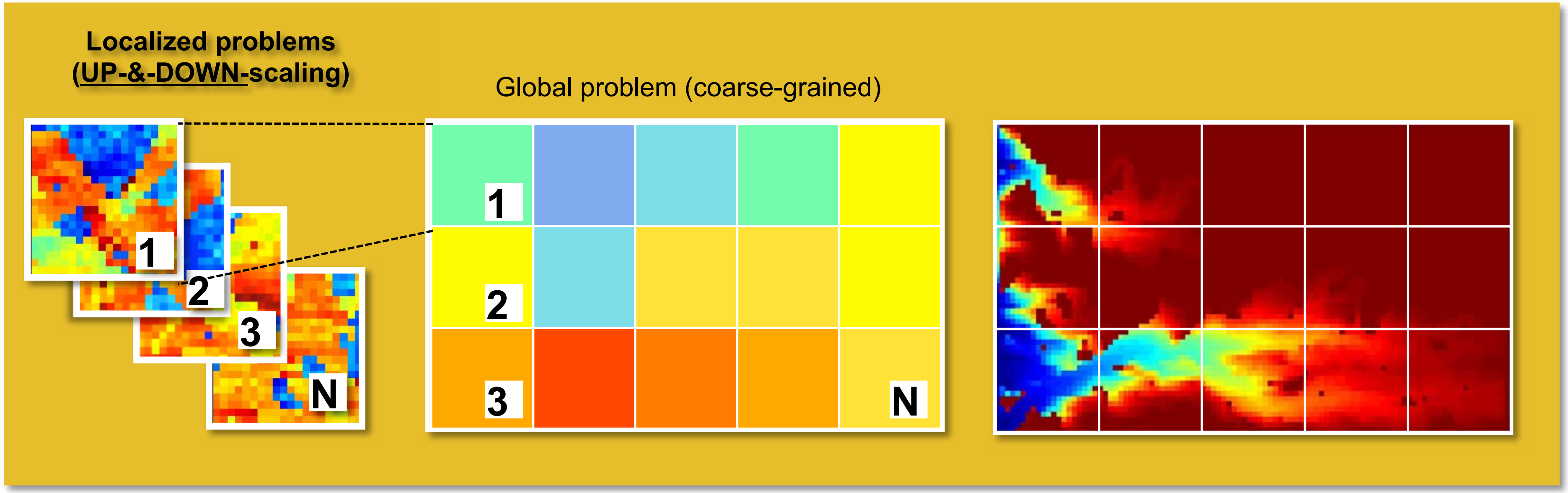

Multiscale Finite Volume (conceptual): operators

Localized problems
(UP-&-DOWN-scaling)

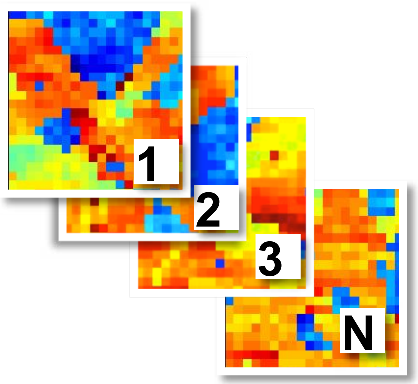

Global problem (coarse-grained)

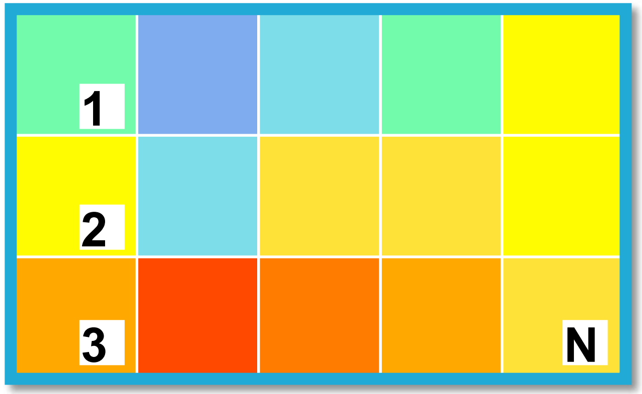

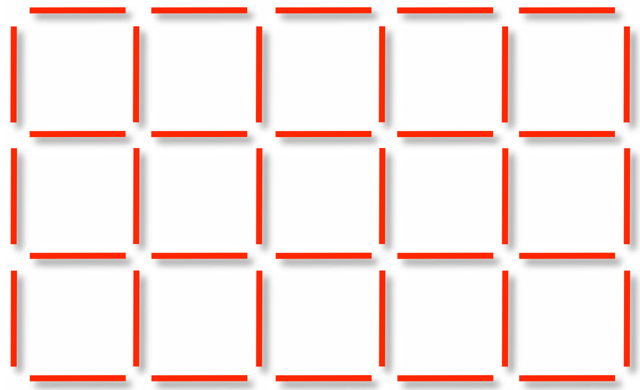

[Pictorial representation: we actually use **two coarse grids** in full analogy with finite-volume (control-volume) discretization]

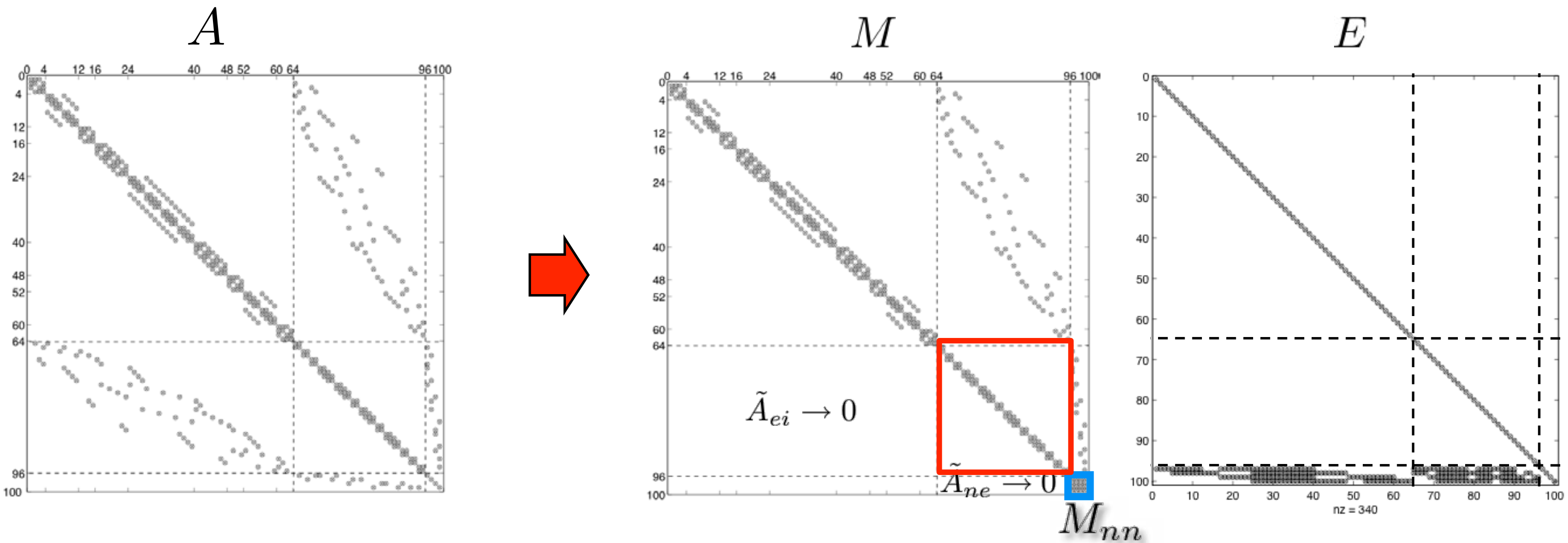

Jenny et al, JCP, 2003; Lunati and Jenny, Comp. Geosci., 2008; Lunati and Lee, MMS, 2009, Lunati, Tyagi, and Lee, JCP, 2011

Multiscale Finite Volume (conceptual): iterative

$$p^{\mu} = p^{\mu-1} + \omega^{\mu-1} M^{-1} E(r - Ap^{\mu-1})$$

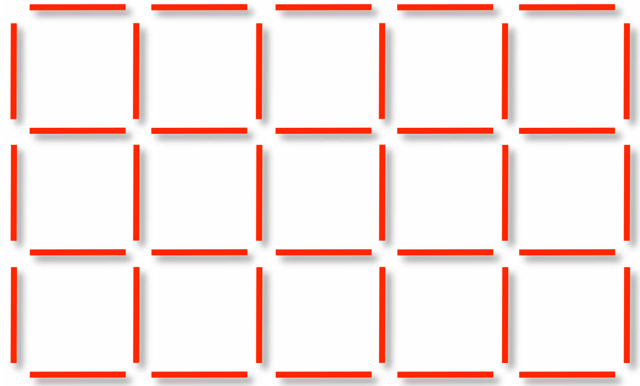

Richardson iterations with GMRES
(but only if more accurate localization is needed)

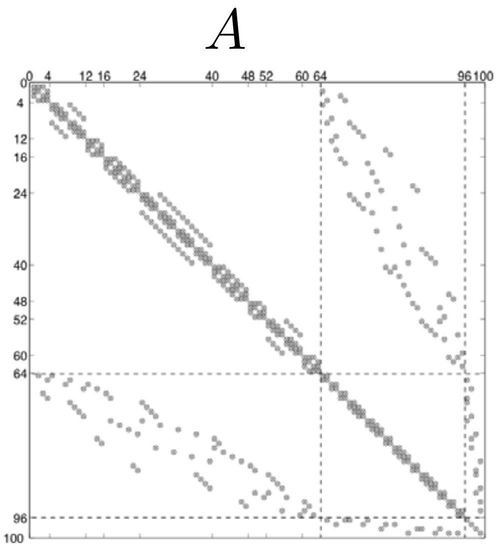

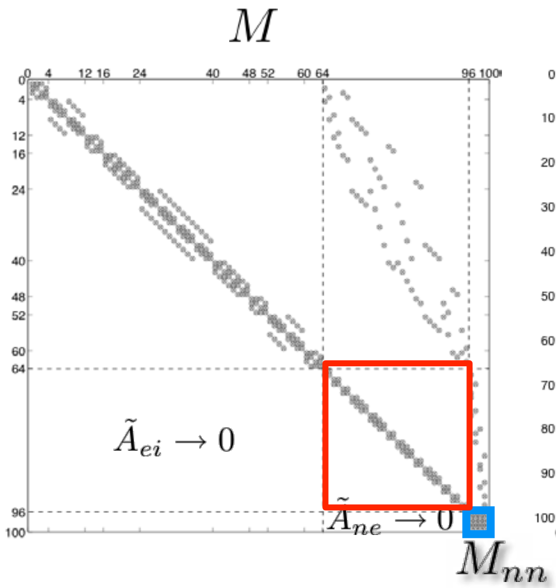

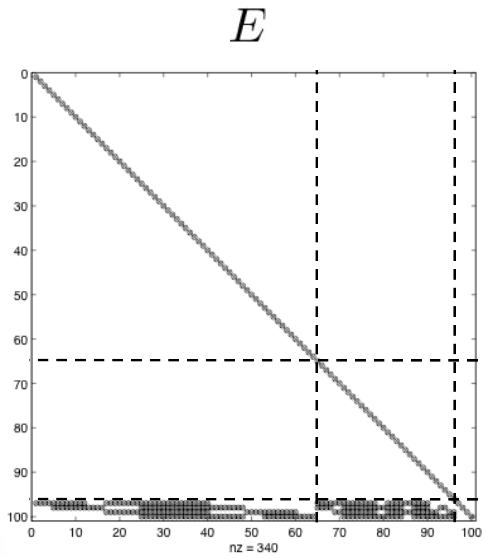

Jenny et al, JCP, 2003; Lunati and Jenny, Comp. Geosci., 2008; Lunati and Lee, MMS, 2009, Lunati, Tyagi, and Lee, JCP, 2011

Computational costs vs. accuracy

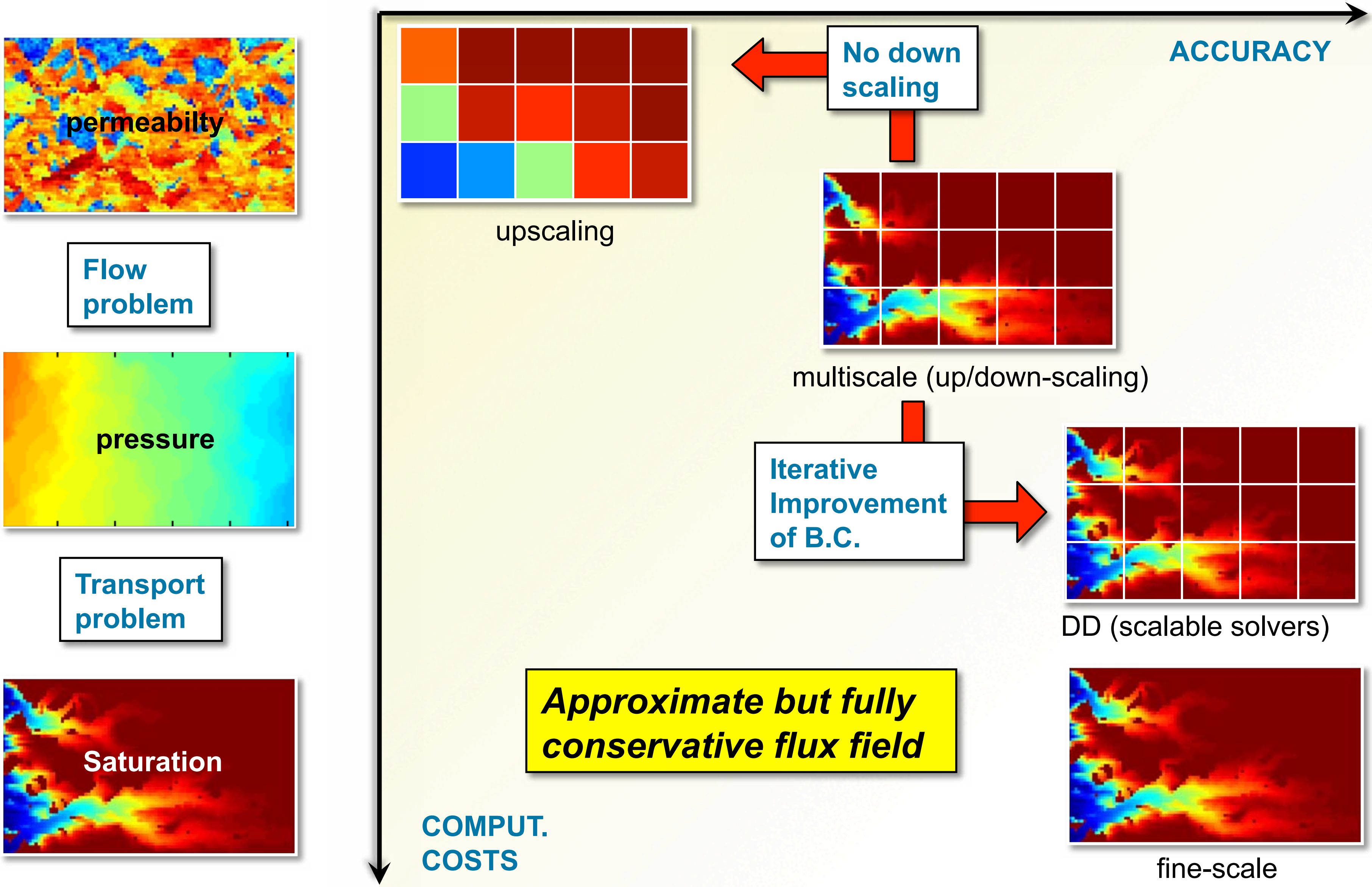

Multiscale Finite-Volume (MsFV) Method

$$-\nabla \cdot \boldsymbol{v} = \nabla \cdot \mathbf{K}\nabla p = r$$

1) Compute an approximate pressure

$$p \approx \cup_e \tilde{p}|_{\tilde{\Omega}^e}$$

2) Compute (construct) an approximate, but **conservative** velocity

$$\boldsymbol{v} \approx \cup_i \boldsymbol{v}|_{\bar{\Omega}_i}$$

3) Then solve transport (sequential implicit coupling)

$$\frac{\partial}{\partial t}(\phi S_\alpha) + \nabla \cdot (f_\alpha \boldsymbol{v}) - q_\alpha = 0$$

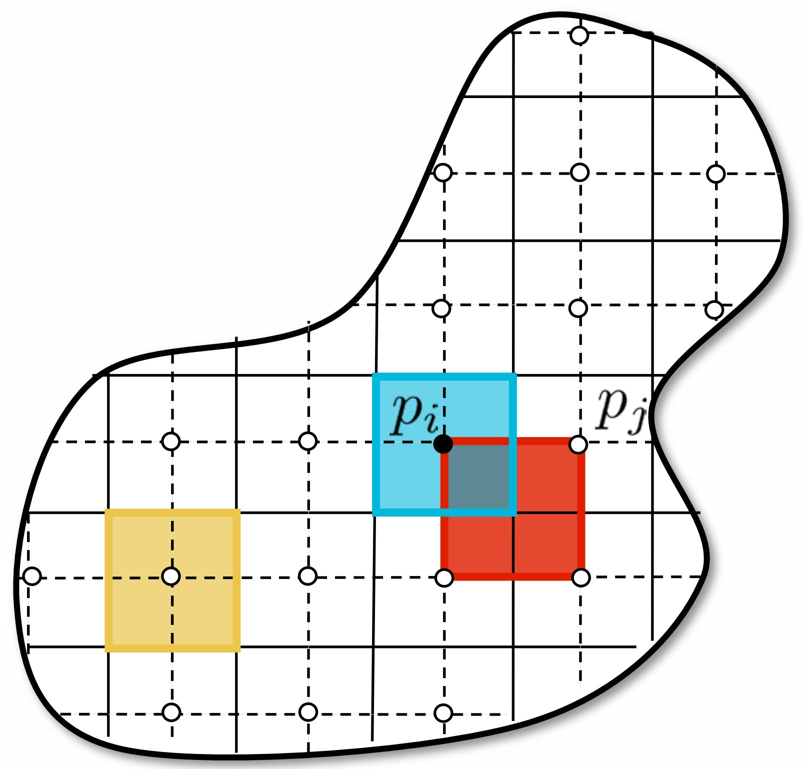

$$\begin{bmatrix} A & 0 & 0 \\ B_{vp} & B_{vv} & 0 \\ C_{sp} & C_{sv} & C_{ss} \end{bmatrix} \begin{bmatrix} p \\ v \\ S \end{bmatrix} = \begin{bmatrix} r \\ q_v \\ q_s \end{bmatrix}$$

Basis functions and correction function

$$p|_{\tilde{\Omega}^e} = \sum_j \tilde{\varphi}_j^e p_j + \tilde{\varphi}_*^e$$

Extension of bilinear basis functions, $\mathbf{K}(\boldsymbol{x})$

$$\begin{cases} \nabla \cdot \mathbf{K} \nabla \tilde{\varphi}_j^e = 0 & \text{in} \quad \tilde{\Omega}^e \\ \nabla_{\parallel} \cdot \mathbf{K} \nabla \tilde{\varphi}_j^e = 0 & \text{on} \quad \partial\tilde{\Omega}^e \\ \tilde{\varphi}_j^e(\boldsymbol{x}_i) = \delta_{ij} & \text{on} \quad \partial\partial\tilde{\Omega}^e \end{cases}$$

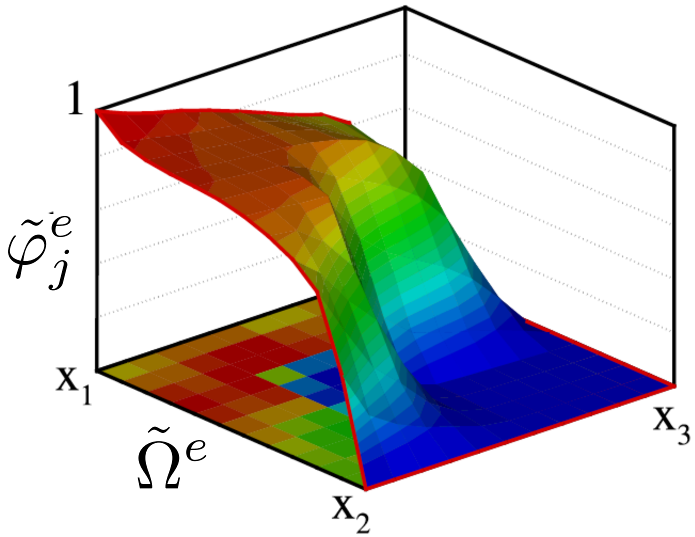

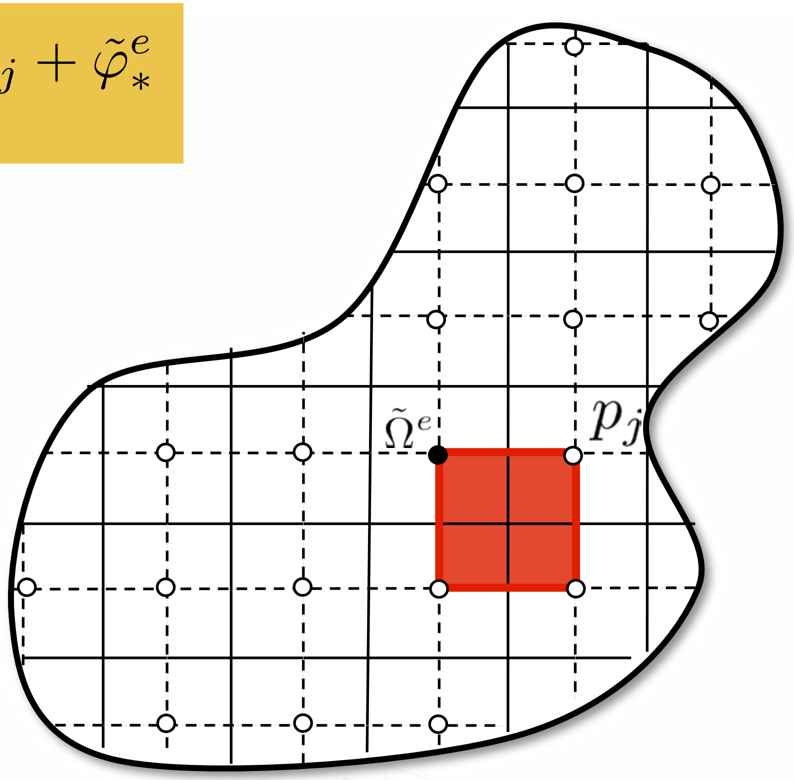

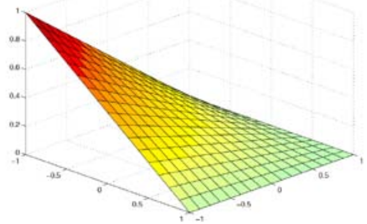

MsFV basis functions take into account heterogeneity
(also MsFE, Hou and Wu, JCP, 1997)

Bilinear basis function

Basis functions and correction function

$$p|_{\tilde{\Omega}^e} = \sum_j \tilde{\varphi}_j^e p_j + \tilde{\varphi}_*^e$$

homogeneous solution

$$\begin{cases} \nabla \cdot \mathbf{K} \nabla \tilde{\varphi}_j^e = 0 & \text{in} & \tilde{\Omega}^e \\ \nabla_\parallel \cdot \mathbf{K} \nabla \tilde{\varphi}_j^e = 0 & \text{on} & \partial\tilde{\Omega}^e \\ \tilde{\varphi}_j^e(\boldsymbol{x}_i) = \delta_{ij} & \text{on} & \partial\partial\tilde{\Omega}^e \end{cases}$$

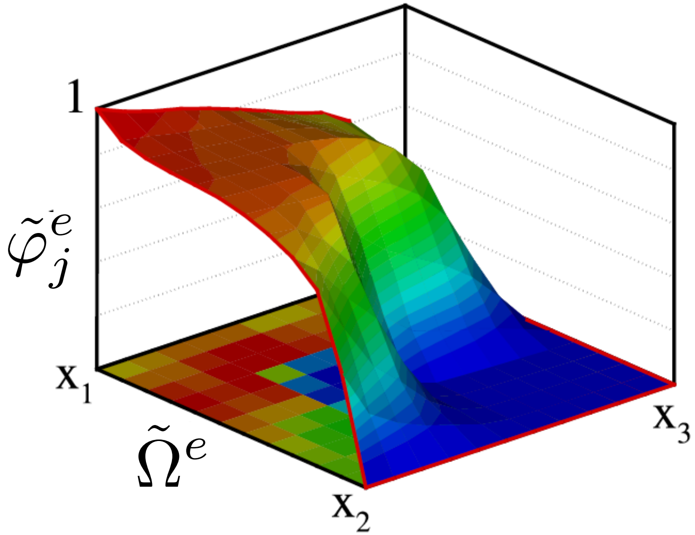

basis functions: describe viscous forces

(Jenny, Lee and Tchelepi, JCP, 2003)

particular solution

$$\begin{cases} \nabla \cdot \mathbf{K} \nabla \tilde{\varphi}_*^e = r & \text{in} & \tilde{\Omega}^e \\ \nabla_\parallel \cdot \mathbf{K} \nabla \tilde{\varphi}_*^e = r_\parallel & \text{on} & \partial\tilde{\Omega}^e \\ \tilde{\varphi}_*^e(\boldsymbol{x}_i) = 0 & \text{on} & \partial\partial\tilde{\Omega}^e \end{cases}$$

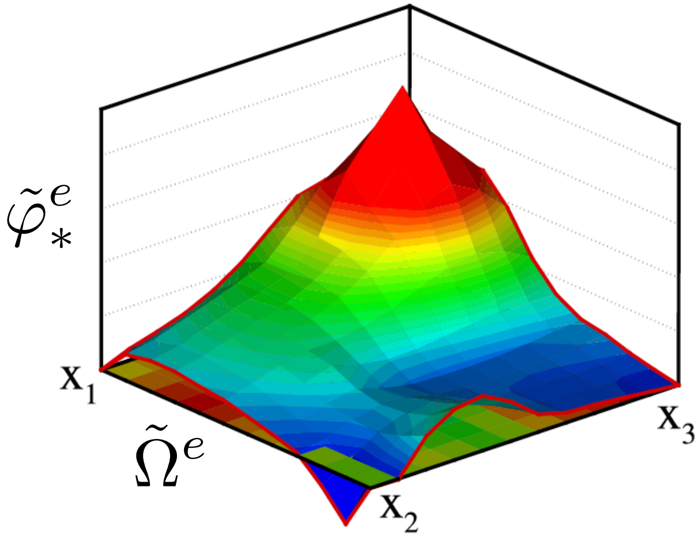

correction function: remaining physics and source terms

(Lunati and Jenny, CMWR, 2006; Comp. Geosci., 2008)

Coarse problem

$$p|_{\tilde{\Omega}^e} = \sum_j \tilde{\varphi}_j^e p_j + \tilde{\varphi}_*^e$$

$$w_i(\boldsymbol{x}) = \chi_{\bar{\Omega}_i}(\boldsymbol{x}) = \begin{cases} 1 & \text{if } \boldsymbol{x} \in \bar{\Omega}_i \\ 0 & \text{otherwise} \end{cases}$$

The coarse problem is obtained integrating over the coarse control volume, $\bar{\Omega}_i$

$$M_{ij} = -\sum_e \int_{\partial\bar{\Omega}_i \cap \tilde{\Omega}^e} \mathbf{K}\nabla\tilde{\varphi}_j^e \cdot \boldsymbol{\eta} d\Gamma$$

$$q_i = \sum_e \int_{\partial\bar{\Omega}_i \cap \tilde{\Omega}^e} \mathbf{K}\nabla\tilde{\varphi}_*^e \cdot \boldsymbol{\eta} d\Gamma - \int_{\bar{\Omega}_i} r d\boldsymbol{x}$$

$$\boxed{\sum_j M_{ij} p_j = q_i}$$

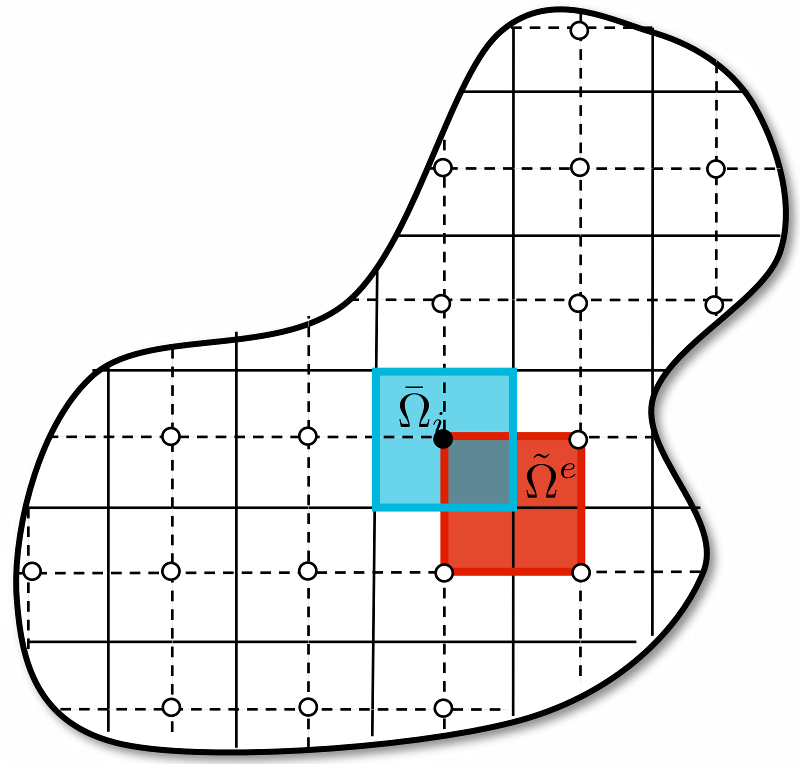

Construction of a conservative velocity

$$p|_{\tilde{\Omega}^e} = \sum_j \tilde{\varphi}_j^e p_j + \tilde{\varphi}_*^e$$

$$\sum_j M_{ij} p_j = q_i$$

The locally conservative velocity is obtained solving problems on coarse control volume

$$\begin{cases} \nabla \cdot \mathbf{K} \nabla \bar{\psi}_i = r & \text{in} \quad \bar{\Omega}_i \\ \nabla_\perp \bar{\psi}_i = \nabla_\perp \tilde{p} & \text{on} \quad \partial\bar{\Omega}_i \end{cases}$$

$$\boldsymbol{v} = \begin{cases} -\mathbf{K} \nabla \bar{\psi}_i & \text{in} \quad \bar{\Omega}_i \\ -\mathbf{K} \nabla \tilde{p} & \text{on} \quad \partial\bar{\Omega}_i \end{cases}$$

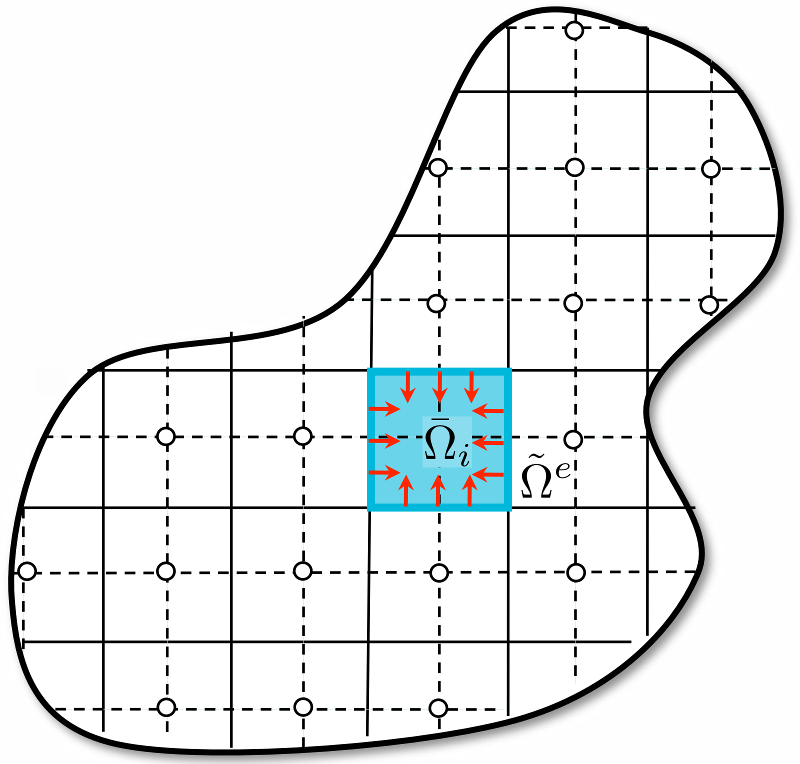

Remark: the conservative velocity cannot be written as the gradient of a scalar field

Divergence and vorticity

$$\nabla \cdot K \nabla p \neq r$$

$$\nabla \times \boldsymbol{v} \neq \nabla(\ln K) \times \boldsymbol{v}$$

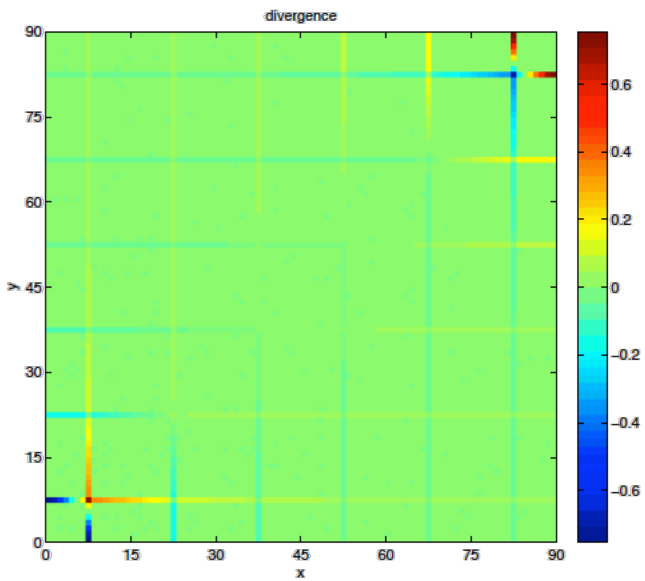

Divergence of dual pressure based velocity

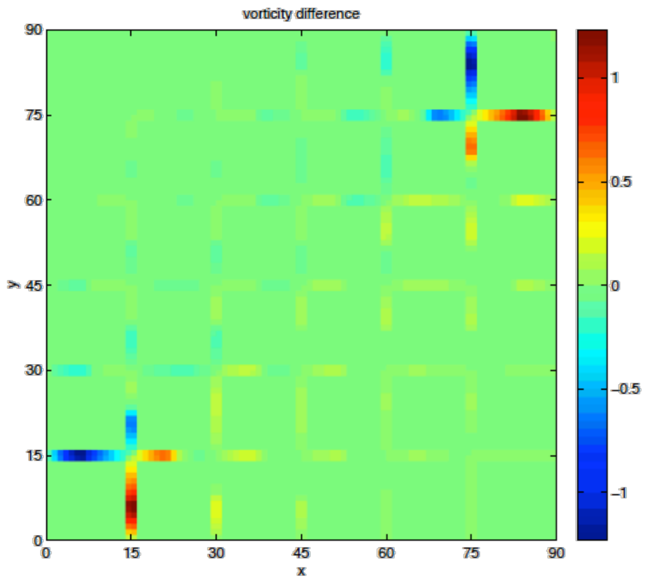

Vorticity of the conservative velocity

(Quarter five spot problem, single phase flow, homogeneous permeability field)

(**Künze & Lunati, IAHR Valencia, 2010**; also Lunati and Jenny MMS, 2007)

Lock-exchange problem

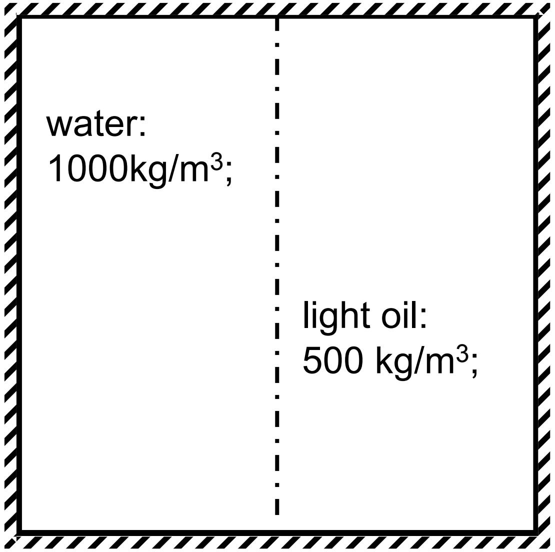

saturation without correction function

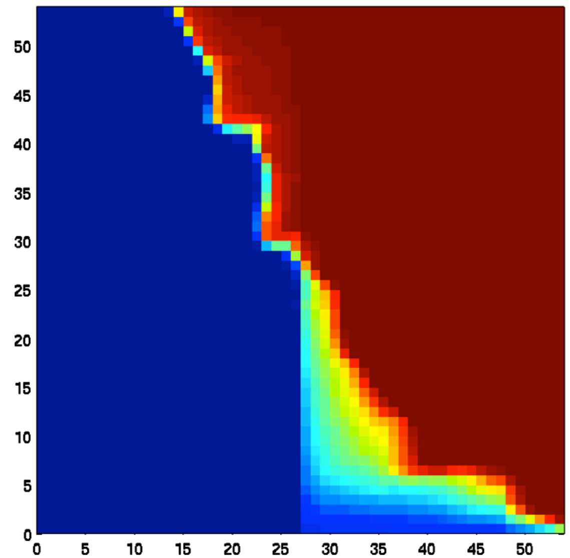

water (blue)
oil (red)

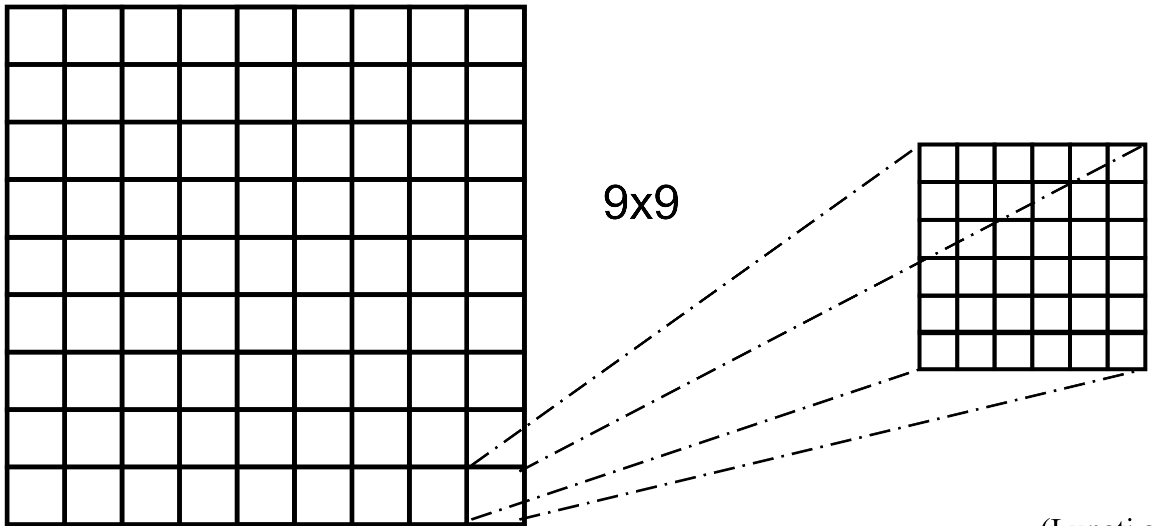

quadratic rel.perms.
$\rho_w/\rho_o = 2$
$\mu_w/\mu_o = 0.1$

(Lunati and Jenny, Comp. Geosci., 2008)

Water-saturation solutions: MsFV vs. reference

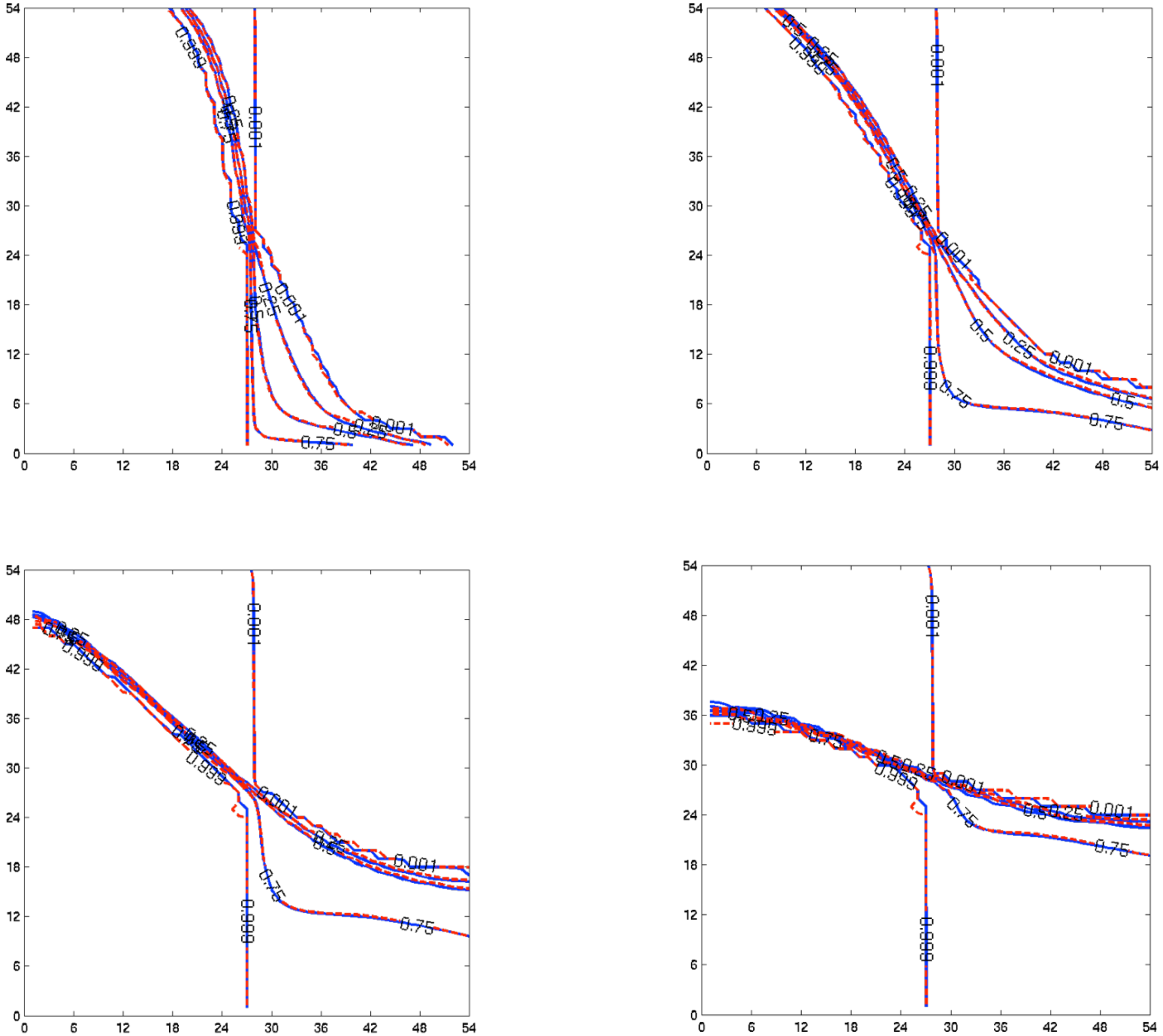

(Lunati and Jenny, Comp. Geosci., 2008)

Gravity currents: lock-exchange problem

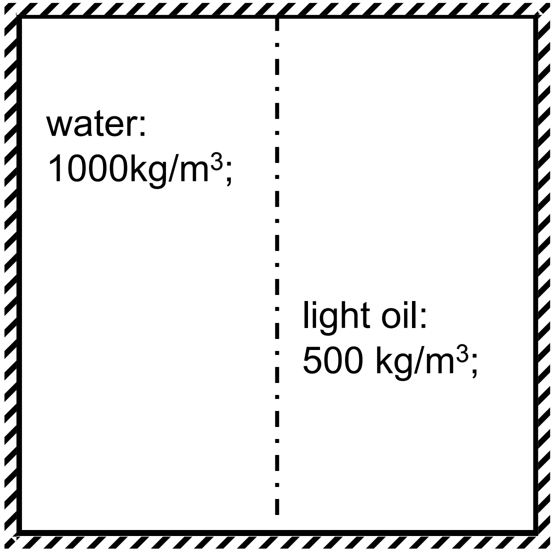

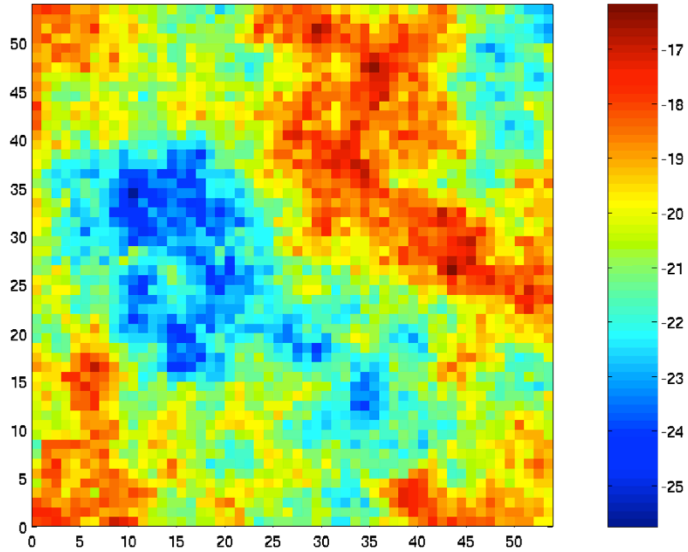

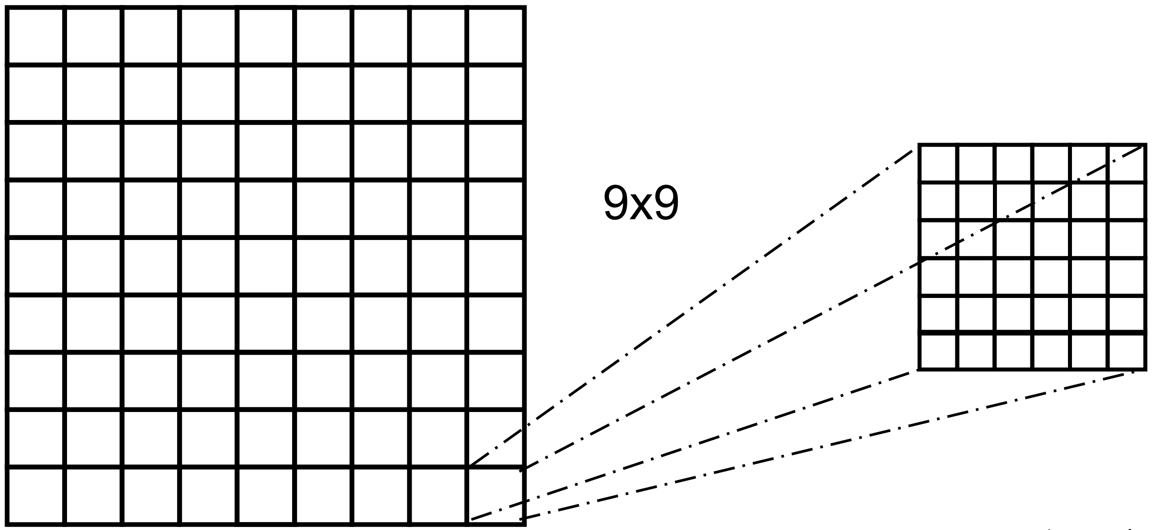

9x9

6x6

quadratic rel.perms.

$\rho_w/\rho_o = 2$

$\mu_w/\ \mu_o = 0.1$

(Lunati and Jenny, Comp. Geosci., 2008)

Lock-exchange in a heterogeneous perm. field

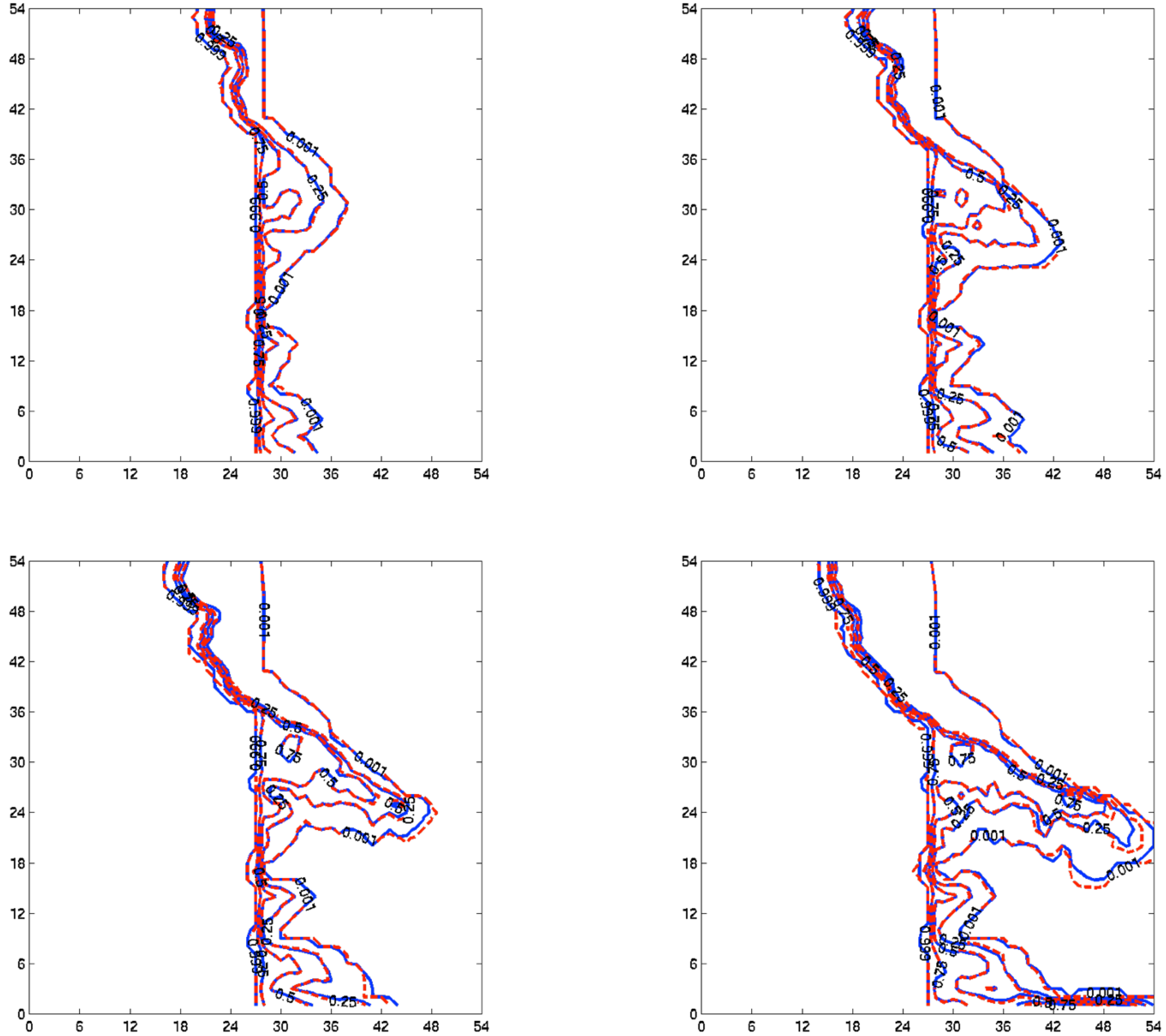

(Lunati and Jenny, Comp. Geosci., 2008)

A 2d model with two wells: strong gravity, $\rho_o = 0.5$, $\rho_w = 1.0$

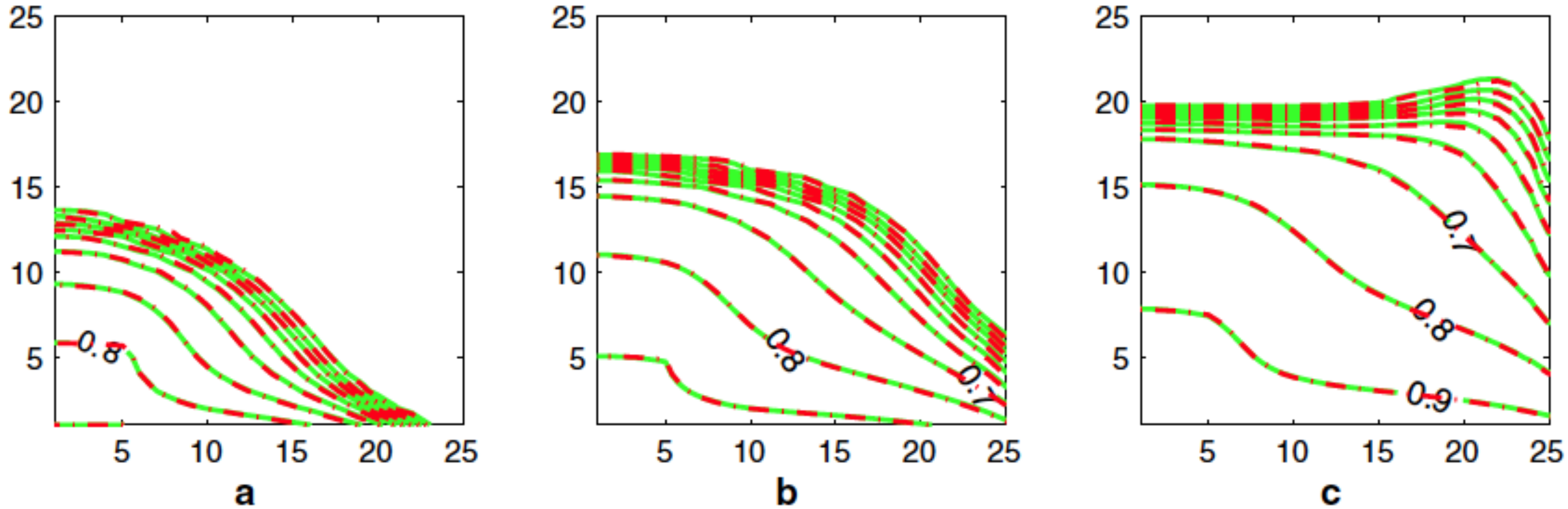

Fig. 5 Contour lines of water saturation for example 2 **a** 0.21 pore volumes injected (PVI), **b** 0.42 PVI, and **c** 0.64 PVI. *Solid contours* represent multiscale, *dashed contours* fine-scale results

(Lee, Wolfsteiner, and Tchelepi, Comp. Geosci., 2008)

A 3D Model with two wells: fine 45x45x30, coarse 9x9x6

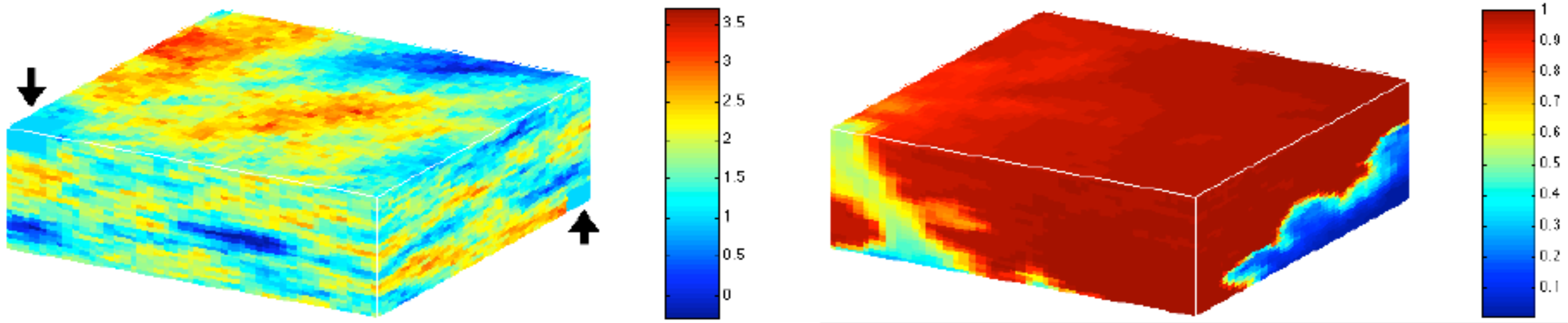

(a) (b)

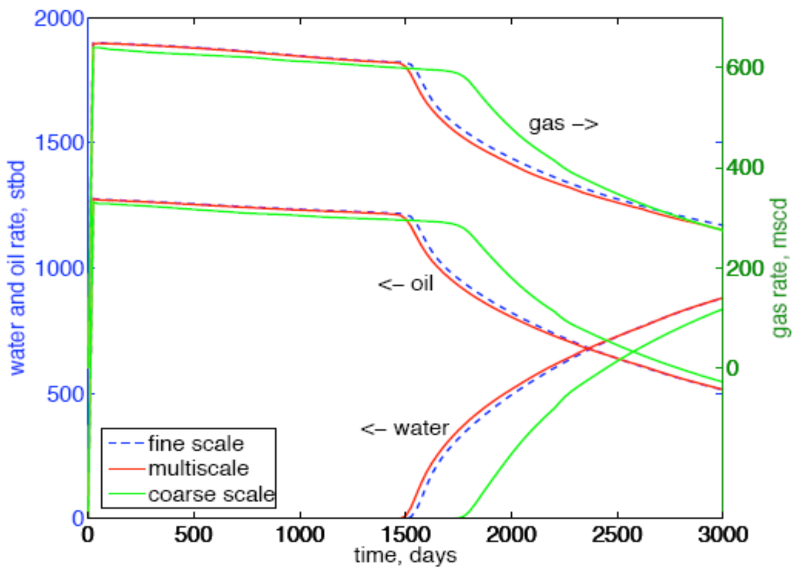

(Lee, Wolfsteiner, and Tchelepi, Comp. Geosci., 2008)

Deterioration of the MsFV solution with anisotropy

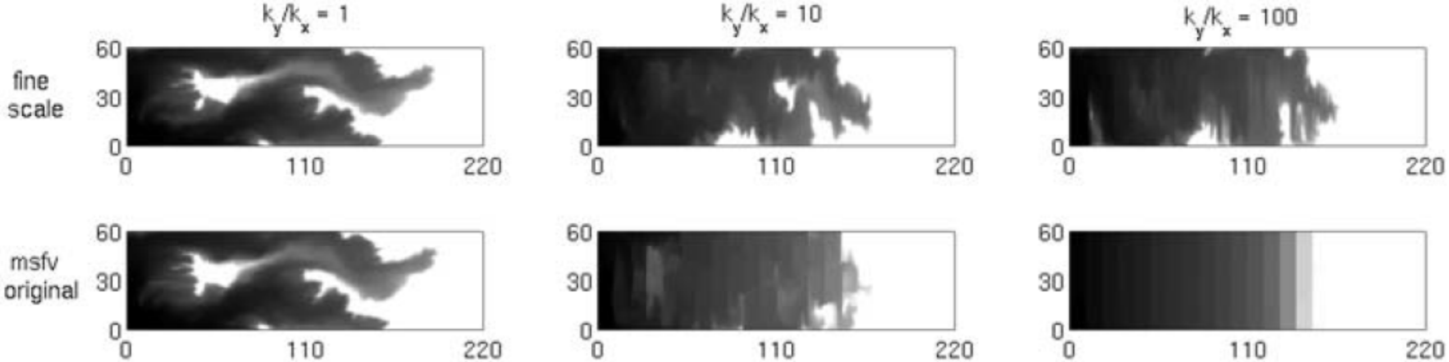

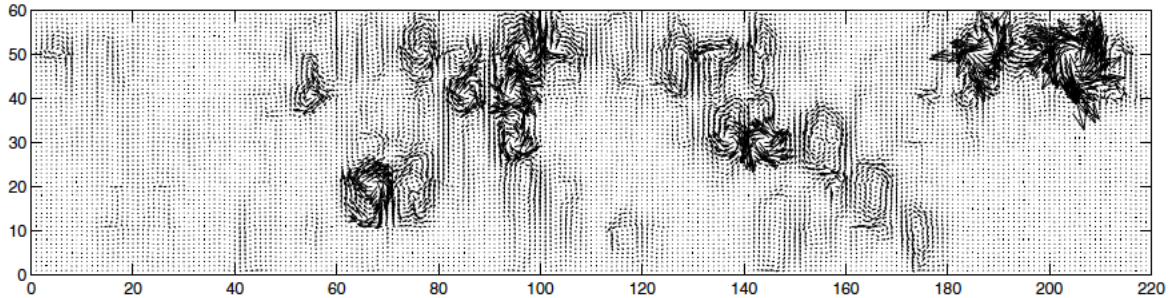

FIG. 5. *Vector plot of the conservative velocity field* $\bar{\mathbf{u}}$ *computed with the original MSFV method for the TOP field at* PVI $= 0.5$.

(**Lunati and Jenny, MMS, 2007**; see also: Kippe et al., Comp. Geosci., 2008)

Localization and reduced problem

$$\nabla \cdot [(\boldsymbol{\eta}\boldsymbol{\eta}^T)\boldsymbol{v}] = [(\boldsymbol{\eta}\boldsymbol{\eta}^T)\nabla] \cdot \boldsymbol{v} = \nabla_\perp \cdot \boldsymbol{v} = 0$$

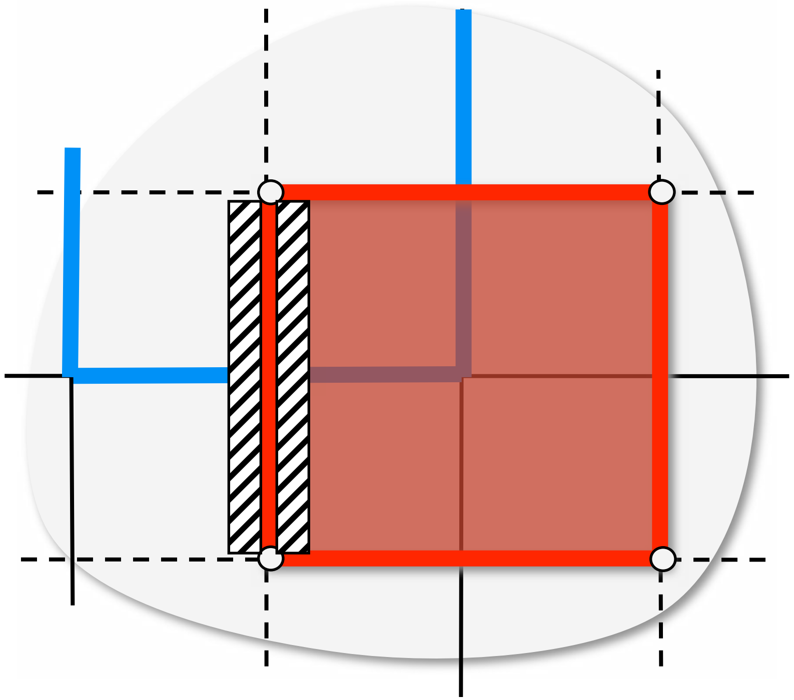

- Reduced problem
  - neglects transversal fluxes
  - reduced dimensionality

Estimate of transverse fluxes

$$\nabla \cdot [(\boldsymbol{\eta}\boldsymbol{\eta}^T)\boldsymbol{v}] = [(\boldsymbol{\eta}\boldsymbol{\eta}^T)\nabla] \cdot \boldsymbol{v} = \boxed{\nabla_\perp \cdot \boldsymbol{v} \approx -\nabla_\perp \cdot \mathbf{K}\nabla p^\star \neq 0}$$

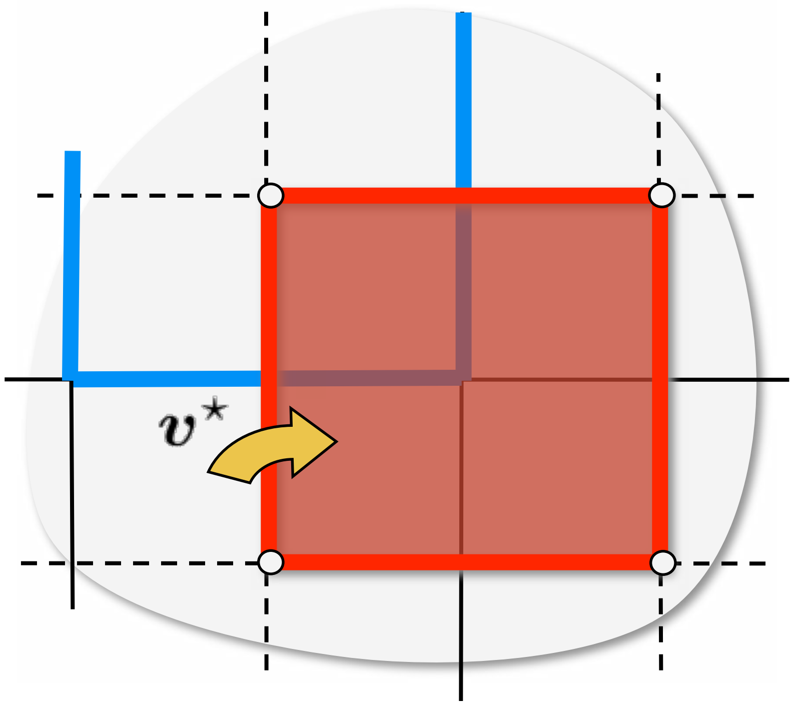

- Two natural candidates
  - approximate pressure (computed on duals)
  - approximate fluxes (computed on coarse cells

Domain decomposition Approach

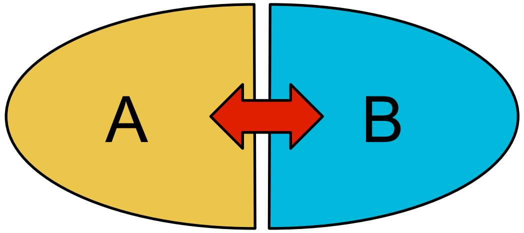

$$\left[\begin{array}{c|c} A\to A & B\to A \\ \hline A\to B & B\to B \end{array}\right]\begin{bmatrix} A \\ B \end{bmatrix} = \begin{bmatrix} q_A \\ q_B \end{bmatrix}$$

Original problem
(mutual interaction)

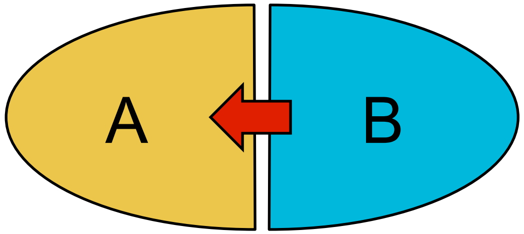

$$\left[\begin{array}{c|c} A\to A & B\to A \\ \hline A\to B & B\to B \end{array}\right]\begin{bmatrix} A \\ B \end{bmatrix} = \begin{bmatrix} q_A \\ q_B + \dots \end{bmatrix}$$

Multiplicative Schwarz
(Gauss-Seidel-like)

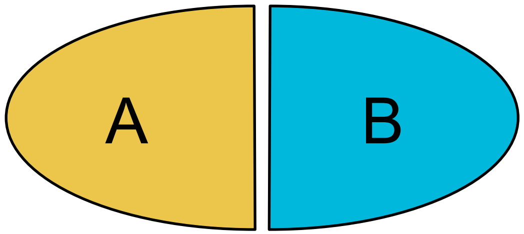

$$\left[\begin{array}{c|c} A\to A & B\to A \\ \hline A\to B & B\to B \end{array}\right]\begin{bmatrix} A \\ B \end{bmatrix} = \begin{bmatrix} q_A + \dots \\ q_B + \dots \end{bmatrix}$$

Additive Schwarz
(Jacobi-like)

Remark: domain decomposition methods are iterative linear solvers

Additive Schwarz on a coarse grid

$Au = r$

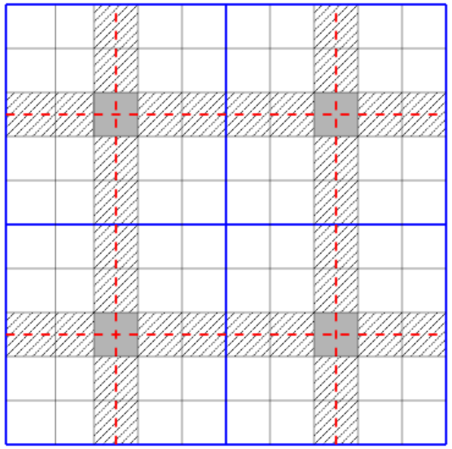

A

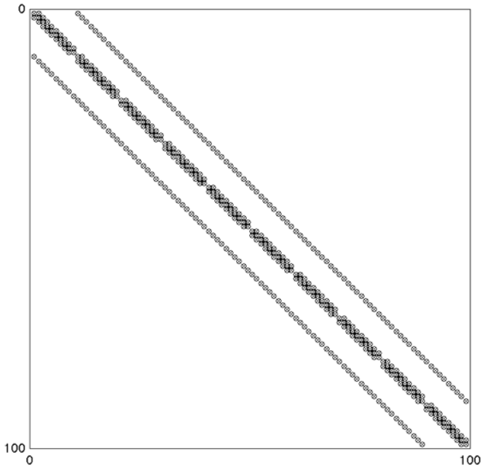

$\bar{A} = \bar{P} A \bar{P}^T$

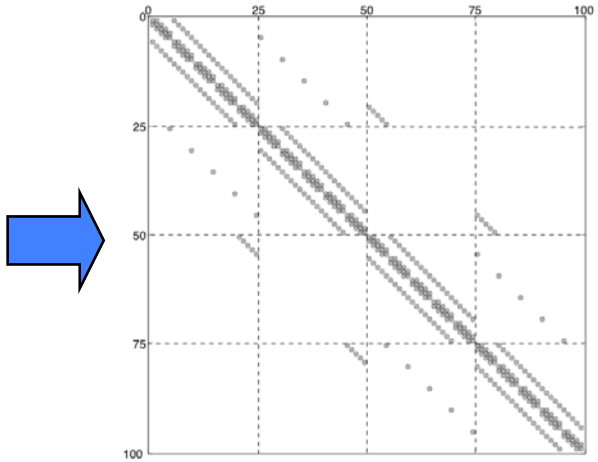

Coarse grid natural reordering

D

Additive Schwarz

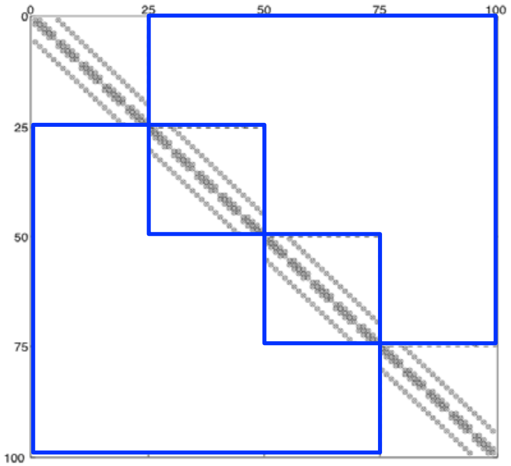

$$\bar{A}\bar{u} = D\bar{u} + (\bar{A} - D)\bar{u} = \bar{r}$$

$$\bar{u}^{\nu+1} = \bar{u}^{\nu} + D^{-1}(\bar{r} - \bar{A}\bar{u}^{\nu})$$

$$\bar{u} \leftarrow \bar{u} + D^{-1}(\bar{r} - \bar{A}\bar{u})$$

Natural reordering based on dual coarse grid

$$Ap = r \qquad A \qquad \tilde{A} = \tilde{P} A \tilde{P}^T$$

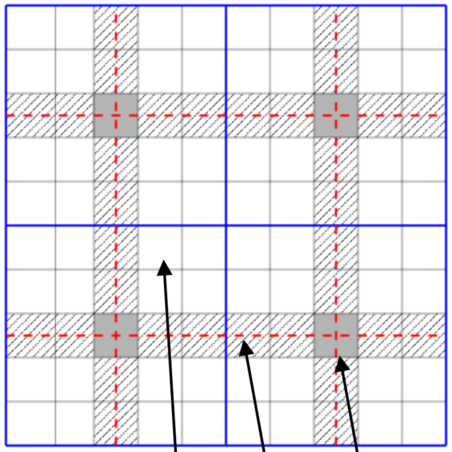

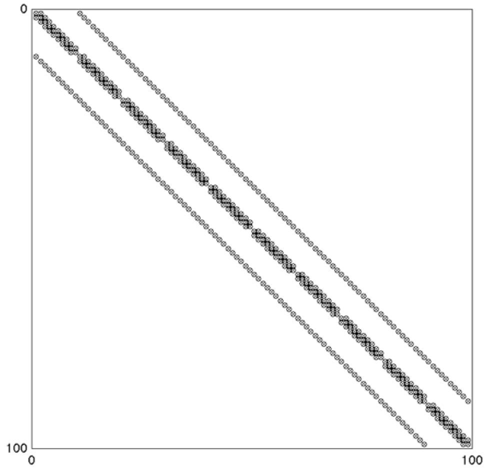

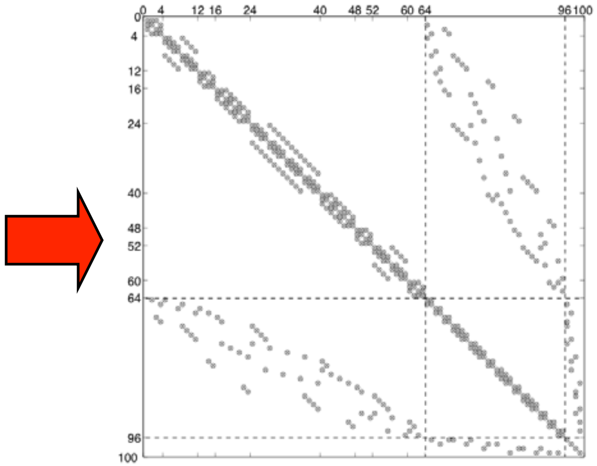

$$\mathcal{I}_f = \mathcal{I}_i \cup \mathcal{I}_e \cup \mathcal{I}_n$$

$$\begin{bmatrix} A_{ii} & A_{ie} & 0 \\ A_{ei} & A_{ee} & A_{en} \\ 0 & A_{ne} & A_{nn} \end{bmatrix} \begin{bmatrix} p_i \\ p_e \\ p_n \end{bmatrix} = \begin{bmatrix} r_i \\ r_e \\ r_n \end{bmatrix}$$

(From here on tildes and bars will be skipped to simplify notation and permutation operators will not be written explicitly; the appropriate reordering must be applied)

The MsFV operator

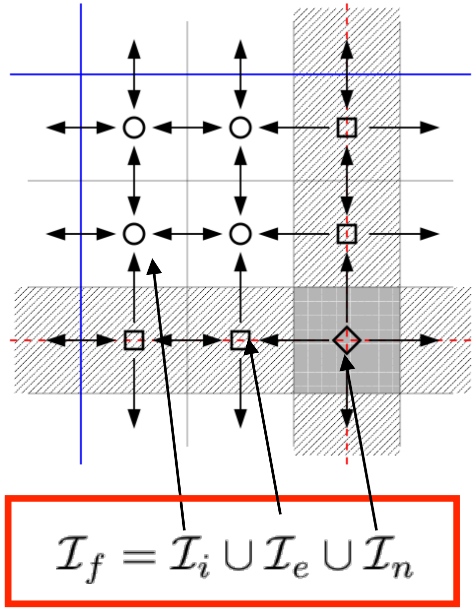

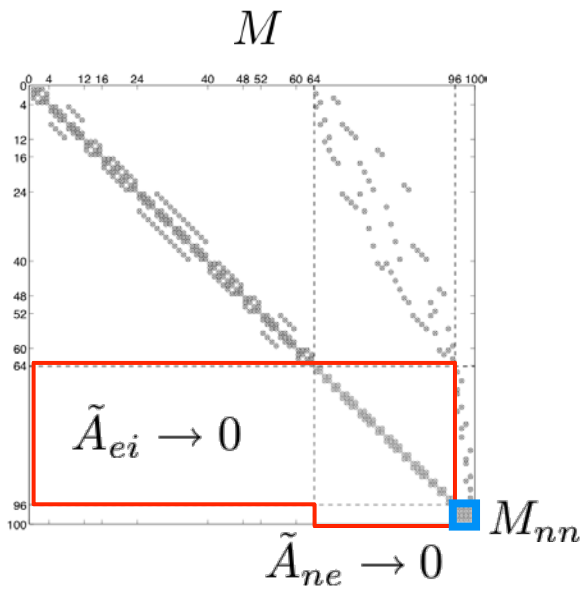

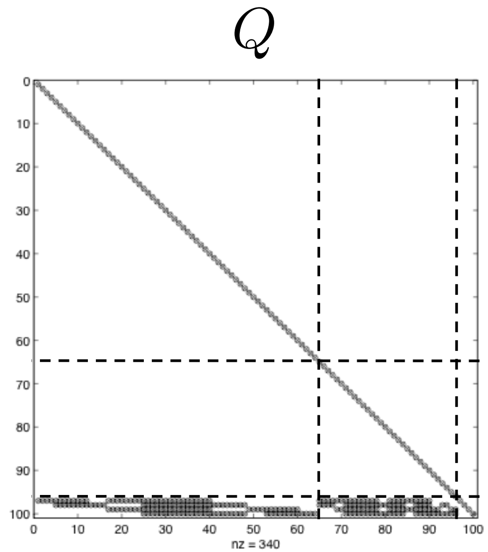

$$Mp = \begin{bmatrix} A_{ii} & A_{ie} & 0 \\ 0 & M_{ee} & A_{en} \\ 0 & 0 & M_{nn} \end{bmatrix} \begin{bmatrix} p_i \\ p_e \\ p_n \end{bmatrix} = \begin{bmatrix} r_i \\ r_e \\ q_n \end{bmatrix} = Qr$$

$$\nabla \cdot [(\boldsymbol{\eta}\boldsymbol{\eta}^T)\boldsymbol{v}] = [(\boldsymbol{\eta}\boldsymbol{\eta}^T)\nabla] \cdot \boldsymbol{v} = \nabla_\perp \cdot \boldsymbol{v} = 0$$

(Lunati et al., CMWR, 2008; Lunati and Lee, MMS, 2009)

The MsFV pressure

$$B = \begin{bmatrix} A_{ii}^{-1} A_{ie} M_{ee}^{-1} A_{en} \\ -M_{ee}^{-1} A_{en} \\ I_{nn} \end{bmatrix}$$

Basis function operator

$$C = \begin{bmatrix} A_{ii}^{-1} & -A_{ii}^{-1} A_{ie} M_{ee}^{-1} & 0 \\ 0 & M_{ee}^{-1} & 0 \\ 0 & 0 & 0 \end{bmatrix}$$

Correction function operator

$$M_{ee} = A_{ee} + \mathrm{diag}\left(\Sigma_i A_{ie}^T\right)$$

Reduce problem operator

$$M_{nn} = \chi A B$$

Coarse-scale operator
(χ is the summation operator)

$$M^{-1} = B M_{nn}^{-1} R + C$$

Inverse of the MsFV operator
($R = [0 \ 0 \ I_{nn}]$ is the restriction operator)

$$Q = I - R^T R + R^T \chi - R^T \chi A C$$

Right-hand-side operator

$$p = M^{-1} Q r$$

MsFV pressure solution

$$M^{-1} Q = B M_{nn}^{-1} (\chi - \chi A C) + C$$

(Identical to the Schur complement with tangential approximation, Nordbotten and Bjørstad, Comp. Geosci., 2008; Lunati and Lee, MMS, 2009)

The MsFV operator

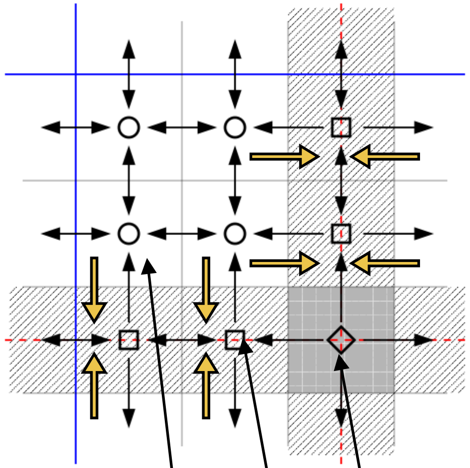

$$\mathcal{I}_f = \mathcal{I}_i \cup \mathcal{I}_e \cup \mathcal{I}_n$$

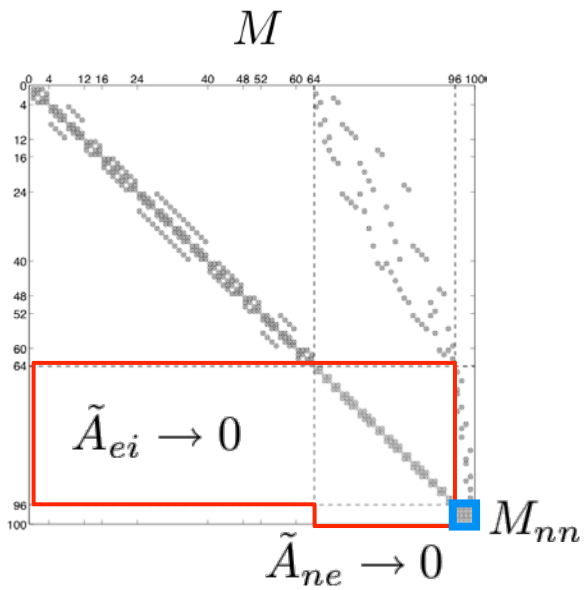

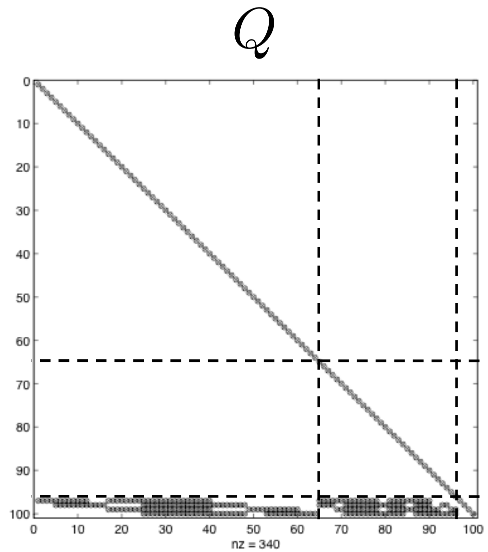

$$Mp = \begin{bmatrix} A_{ii} & A_{ie} & 0 \\ 0 & M_{ee} & A_{en} \\ 0 & 0 & M_{nn} \end{bmatrix} \begin{bmatrix} p_i \\ p_e \\ p_n \end{bmatrix} = \begin{bmatrix} r_i \\ r_e \\ q_n \end{bmatrix} = Qr$$

$$\nabla \cdot [(\boldsymbol{\eta}\boldsymbol{\eta}^T)\boldsymbol{v}] = [(\boldsymbol{\eta}\boldsymbol{\eta}^T)\nabla] \cdot \boldsymbol{v} = \nabla_\perp \cdot \boldsymbol{v} \approx -\nabla_\perp \cdot \mathbf{K}\nabla p^\star \neq 0$$

(Lunati et al., CMWR, 2008; JCP, 2011)

Iterative MsFV method

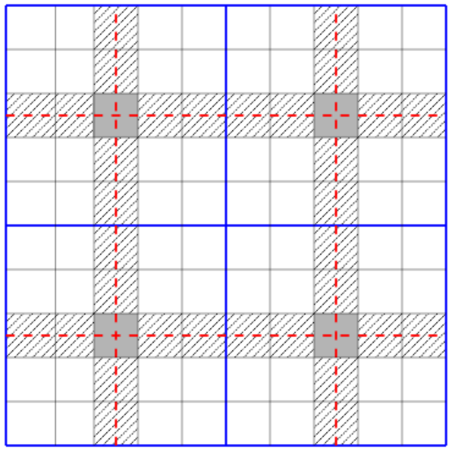

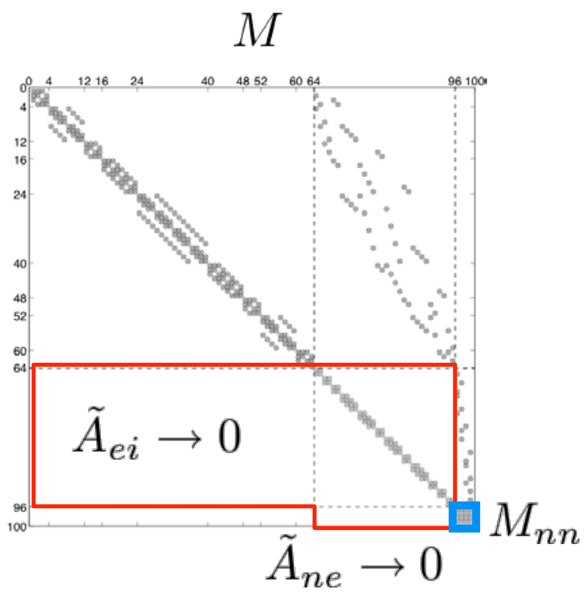

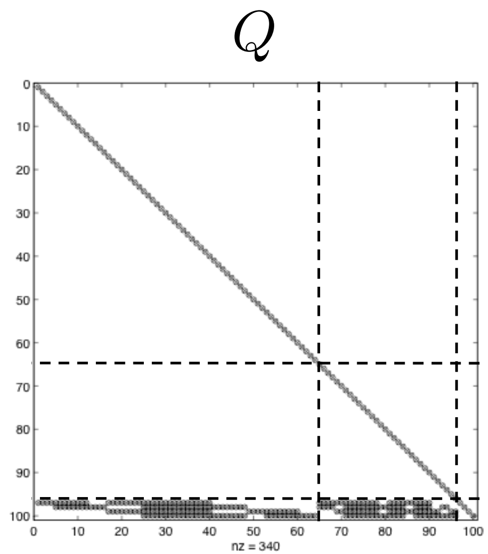

$$p \leftarrow p + M^{-1}Q(r - Ap)$$

Conditionally stable!

$$p \leftarrow M^{-1}Qr + M^{-1}Q\{r - A[p \leftarrow p + S(r - Ap)]\}$$

I-MsFV with smoothers, e.g.
line relaxation Hajibeigi et al., JCP, 2008;
S=D…

$$p \leftarrow p + \omega M^{-1}Q(r - Ap)$$

I-MsFV with Krylov subspace method;
Lunati et al., CMWR, 2008; JCP 2011

Krylov subspace projection methods

$$\boxed{u^{\nu+1} = u^{\nu} + \omega^{\nu} G^{-1} \epsilon^{\nu}}$$

$$\epsilon^{\nu} = (r - Au^{\nu})$$

$G^{-1}\epsilon^{\nu+1} \perp \mathcal{L}$

new residual
(prec.)

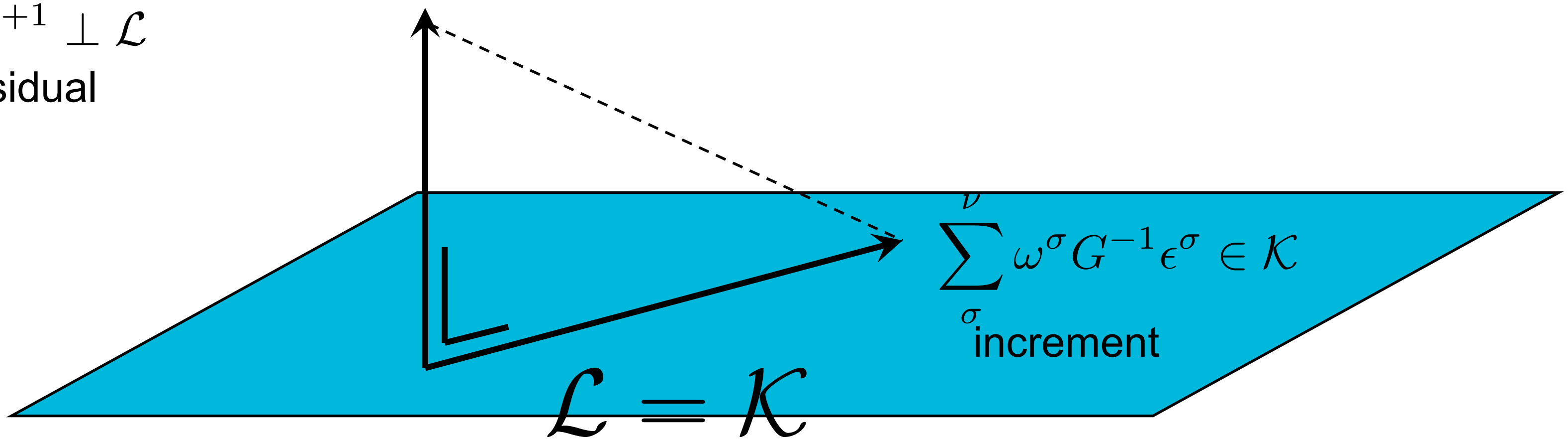

$$\mathcal{K}_{\nu}(G^{-1}\epsilon^{0}, G^{-1}A) = \mathrm{span}\{G^{-1}\epsilon^{0}, (G^{-1}A)G^{-1}\epsilon^{0}, ..., (G^{-1}A)^{\nu-1}G^{-1}\epsilon^{0}\}$$

Steepest Descent $\quad \mathcal{K} = \mathrm{span}\{G^{-1}\epsilon^{0}\} \quad \mathcal{L} = \mathcal{K}$ information from 1 residual

Krylov subspace projection methods

$$u^{\nu+1} = u^{\nu} + \omega^{\nu} G^{-1} \epsilon^{\nu}$$

$$\epsilon^{\nu} = (r - A u^{\nu})$$

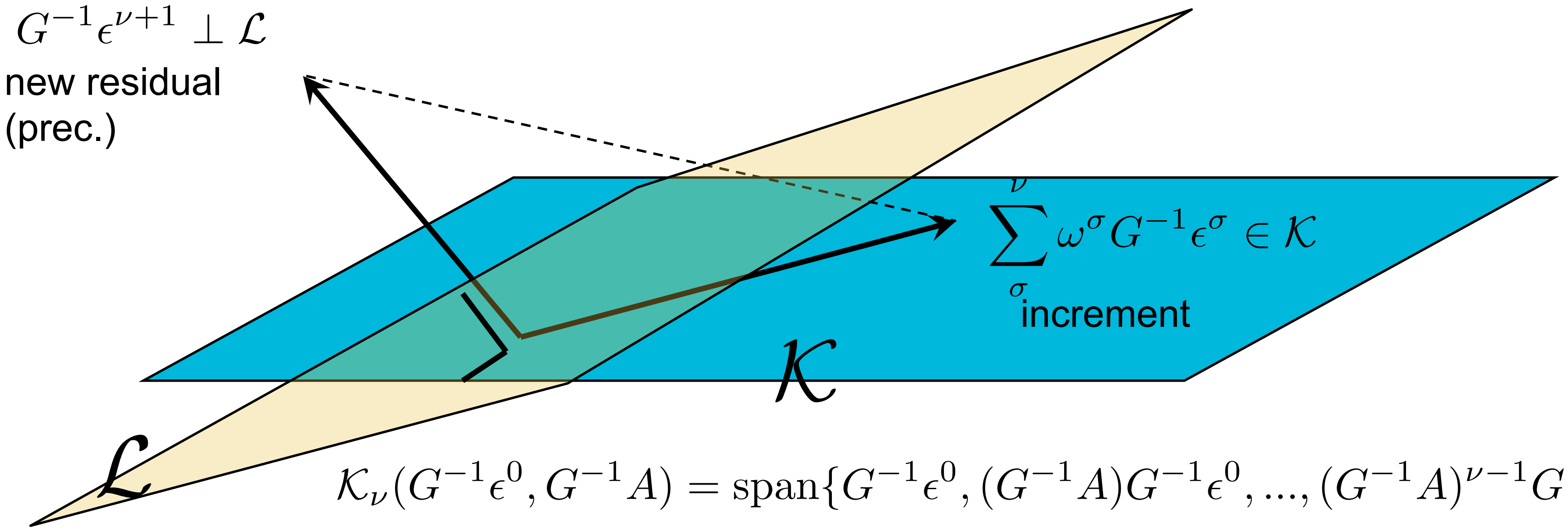

$$\mathcal{K}_{\nu}(G^{-1}\epsilon^0, G^{-1}A) = \mathrm{span}\{G^{-1}\epsilon^0, (G^{-1}A)G^{-1}\epsilon^0, ..., (G^{-1}A)^{\nu-1}G^{-1}\epsilon^0\}$$

Steepest Descent $\mathcal{K} = \mathrm{span}\{G^{-1}\epsilon^0\}$ $\mathcal{L} = \mathcal{K}$ information from 1 residual

GMRES(ν) $\mathcal{K} = \mathcal{K}_{\nu}(G^{-1}\epsilon^0, G^{-1}A)$ $\mathcal{L} = A\mathcal{K}$ information from m residuals

$\min_{\{\omega^{\sigma}\}_{\sigma=1,2,\dots,\nu}} ||G^{-1}\epsilon^{\nu+1}||_2$ ω minimize the L2 norm of the preconditioned residual

Overlapping Domain iterations (2 steps prec.)

$$p \leftarrow p + \omega M^{-1} Q D^{-1} (r - Ap)$$

1st step

preconditioner based on primary coarse grid

Additive Schwarz

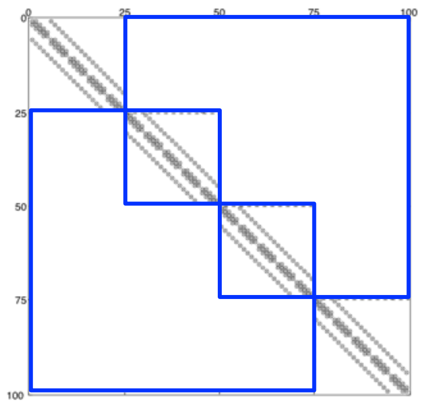

or

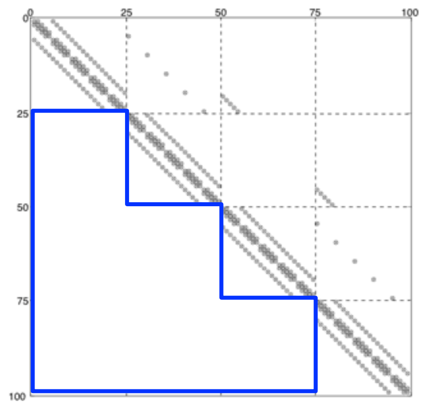

Multiplicative Schwarz

2nd step

preconditioner based on dual coarse grid

M

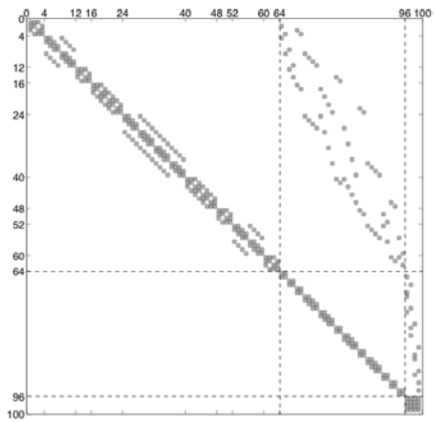

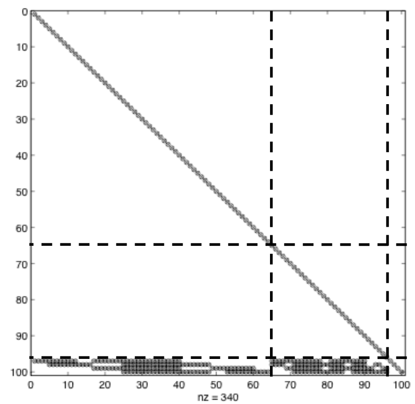

Q

(Lunati, Tyagi, and Lee, CMWR, 2008, JCP 2011)

Conservative velocity and transport

$$p \leftarrow p + \omega M^{-1} Q(r - Ap)$$

Pressure solution

$$D\psi = r - (A - D)p$$

$$v = \begin{cases} \mathcal{D}\psi & \text{in} \quad \Omega_i \\ \mathcal{D}p & \text{on} \quad \partial\Omega_i \end{cases}$$

Conservative velocity

$$A_T S = r_T$$

Transport problem
(A_T depends on v –advective
Part- and on the diffusive part)

$$S \leftarrow S + D_T^{-1}(r_T - A_T S)$$

Schwarz iterations

Anisotropy

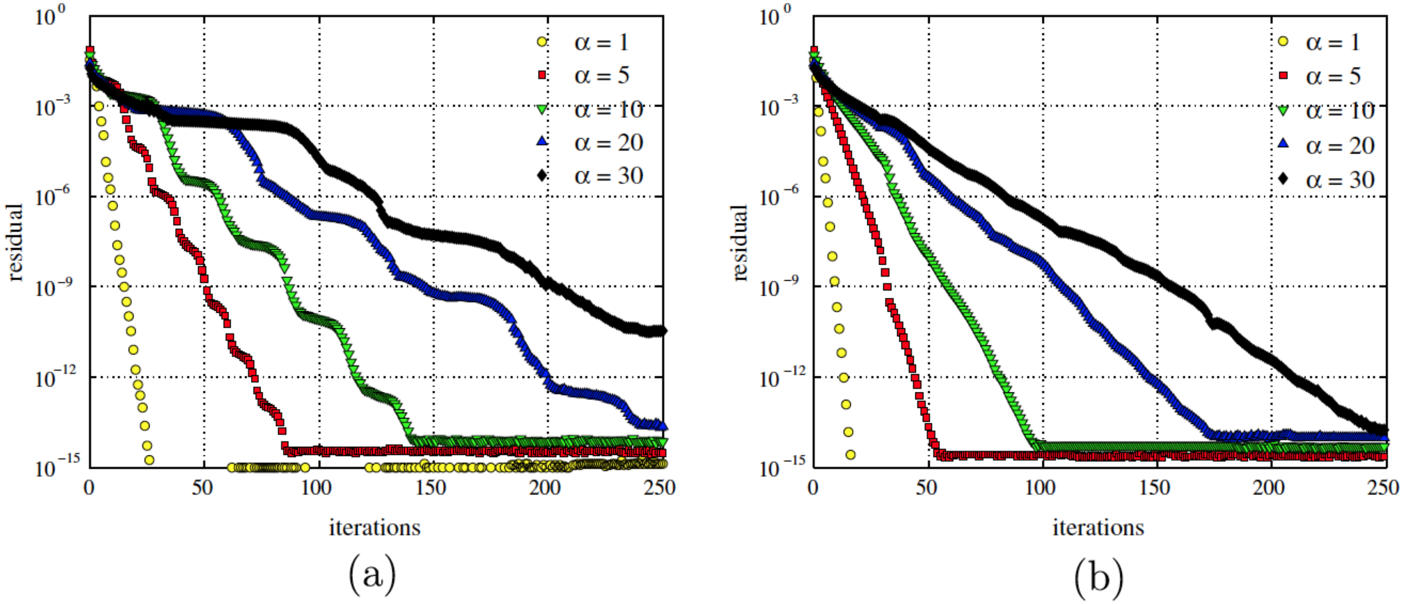

Fig. 7. Convergence history for varying grid aspect ratio $\alpha = \Delta x/\Delta y$ in a homogeneous permeability field. The simulations are performed on a 100 × 100 fine grid with a 20 × 20 coarse grid for the QFS flow configuration employing: (a) MsFV-GMRES; (b) MsFV-OD with DMS.

(Lunati, Tyagi, and Lee, CMWR, 2008, JCP 2011)

Impermeable shale layers: convergence history

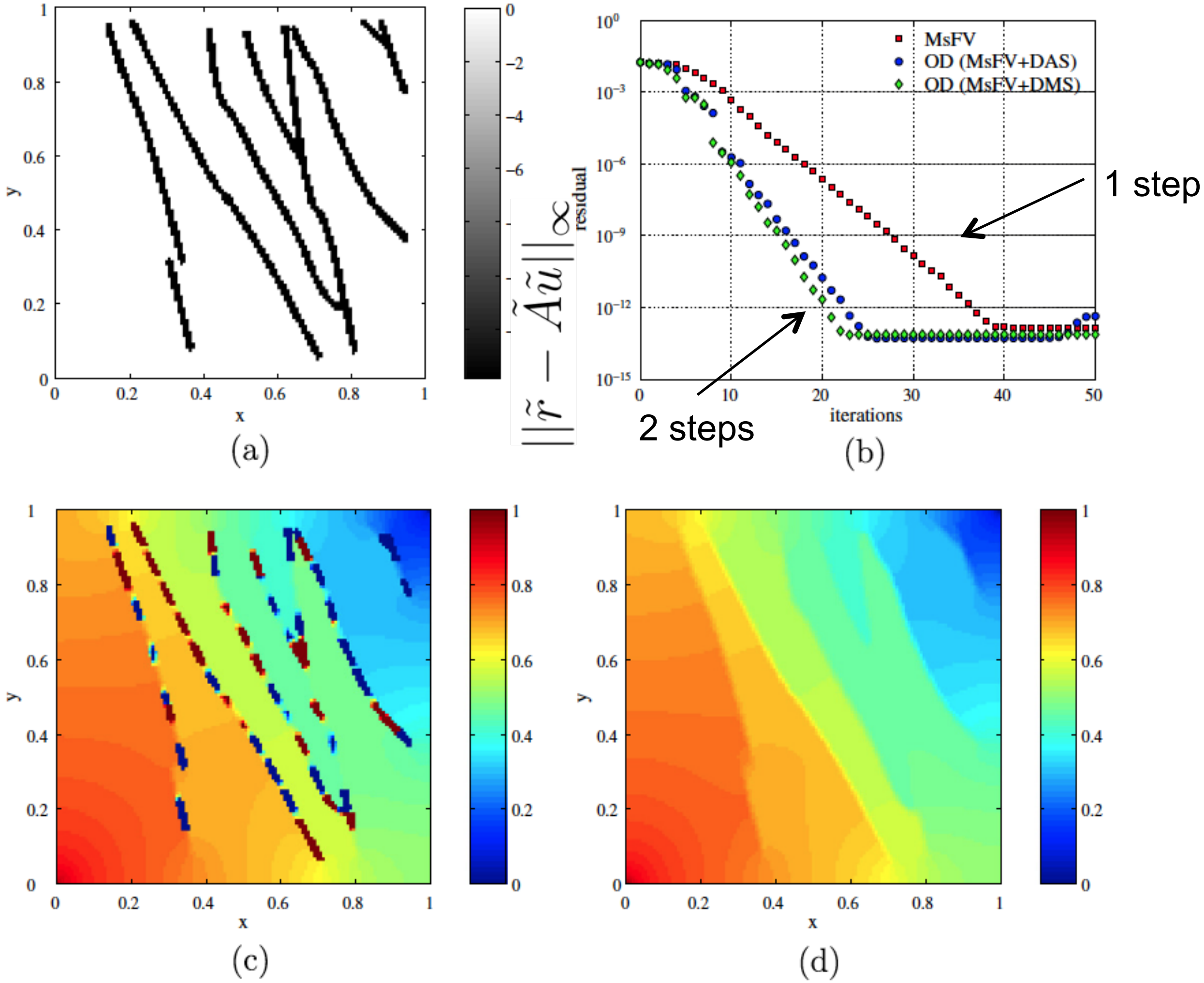

Fig. 9. (a) The natural logarithm of heterogeneous field consisting of multiple shale layers embedded in a 10^6-times more transmissive matrix (SHALE-field). The field is represented on a 125×125 grid and MsFV simulations employ a 25×25 coarse grid. (b) Convergence history of MsFV and MsFV-OD iterations for a quarter five spot (QFS) configuration (wells are at the top-left and bottom-right corners). (c) Approximate pressure solutions obtained with the original MsFV method. (d) Converged pressure solution.

(Lunati, Tyagi, Lee., SIAM Denver, 2009; JCP 2011)

SPE 10 bottom layer: pressure

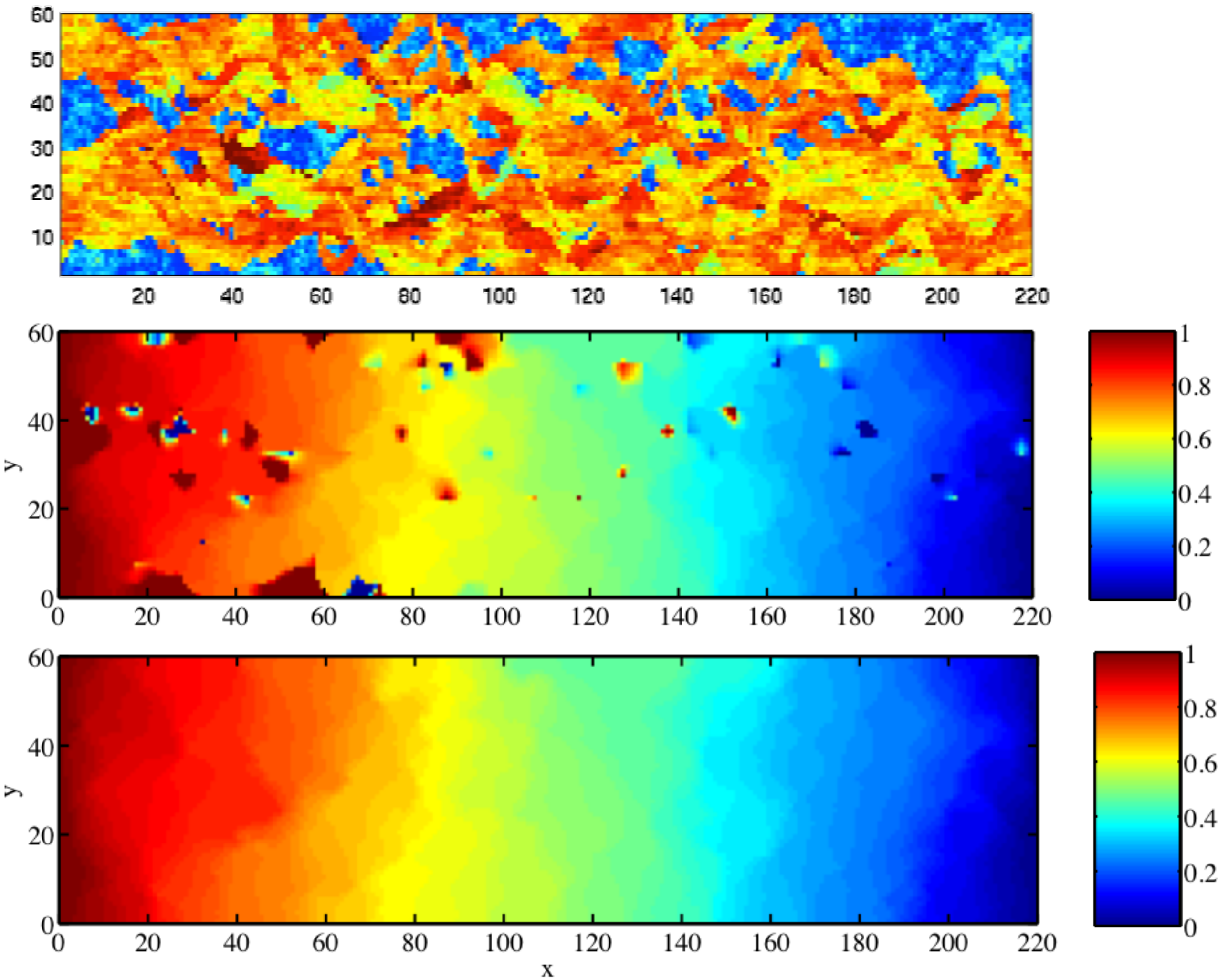

(Lunati, Tyagi, Lee., SIAM Denver, 2009; JCP 2011)

SPE 10 bottom layer: convergence history

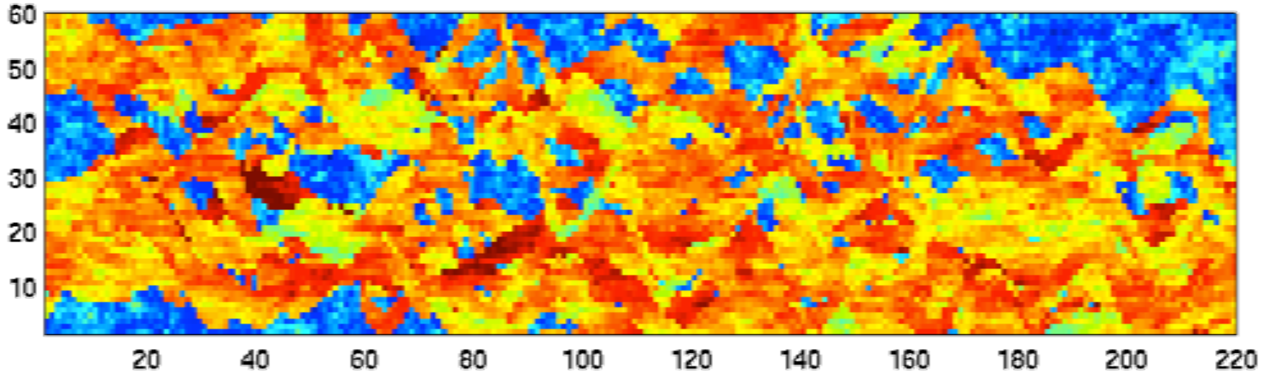

$$||\tilde{r} - \tilde{A}\tilde{u}||_{\infty}$$

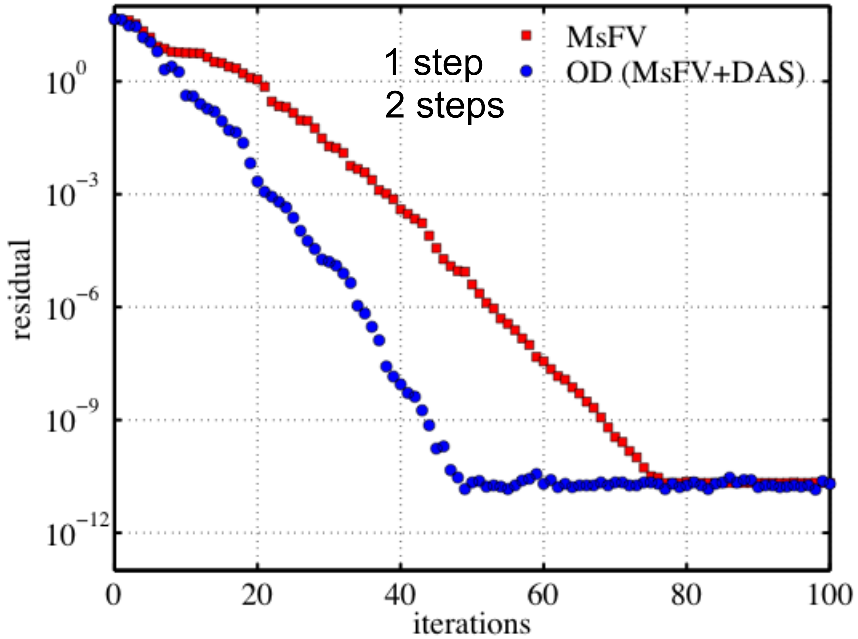

(Lunati, Tyagi, Lee., SIAM Denver, 2009; JCP 2011)

Effects of restart – SPE10 bottom layer

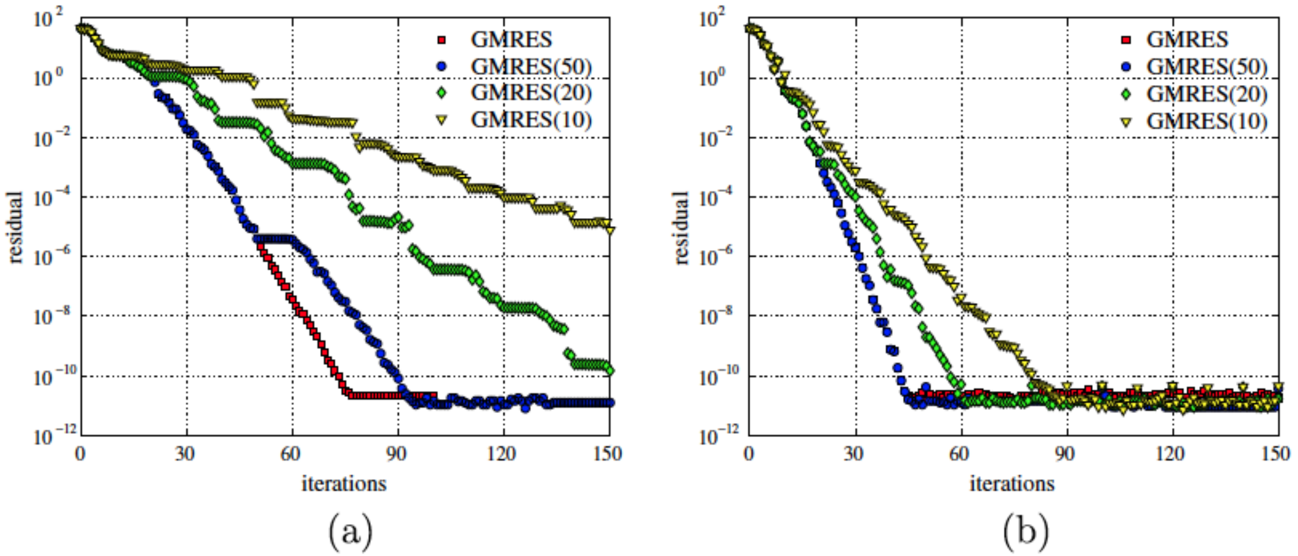

Fig. 12. Effects of restart for the SPE10 bottom layer test case with a 44 × 12 coarse grid and upscaling factor 5 × 5 (Fig. 10(a)): (a) MsFV-GMRES; (b) MsFV-OD with DMS.

(Lunati, Tyagi, Lee., SIAM Denver, 2009; JCP 2011)

Compressible flow

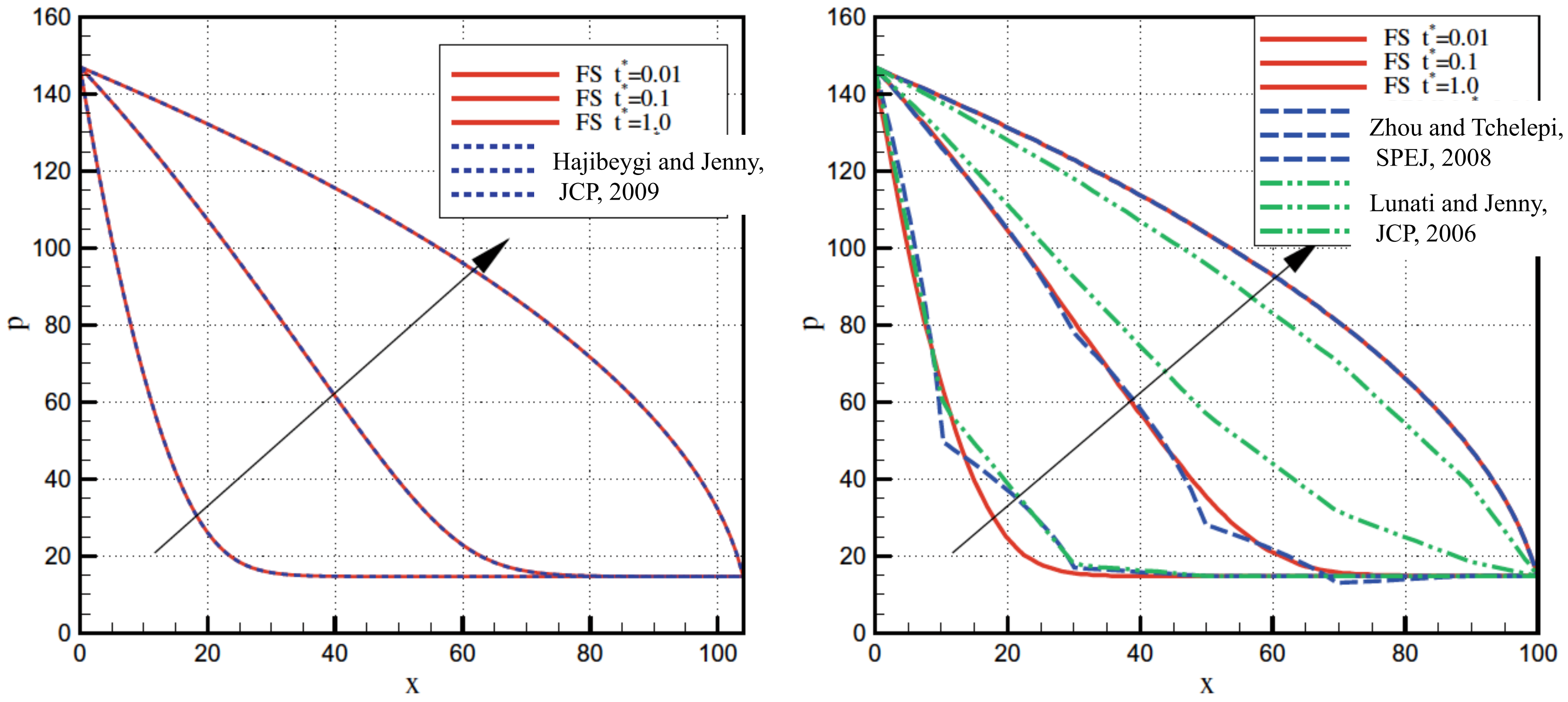

Fig. 4. 1D single-phase gas injection test case: pressure at three different times. Shown are the new MSFV and fine-scale reference solutions (left) using 105 fine and 5 coarse cells together with previous multiscale solutions presented in [25] (right) using 100 fine and 5 coarse cells. FSA based multiscale method was developed by Lunati and Jenny [24] and OBMM method was developed by Zhou and Tchelepi [25].

(**Hajibeygi and Jenny, JCP, 2009**; see also Lunati and Jenny, CMWR, 2006)

Magnetic Resonance Imaging of 3D Density Fingers

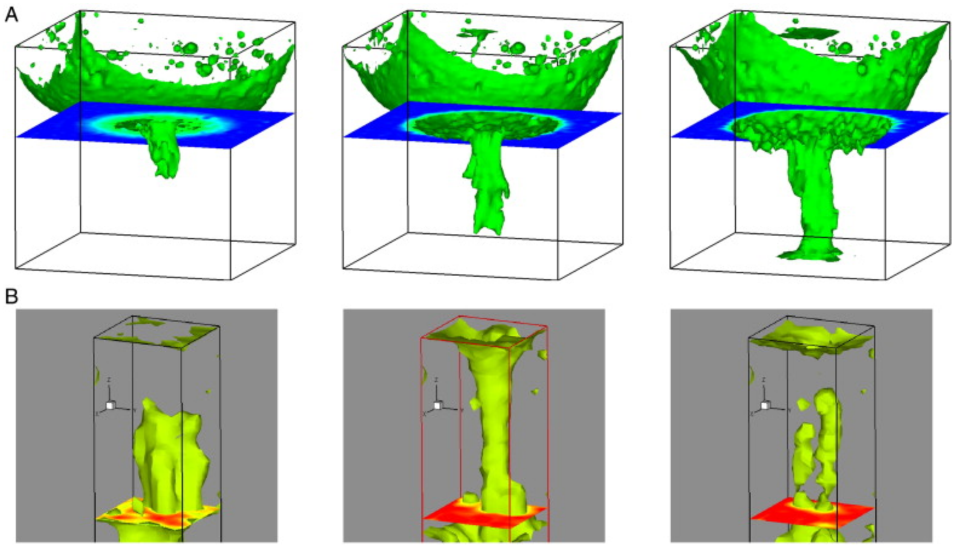

(Oswald, Spiegel, and Kinzelbach, M.R. Imag., 2007)

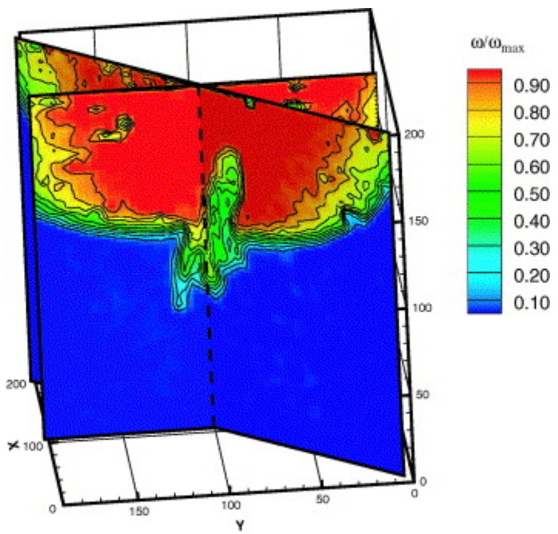

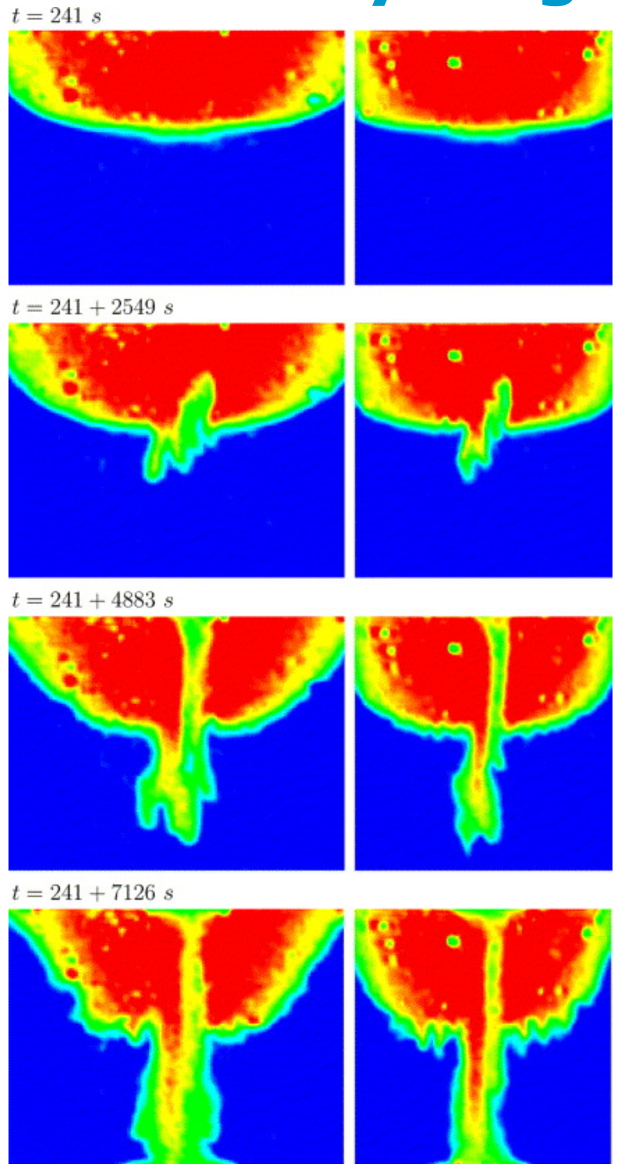

(Johannsen, Oswald, Held, Kinzelbach, Adv. Water. Res., 2006)

Density-driven fingers (single phase)

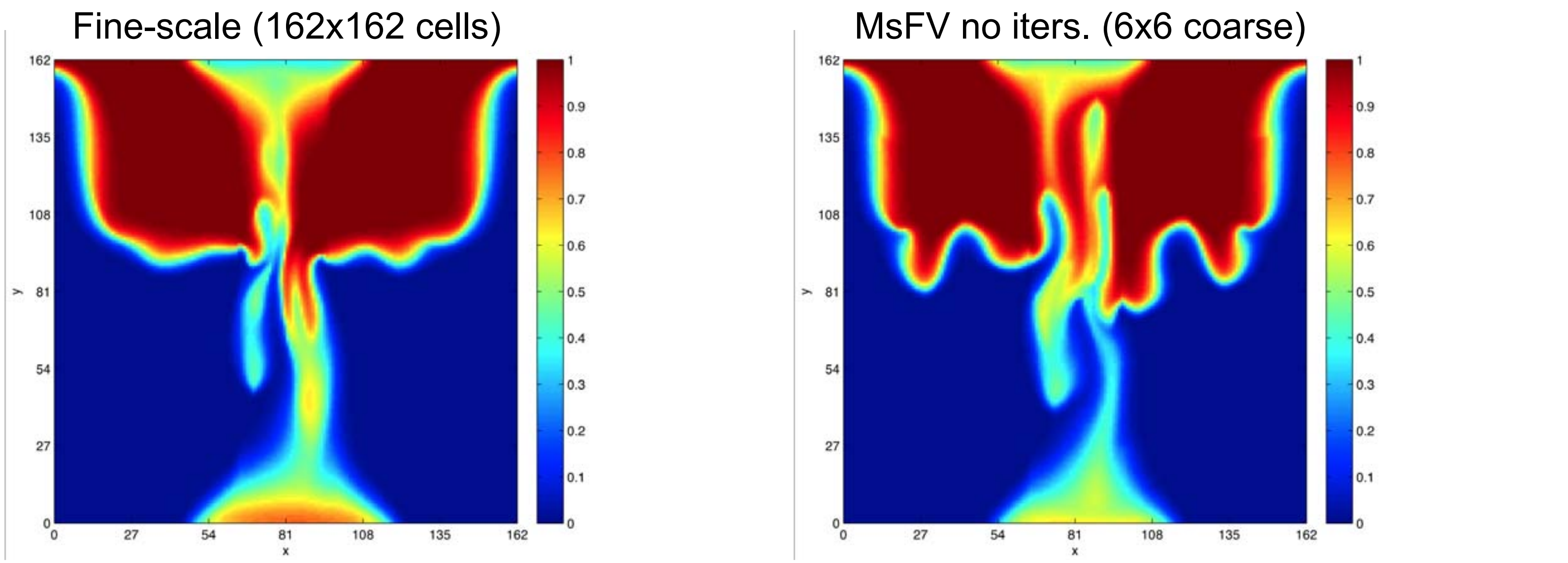

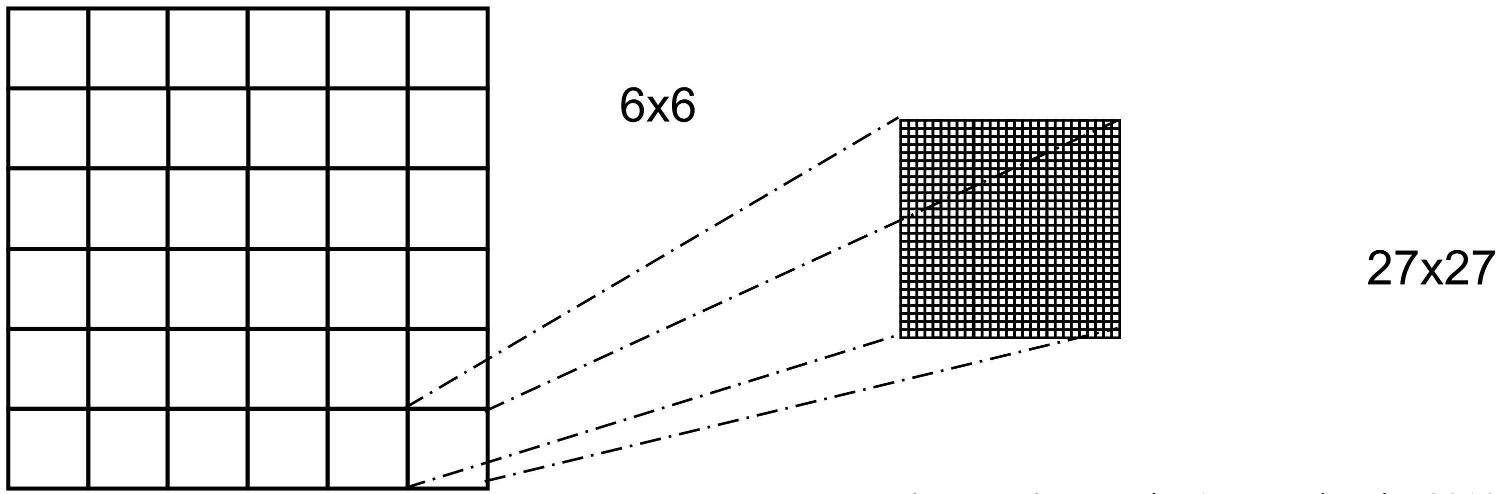

(Künze & Lunati, IAHR Valencia, 2010)

Density-driven fingers (single phase – 2D)

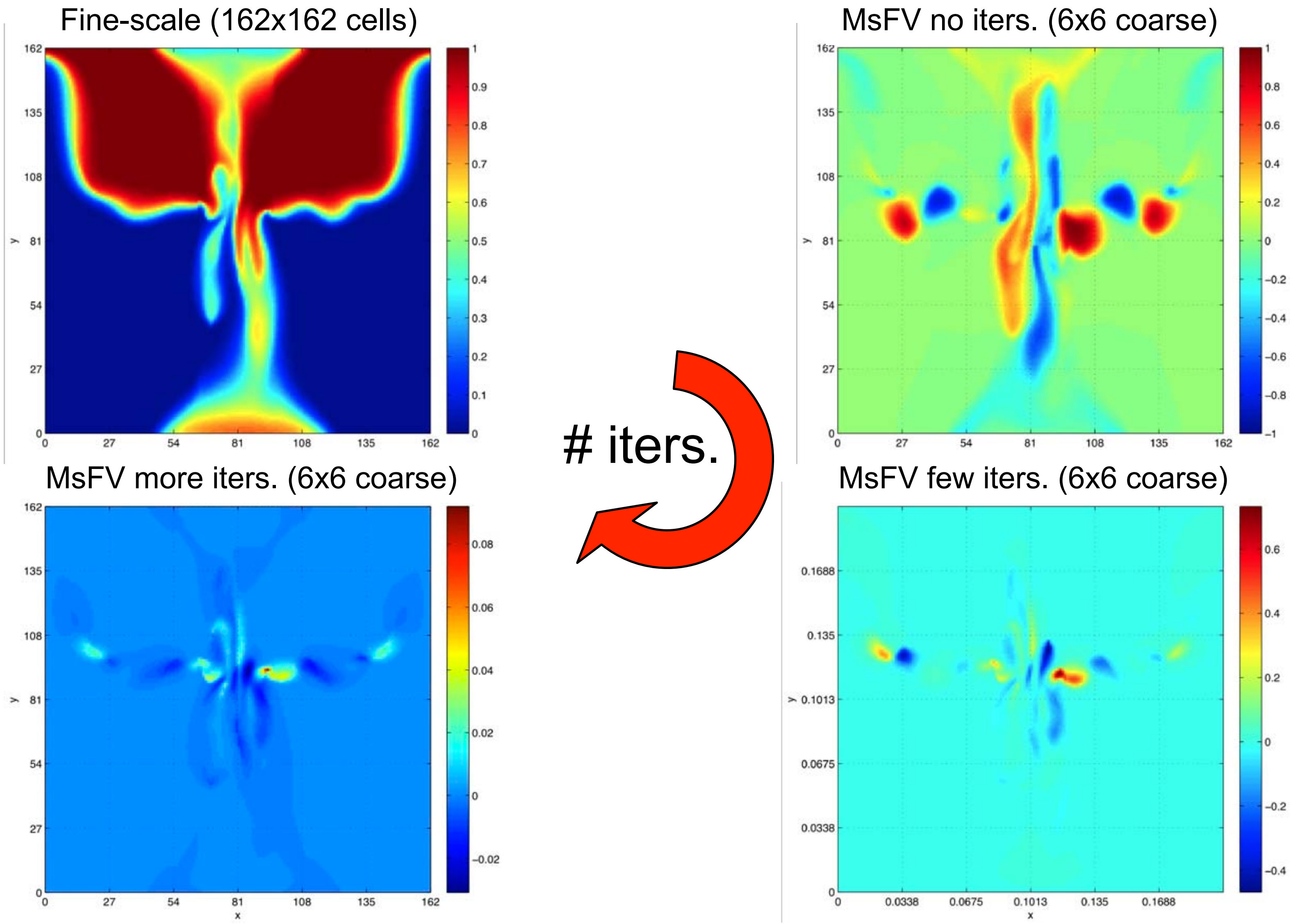

(Künze & Lunati, IAHR Valencia, 2010)

Multiscale simulation of gravity fingers

2D simulation

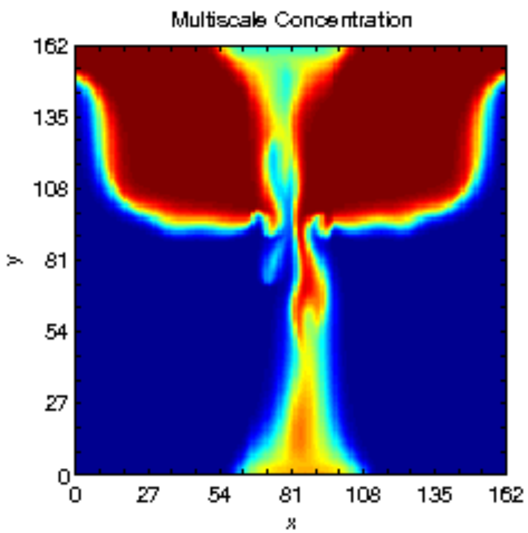

Künze and Lunati, *IAHR Valencia*, 2010

3D experiment

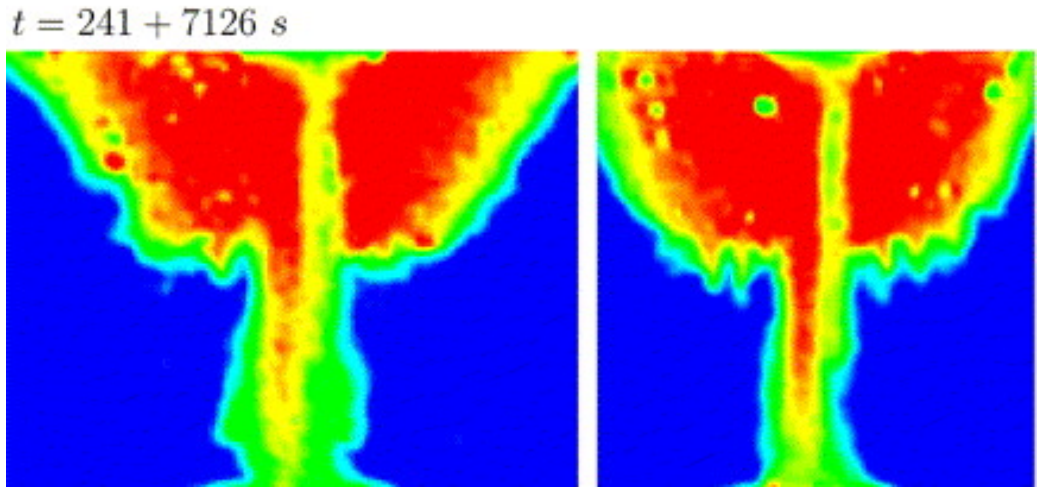

(Johannsen, Oswald, Held, Kinzelbach, Adv. Water. Res., 2006)

Adaptive iteration to improve localization

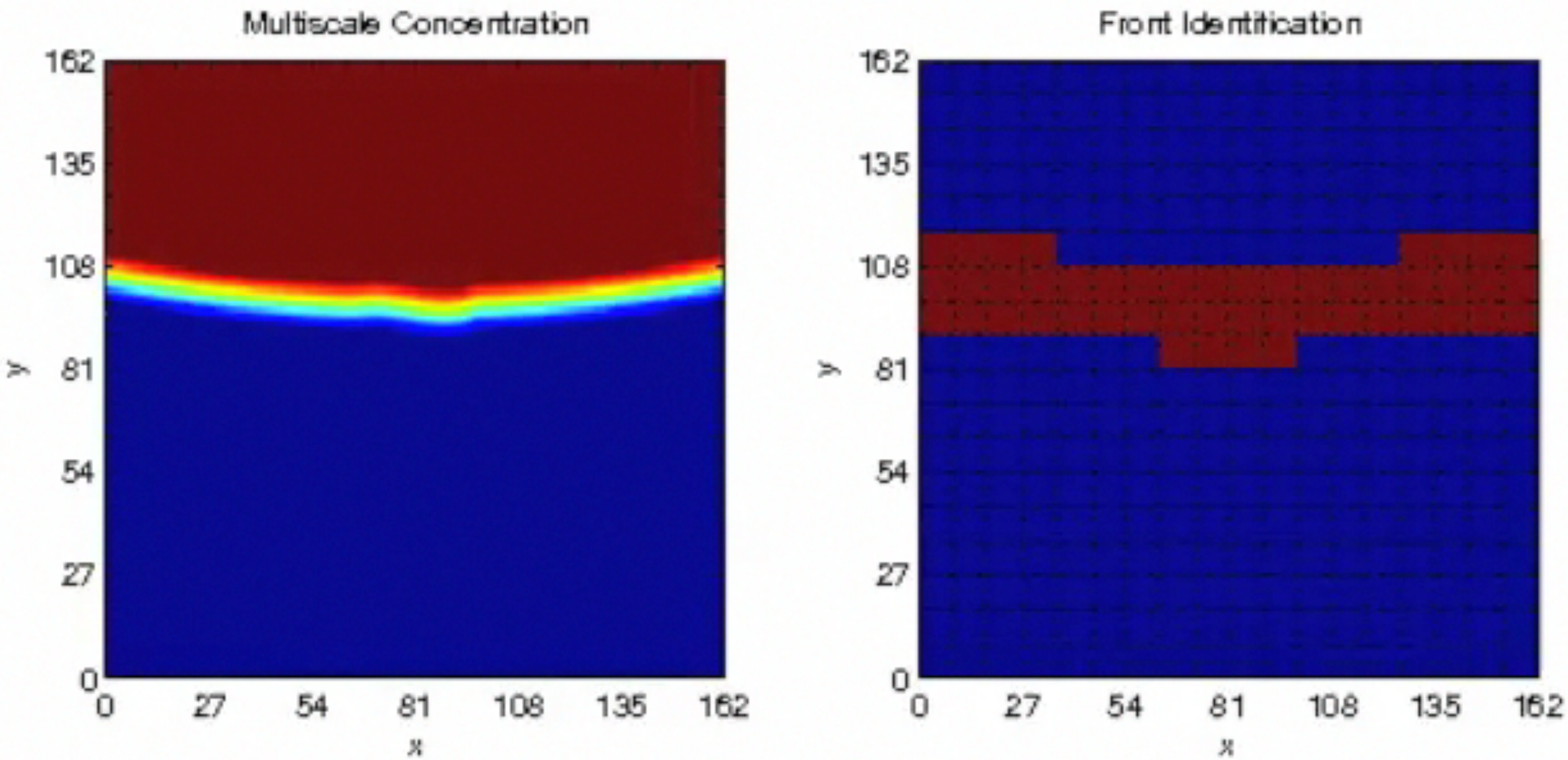

Not only numerical efficiency, but "*better than fine-scale*" simulation:
The MsFV method as a **grid refinement** (**downscaling**) technique, or
as a platform for hybrid models (Navier-Stokes/Darcy flow)

Künze and Lunati, *IAHR Valencia*, 2010; Künze and Lunati, preprint, [in preparation]

Complex behavior after CO_2 injection

Hydrodynamic trapping

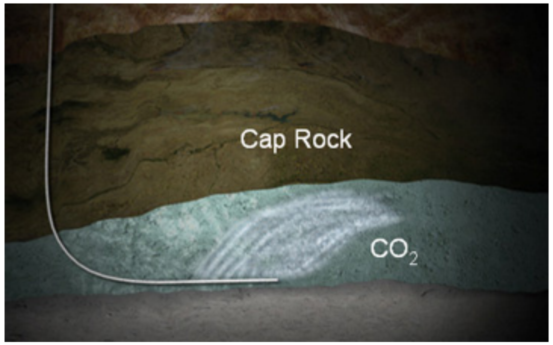

solution trapping (+ mineral trapping)

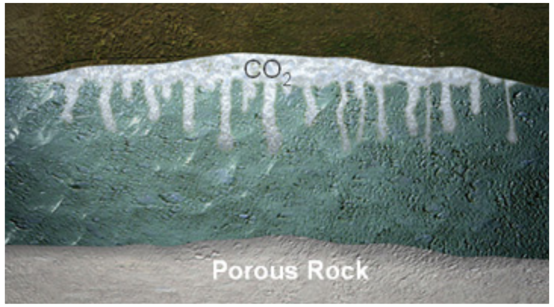

residual trapping (hysteresis)

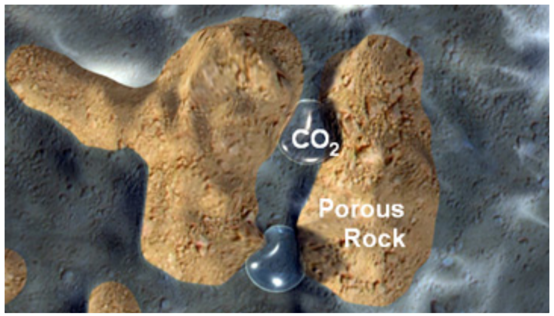

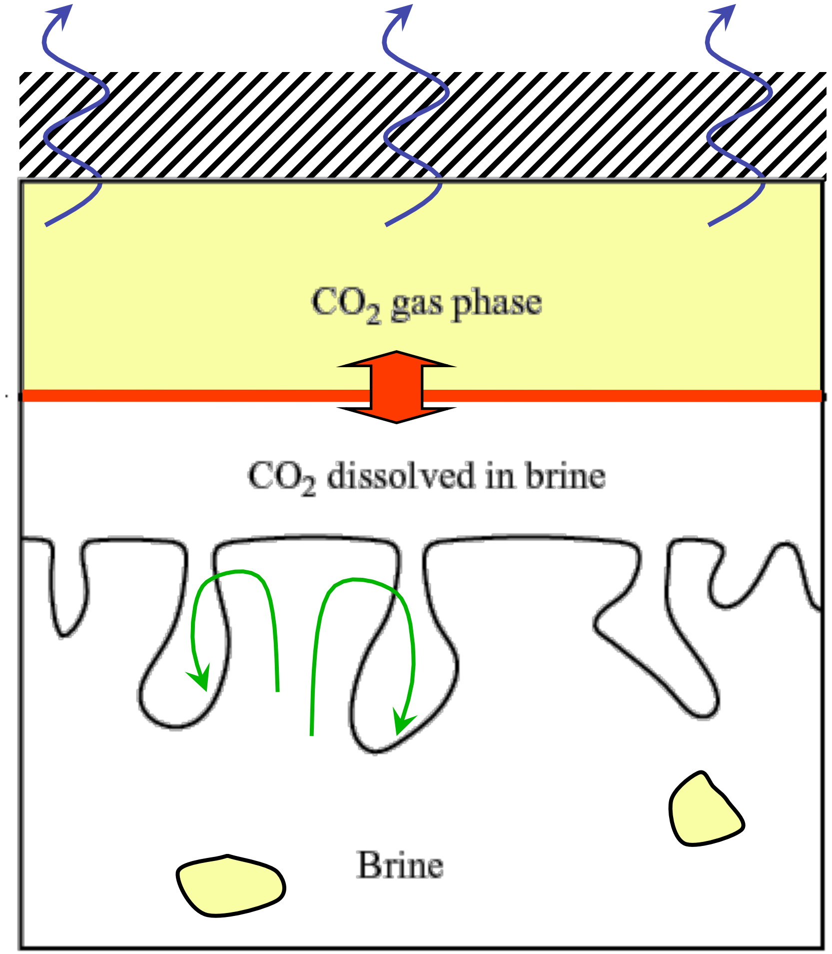

leaking

gas solution

water diffusion

density driven convection

(Photo: http://www.co2captureproject.org/ Sketch adapted from Riaz and Tchelepi)

CO_2 fingering in a Hele-Shaw cell

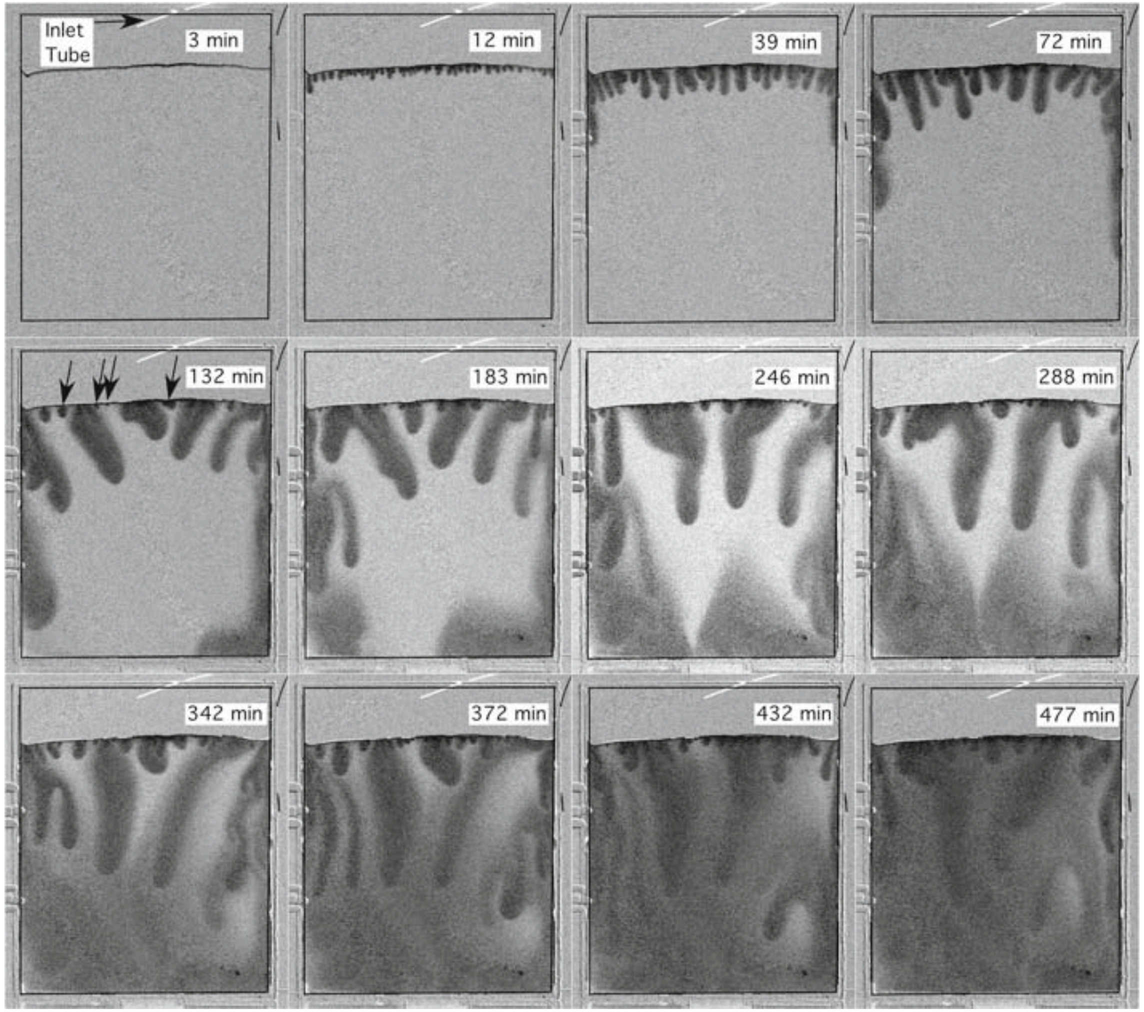

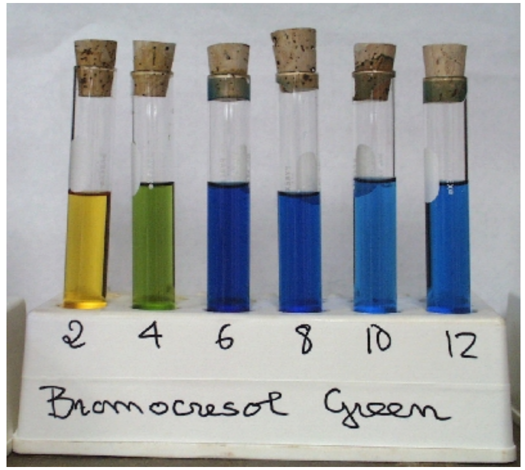

Fluid properties	
Temperature	$T = 22°C$
Pressure	$P = 1.013$ bar
Salinity	$X_s = 0$
Dissolved CO_2 concentration	$X = 0$
Viscosity	$\mu = 0.954766 \times 10^{-3}$ Pa-s
Water density	$\rho = 997.889$ kg/m^3
Dissolved CO_2 mass fraction at the top boundary	$X_0 = 1.53377 \times 10^{-3}$
Density increase of aqueous phase from CO_2 dissolution	$\Delta\rho = 0.287$ kg/m^3
Diffusivity	$D = 10^{-9}$ m^2/s
Formation properties	
Porosity	$\phi = 1.0$
Permeability	$k = 4.08 \times 10^{-8}$ m^2
Model domain	
Height	$H = 0.24$ m
width	$W = 0.24$ m

Kneafsey and Pruess, *Laboratory Flow Experiments for Visualizing Carbon Dioxide-Induced, Density-Driven Brine Convection*, **TPM**, 2010

Density-driven convections: CO_2 fingers

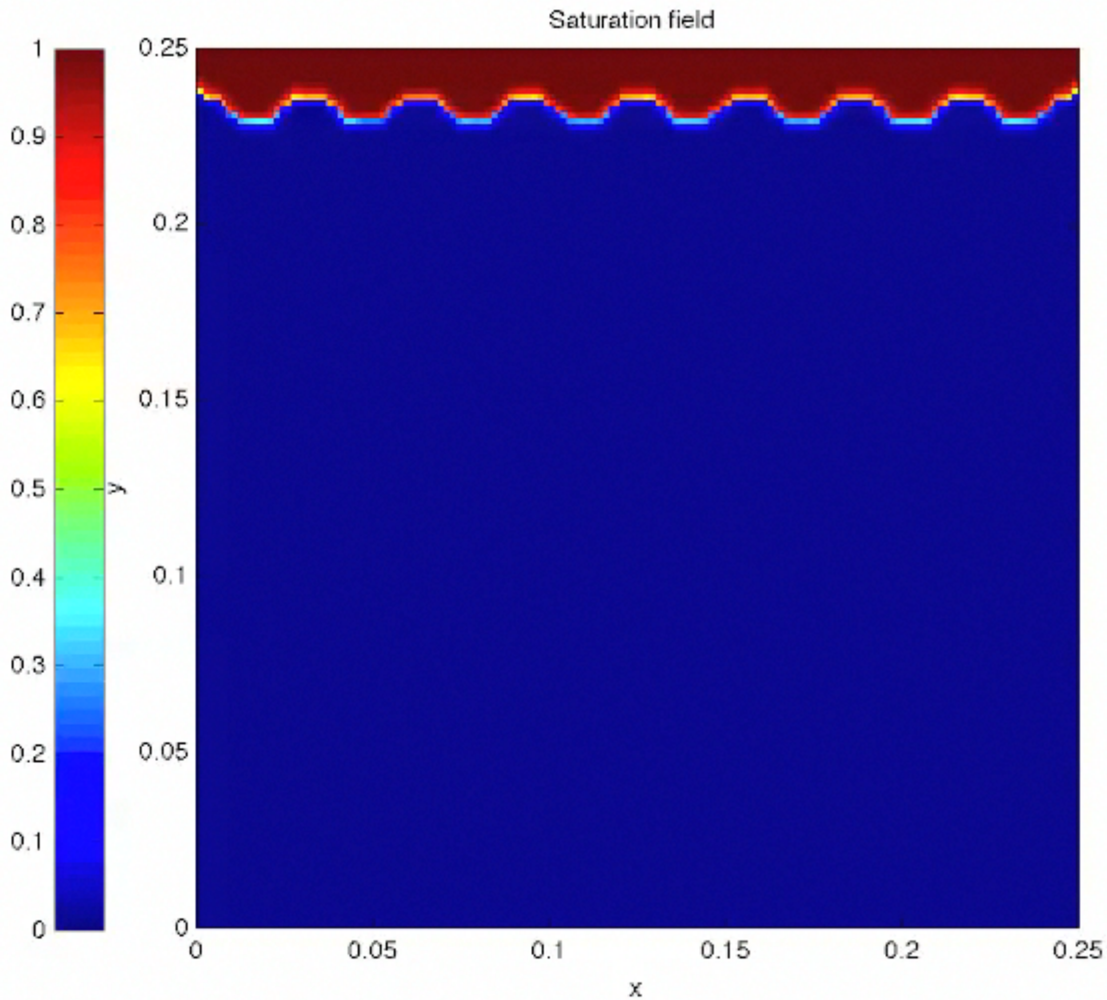

Hybrid models (Darcy flow and pore flow)

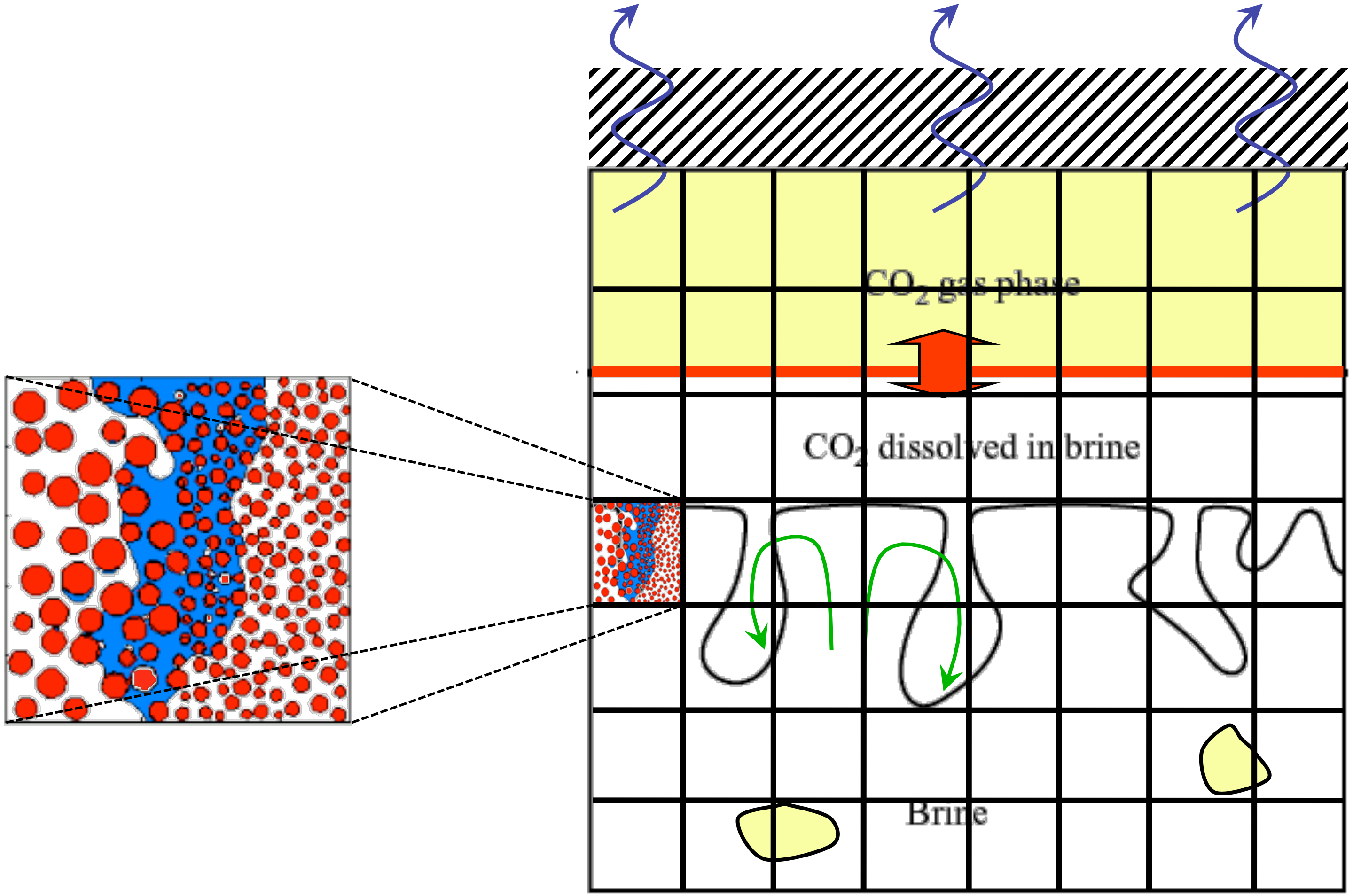

leaking

gas solution

water diffusion

density driven
convection

Iterative error reduction

Fine-scale

MsFV
(up-factor 11x5)

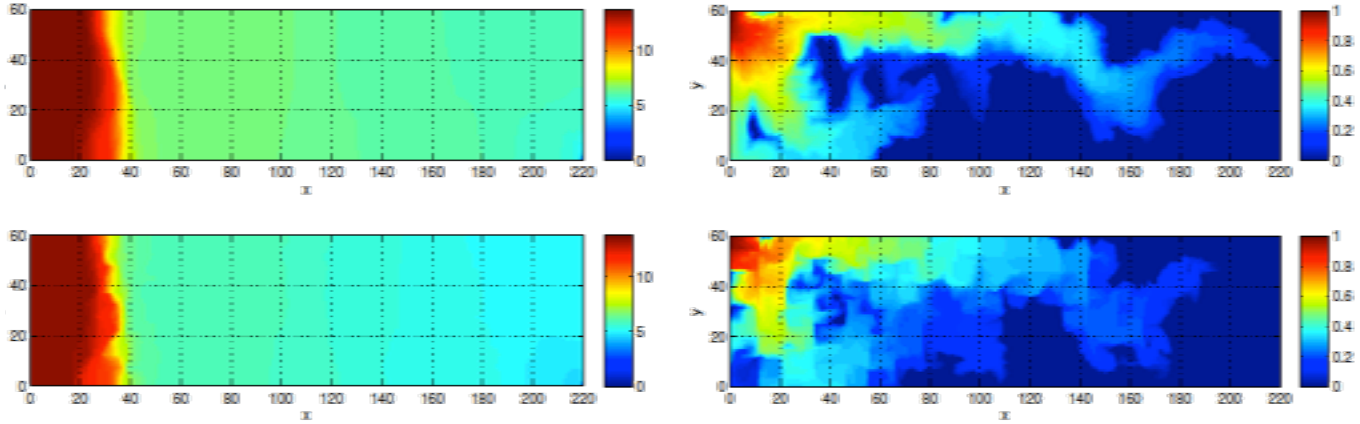

Figure 3: Fine-scale reference results after 0.2 PVI gas injection obtained by 220 × 60 grid cells: pressure (top-left) and saturation (top-right) maps. Also shown are the original non-iterative MSFV results after the same 0.2 PVI injection of gas using a 20 × 12 coarse grid: pressure (bottom-left) and saturation (bottom-right) maps.

MsFV
(up-factor 11x5)

I-MsFV
~1.3 its/p-solve
(up-factor 11x5)

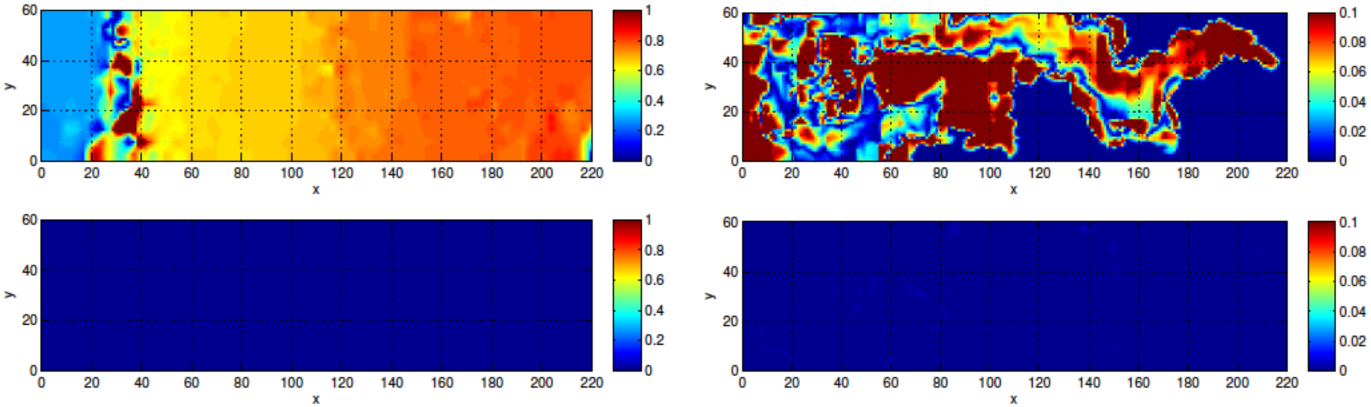

Figure 4: Error maps of the MSFV results corresponding to the results of Fig. 3: pressure error (top-left) and saturation error (top-right) maps. Also shown on the bottom row are the error maps of the i-MSFV results with $\epsilon = 2 \times 10^{-2}$: pressure error (bottom-left) and saturation error (bottom-right) maps. Note that error is defined as difference with respect to the fine-scale reference solution.

(Hajibeygi, Lunati, and Lee, SPE, 2011)

Iterative error reduction

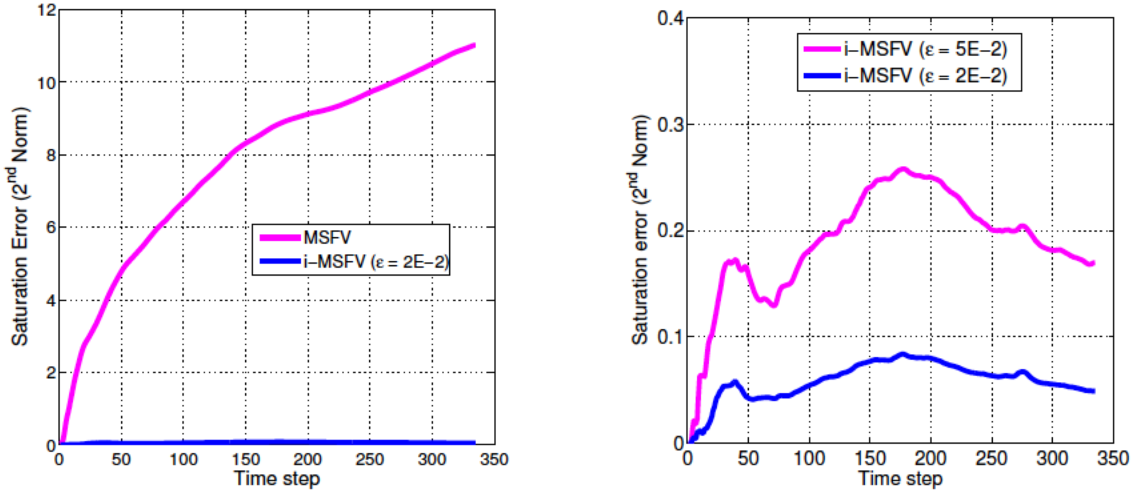

Figure 5: Saturation error second norm growth during the simulation time for the i-MSFV simulations with $\epsilon = 5 \times 10^{-2}$ and $\epsilon = 2 \times 10^{-2}$ which result in 0.55 and 1.36 additional iterations per pressure solver call, respectively.

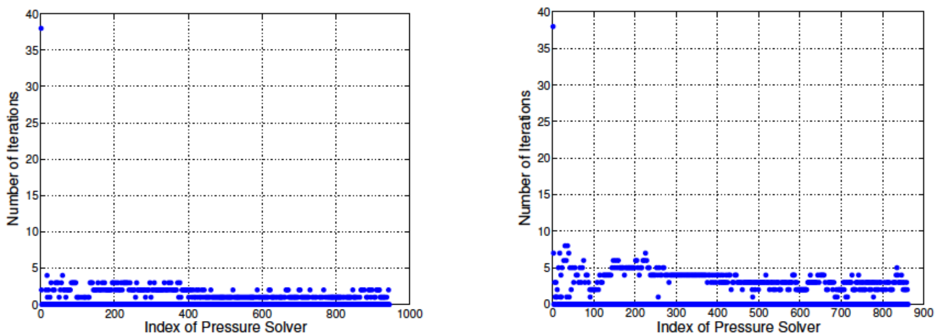

Figure 6: I-MSFV iteration histories for $\epsilon = 5 \times 10^{-2}$ (left) and $\epsilon = 2 \times 10^{-2}$ (right) vs. the pressure call index, corresponding to the results of Fig. 5. Note that with the same tight criterion for the pressure-saturation outer loop convergence, i.e. $||S^{v+1} - S^{v}||_{\infty} < 10^{-3}$, loosening the residual threshold value results in more employed outer iterations. This effect will be minimal if slightly looser convergence criteria are used.

(Hajibeygi, Lunati, and Lee, SPE, 2011)

SPE10 bottom layer (channelized k-field)

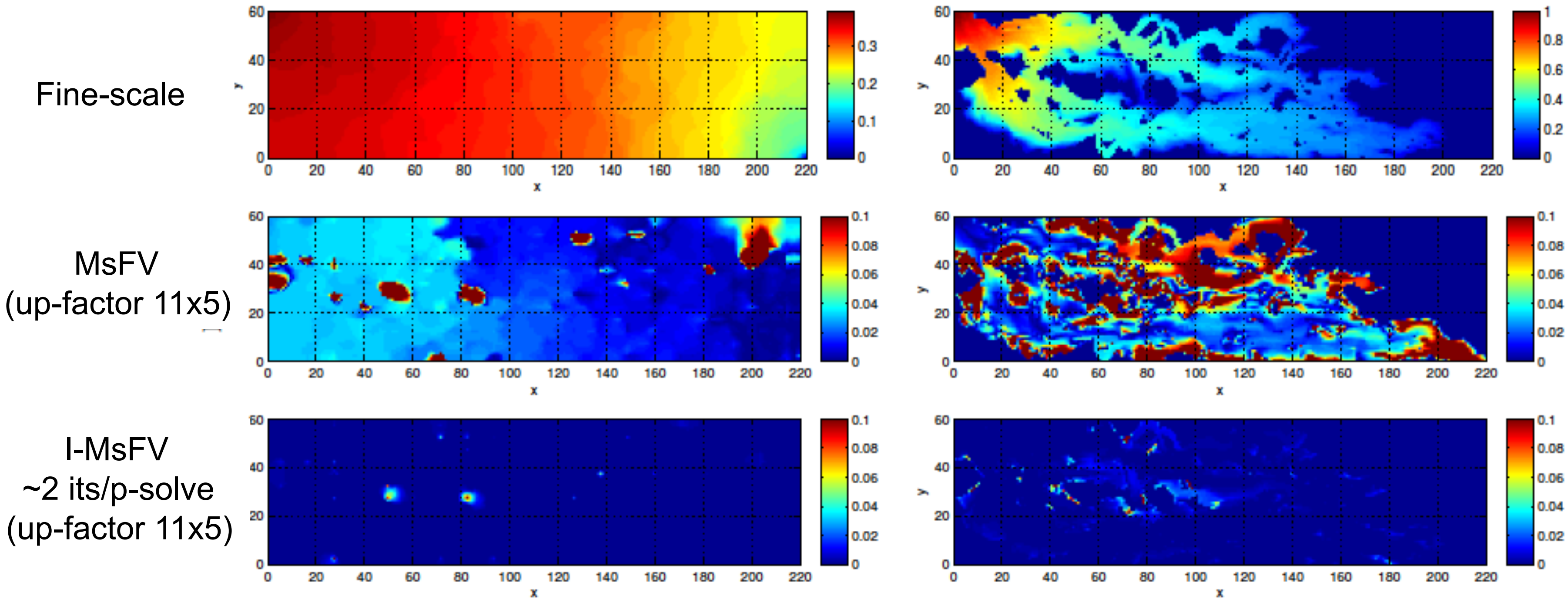

Figure 8: Fine-scale pressure (top-left) and gas saturation (top-right) maps. Also shown are the MSFV and i-MSFV error maps: MSFV pressure error (middle-left), MSFV saturation error (middle-right), i-MSFV pressure error (bottom-left), and i-MSFV saturation error (bottom-right). The i-MSFV results are obtained with $\epsilon = 5 \times 10^{-2}$ leading to 2.1 average additional iterations.

(Hajibeygi, Lunati, and Lee, SPE, 2011)

Saturation error and mass conservation

- What happens if we do not iterate till convergence?

$$\boldsymbol{v} = \boldsymbol{v}^* + \boldsymbol{v}'$$ approximate velocity = exact + deviation

- If the approximate velocity is mass conservative, errors are introduced only where f varies

$$\frac{\partial}{\partial t}(\phi S_\alpha) + \nabla \cdot (f_\alpha \boldsymbol{v}^*) - q_\alpha = -\epsilon_s$$

$$\epsilon_s = \nabla \cdot (f_\alpha \boldsymbol{v}') = f_\alpha \nabla \cdot \boldsymbol{v}' + \boldsymbol{v}' \cdot \nabla f_\alpha$$

  - error clearly depends from the pressure residual

$$\epsilon_s \sim r - Ap$$ acts a spurious source term

Remark: For the same pressure residual, the saturation error is greatly reduced if the approximate velocity is conservative

Saturation error and pressure residual

$$\epsilon_s = \nabla \cdot (f_\alpha \boldsymbol{v}^*) = f_\alpha \nabla \cdot \boldsymbol{v}' + \boldsymbol{v}' \cdot \nabla f_\alpha$$

$$\epsilon_s \sim r - Ap$$

$$\epsilon_s = \boldsymbol{v}' \cdot \nabla f_\alpha \approx \left\{ \underbrace{-K\lambda_t \nabla}_{\mathcal{D}} \underbrace{\left[(-\nabla \cdot K\lambda_t \nabla)^{-1}\right.}_{A^{-1}} \underbrace{\left.(q_t + \nabla \cdot K\lambda_t \nabla \tilde{p}^\nu)\right]}_{\epsilon_p = r - Ap} \right\} \cdot \underbrace{\nabla f_\alpha}_{df}$$

$$\boxed{\epsilon_s \approx [\mathcal{D}A^{-1}\epsilon_p]^T [df] \approx [\mathcal{D}M^{-1}\epsilon_p]^T [df]}$$

Remark: For the same pressure residual, the saturation error is greatly reduced if the approximate velocity is conservative -> fewer iterations…

A summary of adaptive strategies

- Adaptive update of the MsFV operator
  - Adaptive update basis functions in multiphase flow
- Adaptive iterations
  - Do not iterate convergence, only to obtain the desired S accuracy
- Space adaptive iterations
  - Iterations only in region of large residuals
- Adaptive refinement
  - Local fine scale are solved only where needed
  - MsFV/IMsFV as a grid refinement (downscaling) technique

- Adaptive physical description (NS/Darcy)
  - MsFV as a framework to couple different physical descriptions
  - Consistent description without needs iteration

UNIL | Université de Lausanne

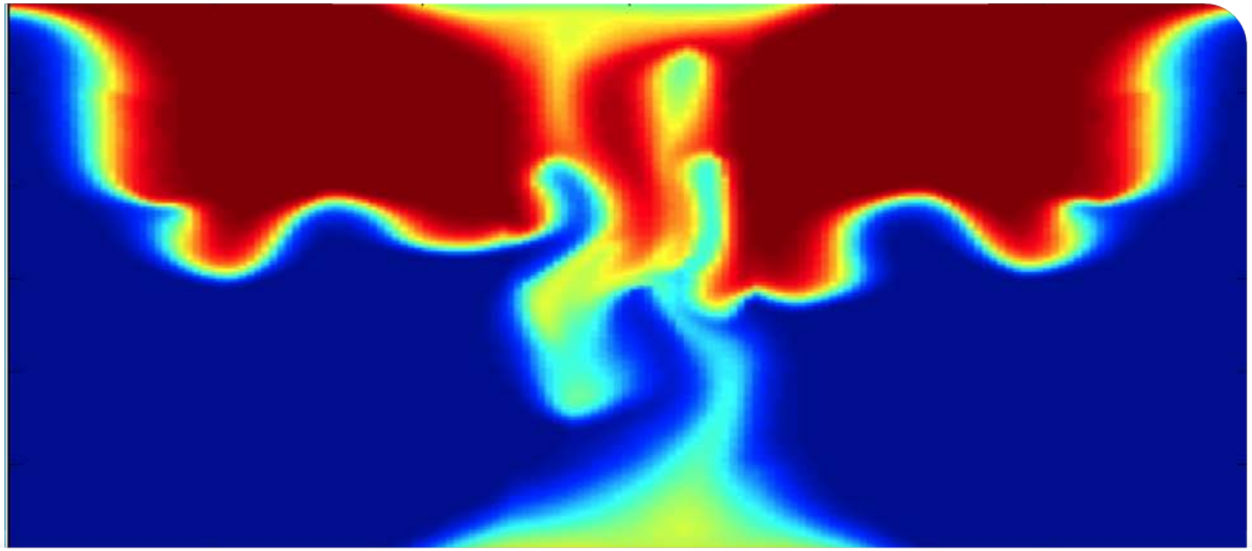

Direct pore-scale simulation of interfaces

| le savoir vivant |

 ivan.lunati@unil.ch 1/26/11

regional scale
(aquifer or
reservoir)
~ 1 km – 100 km

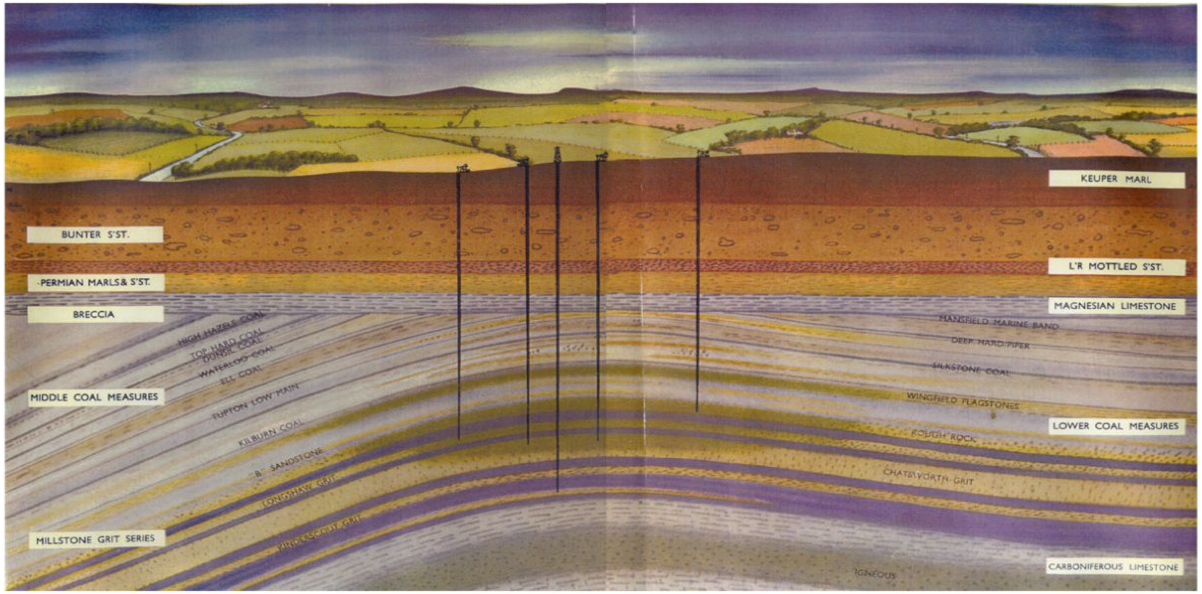

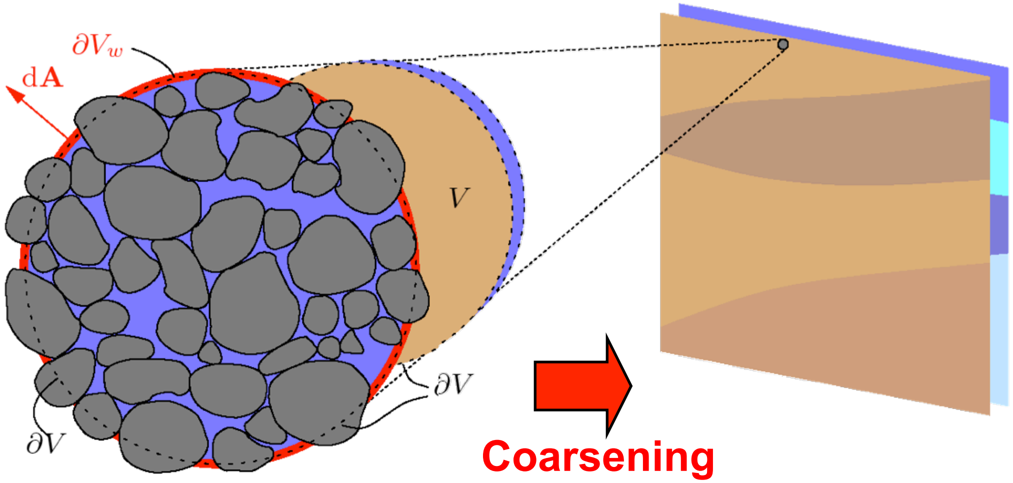

Darcy scale
(continuum scale)
~ 1 m – 10 m

pore scale
< 10 μm – 1 cm

Coarsening
(Volume averaging)

Linear vs. nonlinear flow in a fracture

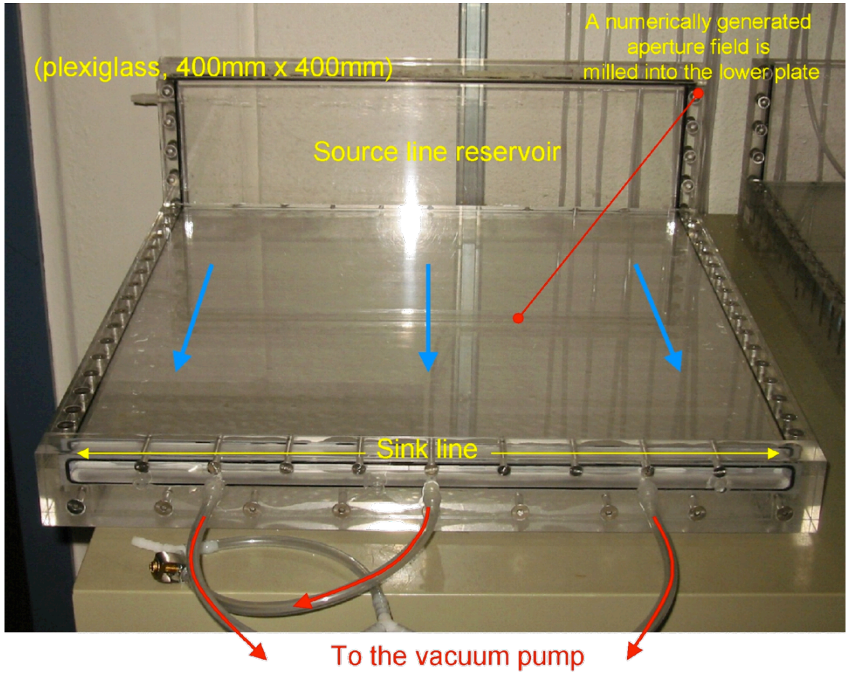

Linear (Ideal tracer)

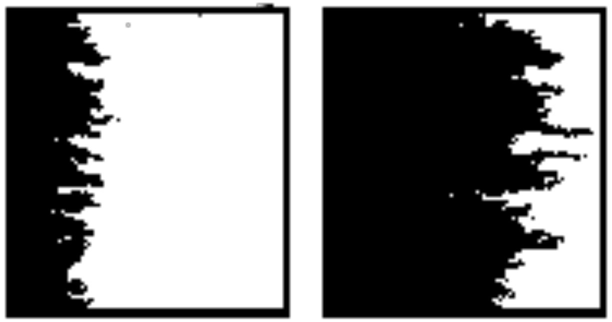

fracture aperture

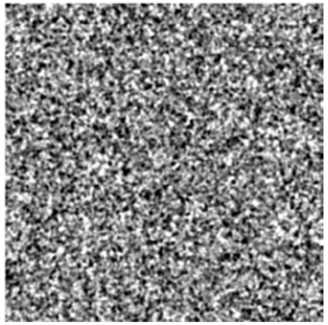

Lunati et al., *J. Cont. Hydr.*, 2003
Marschall and Lunati (Eds.), *NTB – Nagra Technical Report, 03-11, Dec. 2006*

Linear vs. nonlinear flow in a fracture

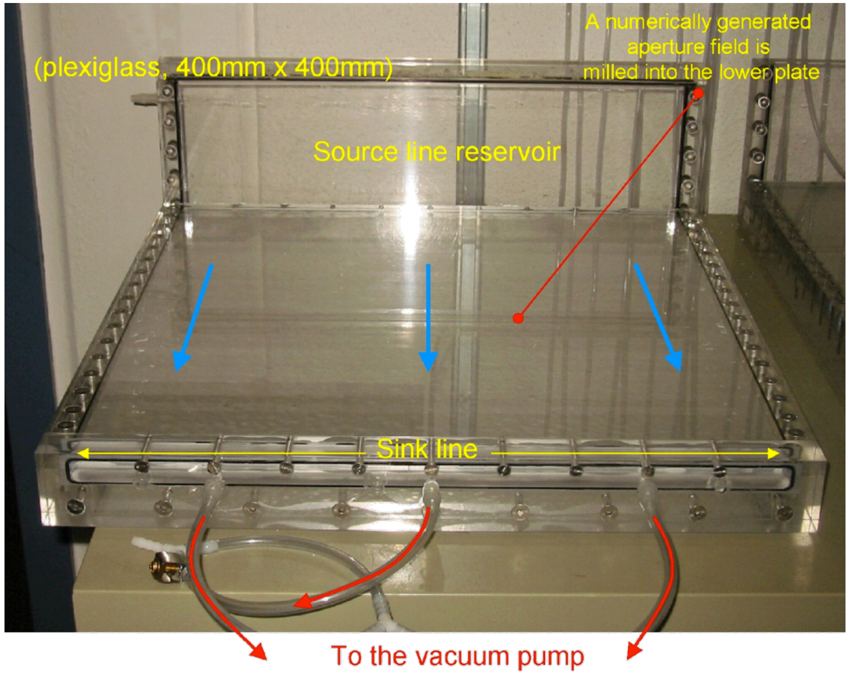

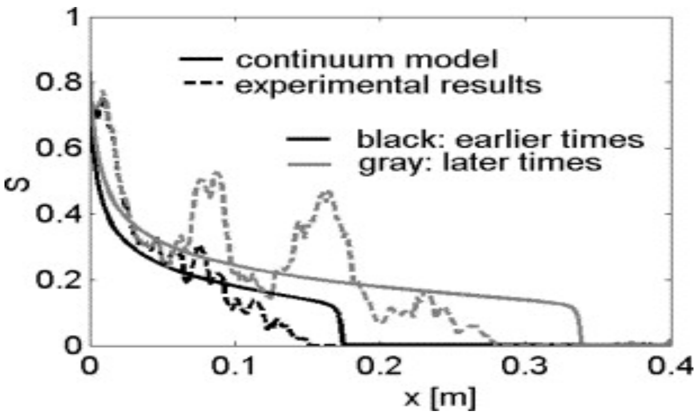

Neuweiler, Soerensen, and Kinzelbach, *Adv. Water Res.*, 2004

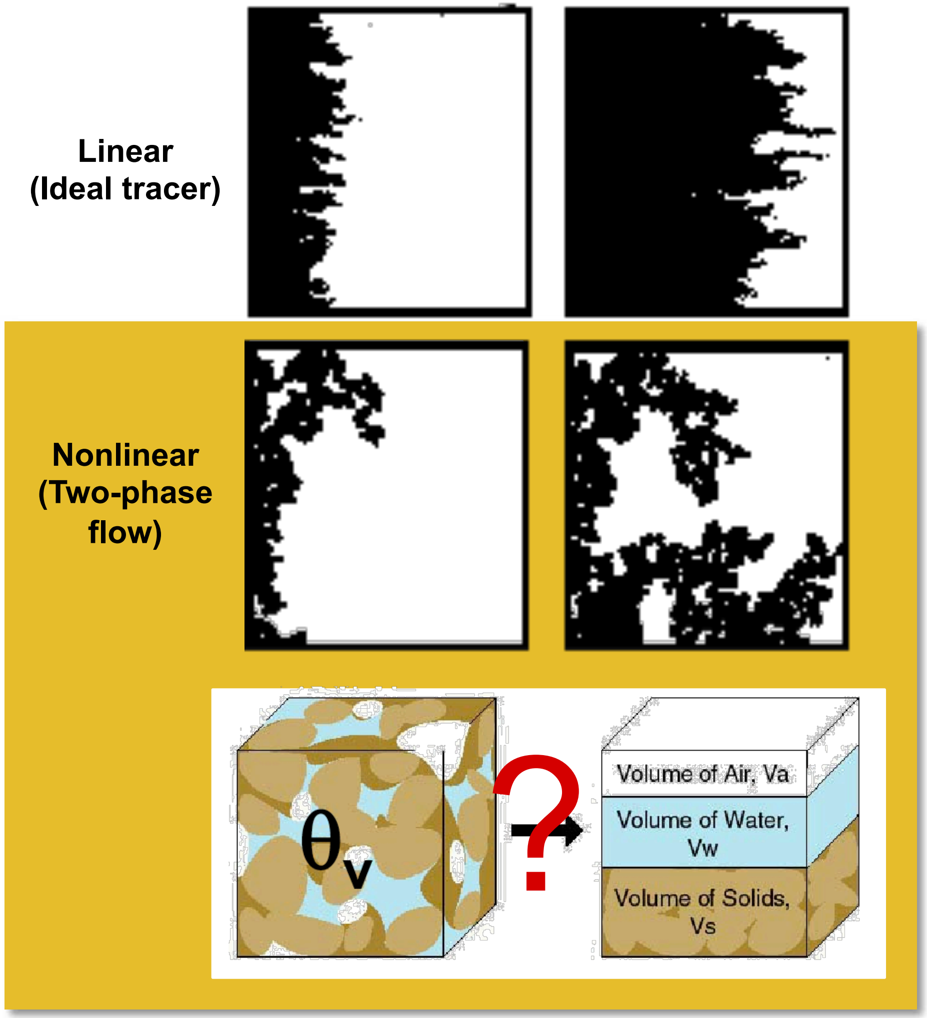

Lunati et al., *J. Cont. Hydr.*, 2003
Marschall and Lunati (Eds.), *NTB – Nagra Technical Report, 03-11*, *Dec. 2006*

limitation of the continuum approach

- difficulties in applying the continuum approach in case of
  - multiphase flow
  - instabilities (intermittency)
  - non-equilibrium processes

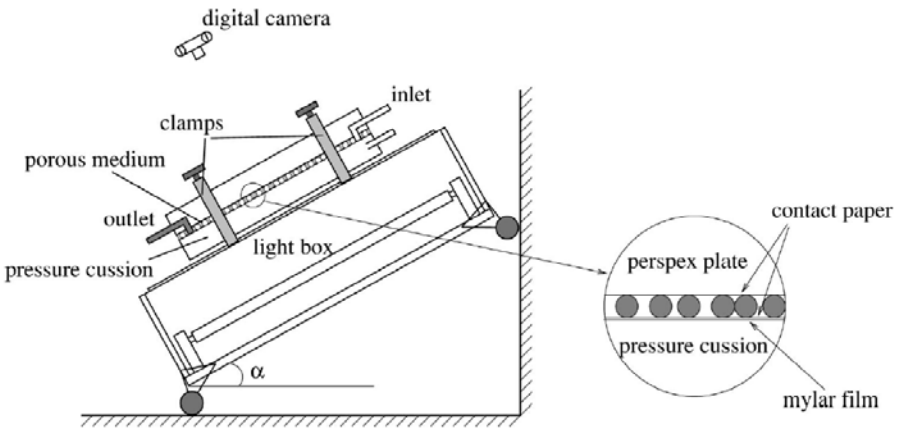

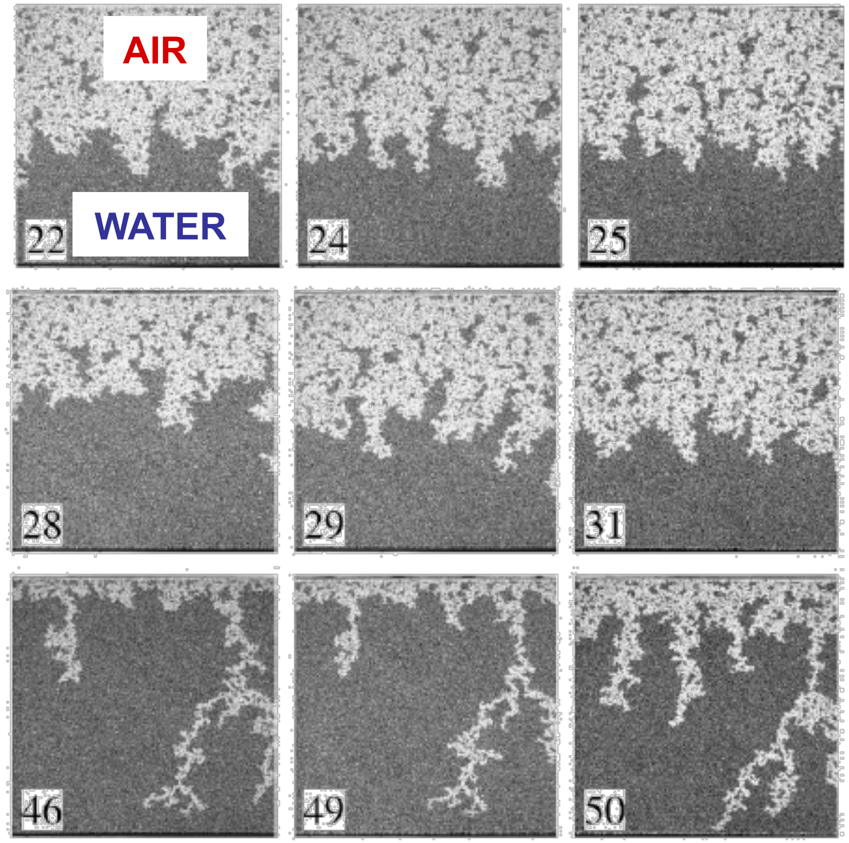

Méheustet al., *Phys. Rev. E*, 2002

Flow regimes in the parameter space

Lenormand et al., JFM., 1988

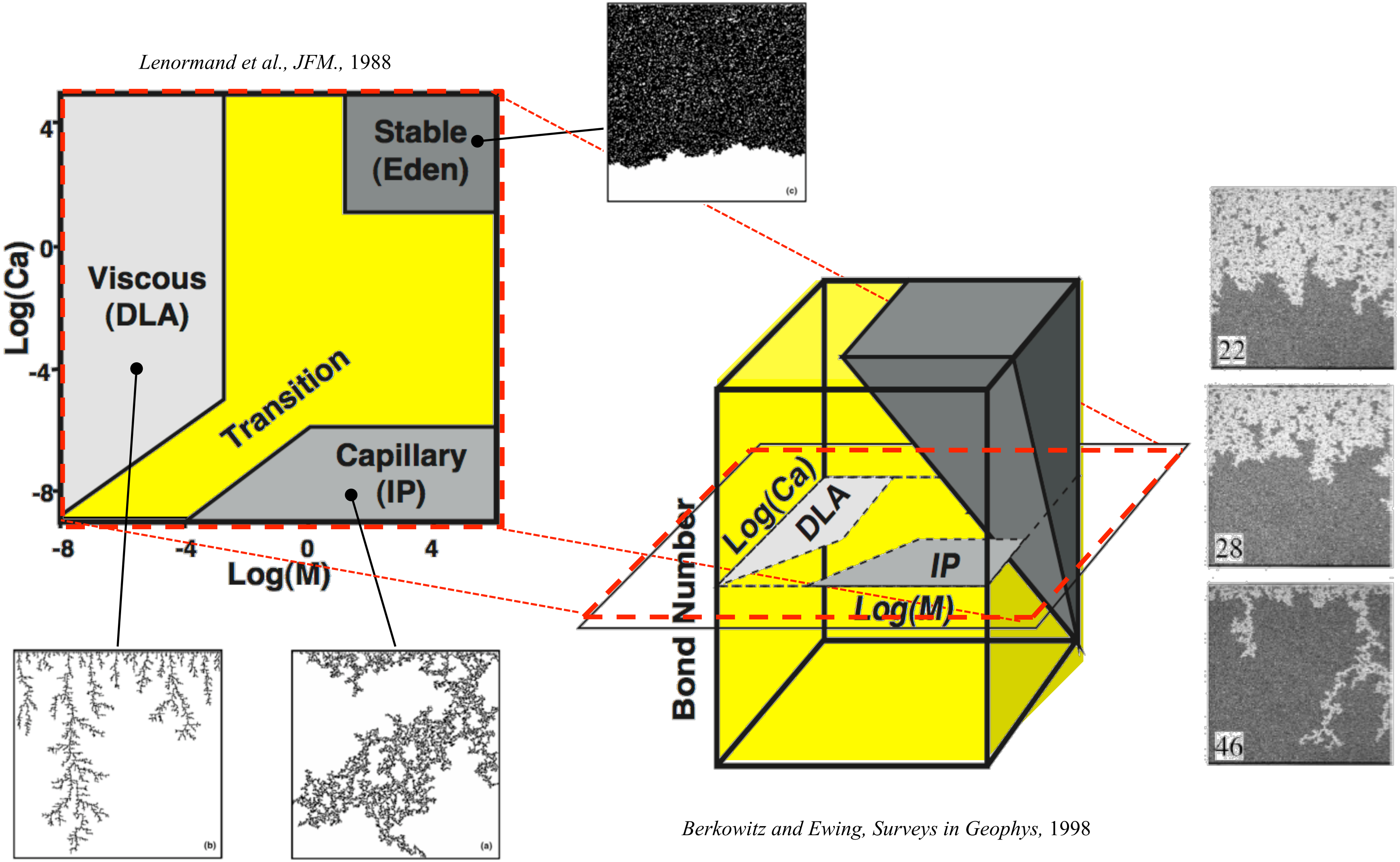

(Méheust et al., Phys. Rev. E, 2002)

Berkowitz and Ewing, Surveys in Geophys, 1998

gravity instability - decreasing the velocity (Ca)

- water, but θ = 90°; Bo ~ 0.08;
- an extension of Saffman-Taylor stability criterion:
  – $\mathrm{Bo}^* = \mathrm{Bo} - \mathrm{Ca}\ b^2/k$
    - (e.g., Méheust et al., 2002)
  – $\mathrm{Bo}^* = \mathrm{Bo} - f\,\mathrm{Ca}$

$$\mathrm{Ca} = \frac{\mu U}{\gamma}$$

$$\mathrm{Bo} = \frac{\rho g b^2}{\gamma\,(d-1)}$$

$$f = \int_{\Sigma_M} \frac{\partial u'_{\parallel}}{\partial x'_{\perp}} da'$$

$$k = b^2/f$$

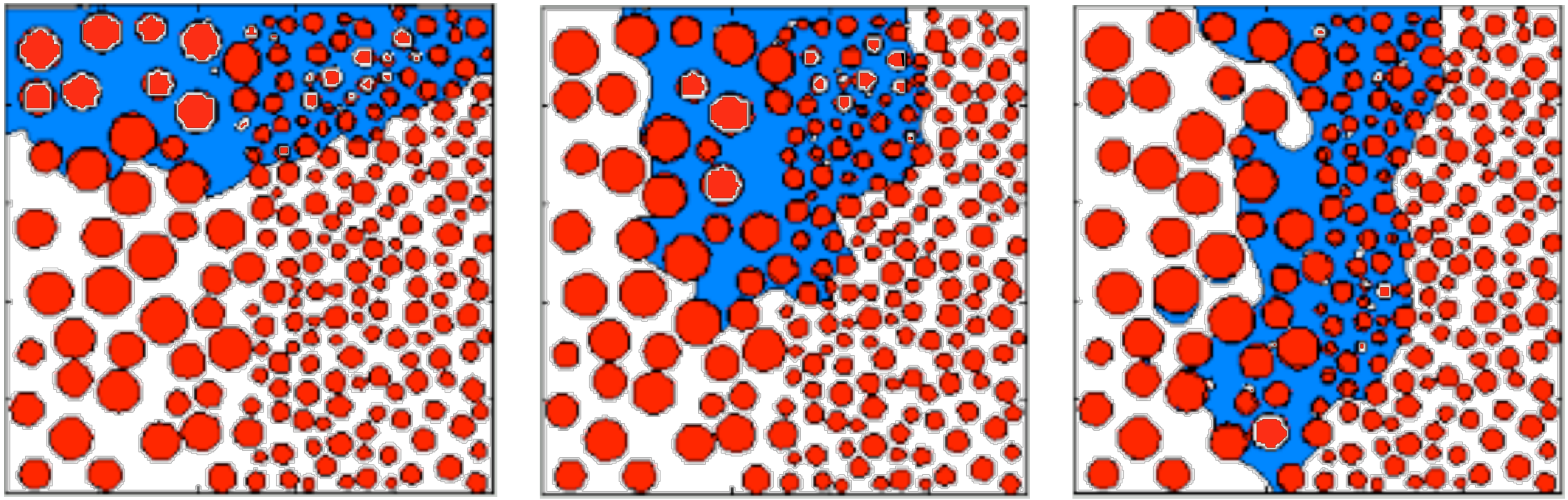

Lunati , 2007 [unpubl.]

Volume of fluid method - VoF

- Well-established technique for modeling free surfaces
  - computational fluid dynamics
    - splash of drops
- Interface tracking coupled with grid-based NS solver
  - finite volume to compute the velocity field
    - solution of NS equations
  - VoF for interface advection
    - the interface in not tracked directly
    - the fluid indicator function F is advected
      - $F = 1$ in the fluid;
      - $F = 0$ in the void;
      - $0<F<1$ at the surface
    - interface is reconstructed
- For fractures and porous media: contact angle model

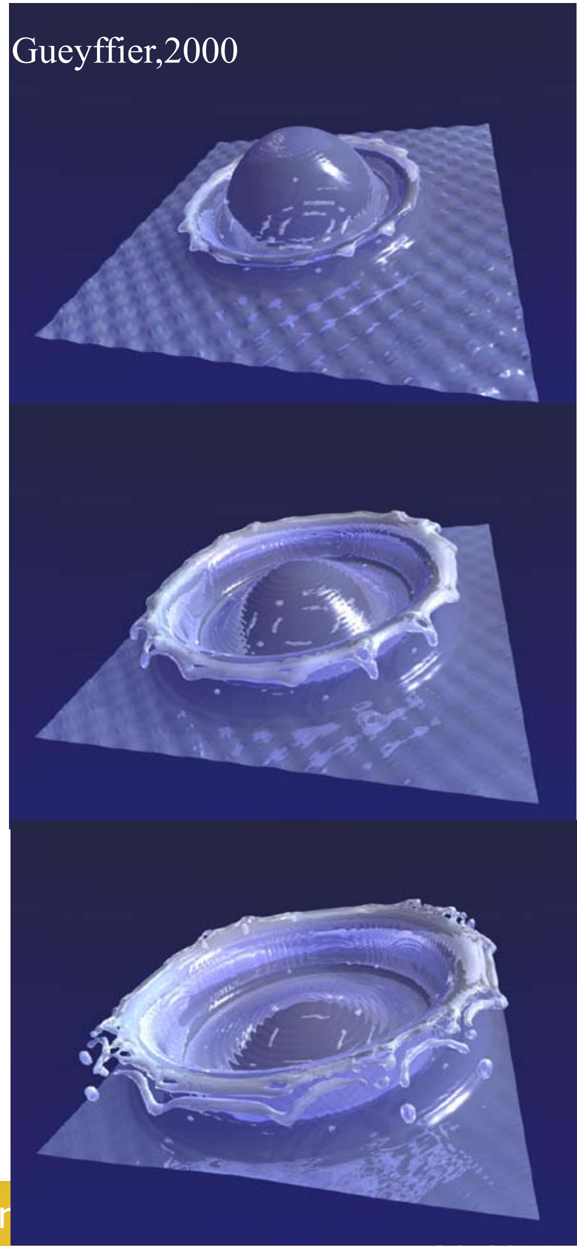

Velocity and Continuum Surface Force model

- finite-volume discretization
  - two-step projection method for incompressible NS equations
    - 1. $$\frac{\mathbf{V}^* - \mathbf{V}^{(i)}}{\Delta t} + \left(\mathbf{V}^{(i)} \cdot \nabla\right)\mathbf{V}^{(i)} = \frac{\mu}{\rho}\nabla^2\mathbf{V}^{(i)} + \frac{1}{\rho}\mathbf{F}_{\mathbf{b}}^{(i)}$$
    - 2. $$\frac{\mathbf{V}^{(i+1)} - \mathbf{V}^*}{\Delta t} = -\frac{1}{\rho}\nabla P^{(i+1)} \quad \& \quad \nabla \cdot \mathbf{V}^{(i+1)}$$
  - continuum surface force (csf - Brackbill et al. 1992)

$$\lim_{\Delta v \to 0} \int_{\Delta v} \mathrm{F}_{sv}(\mathrm{x})dv = \int_{\Delta s} \mathrm{F}_{sa}(\mathrm{x}_s)ds$$

$$\mathbf{F}_{sa}(\mathbf{x}_s) = \sigma\kappa(\mathbf{x}_s)\mathbf{n}(\mathbf{x}_s)$$

$$\mathbf{F}_{sv}(\mathbf{x}) = \sigma\kappa(\mathbf{x})\nabla F$$

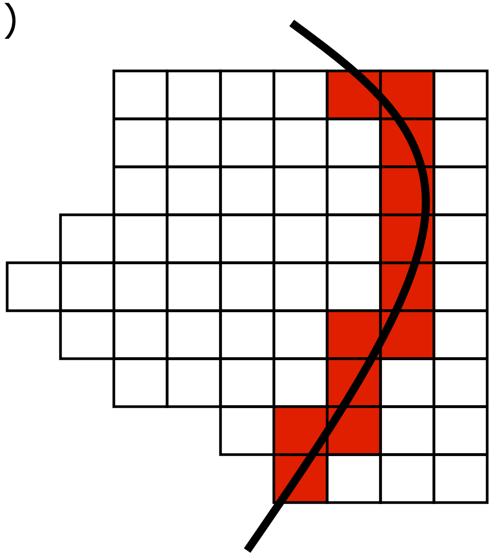

  - stability constraints
    - viscous flow; csf stability; Courant (VoF)

interface advection and reconstruction

- advection of fluid function

$$\frac{\partial F}{\partial t} + \mathbf{V} \cdot \nabla F = \frac{\partial F}{\partial t} + \nabla \cdot (\mathbf{V} F) = 0 \qquad F(\vec{x}, t) = \begin{cases} 1, & \text{in the fluid;} \\ > 0\,, < 1, & \text{at the free surface;} \\ 0, & \text{in the void.} \end{cases}$$

- Young's reconstruction (piecewise linear interface calculation - PLIC)

$$\mathbf{n} = \frac{\nabla F}{|\nabla F|}$$

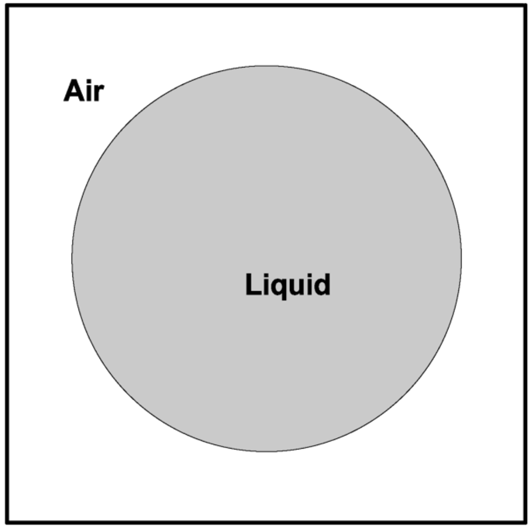

0.00	0.00	0.00	0.00	0.00	0.00	0.00	0.00
0.00	0.03	0.58	0.94	0.94	0.58	0.03	0.00
0.00	0.58	1.00	1.00	1.00	1.00	0.58	0.00
0.00	0.94	1.00	1.00	1.00	1.00	0.94	0.00
0.00	0.94	1.00	1.00	1.00	1.00	0.94	0.00
0.00	0.58	1.00	1.00	1.00	1.00	0.58	0.00
0.00	0.03	0.58	0.94	0.94	0.58	0.03	0.00
0.00	0.00	0.00	0.00	0.00	0.00	0.00	0.00

Huang et al.,2005

boundary condition at the wall

- advection of fluid function

$$\frac{\partial F}{\partial t} + \mathbf{V} \cdot \nabla F = \frac{\partial F}{\partial t} + \nabla \cdot (\mathbf{V}F) = 0 \qquad F(\vec{x}, t) = \begin{cases} 1, & \text{in the fluid;} \\ > 0\,, < 1, & \text{at the free surface;} \\ 0, & \text{in the void.} \end{cases}$$

- if solid surfaces, need for wetting description
  - contact angle model

$$\mathbf{n} = \frac{\nabla F}{|\nabla F|}$$

$$\mathbf{n}(\mathbf{x})|_{wall} = \mathbf{n}_w \cos(\theta_{eq}) + \mathbf{t}_w \sin(\theta_{eq})$$

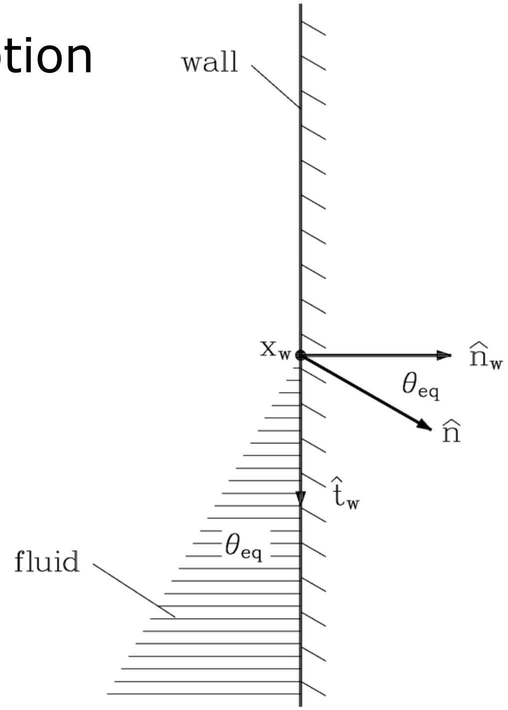

contact angle adjustment in the VoF method

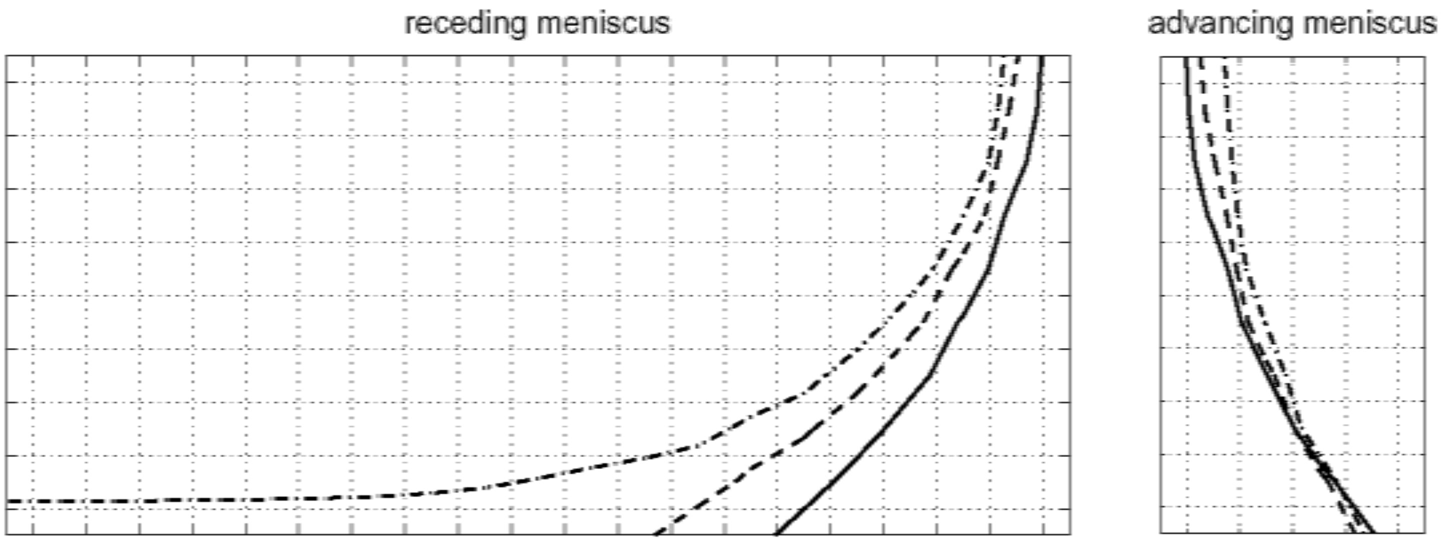

FIGURE 6. The shape of the advancing (right) and receding (left) menisci obtained with the VOF method for a partially wetting liquid ($\theta_m = 40^\circ$). Shown are the meniscus shapes of three different slugs of dimensionless size $1/\epsilon = 4$ (solid line), 20 (dashed line), and 40 (dashed-dotted line).

(Lunati and Or, *Phys. Fluids*, 2009)

Dynamic contact angle

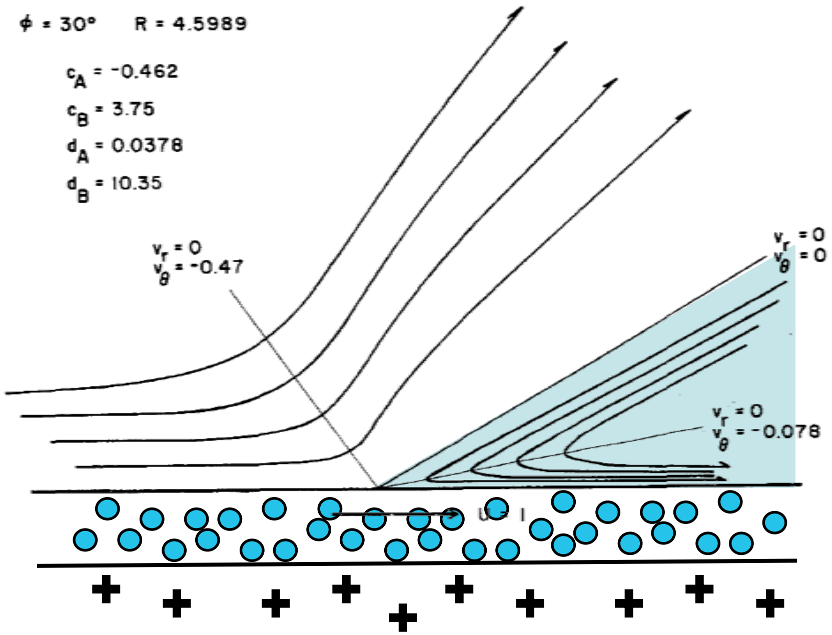

$$f_w \sim \mathrm{Ca} \int \frac{1}{h} dh = \infty$$

- singularity at the contact line
  - friction is logarithmically infinite
    - » *"not even Herakles could sink a solid if the physical model were entirely valid, which is not."* Hue and Scriven, *J. Colloid Interf. Sci.*, 1971

Dynamic contact angle

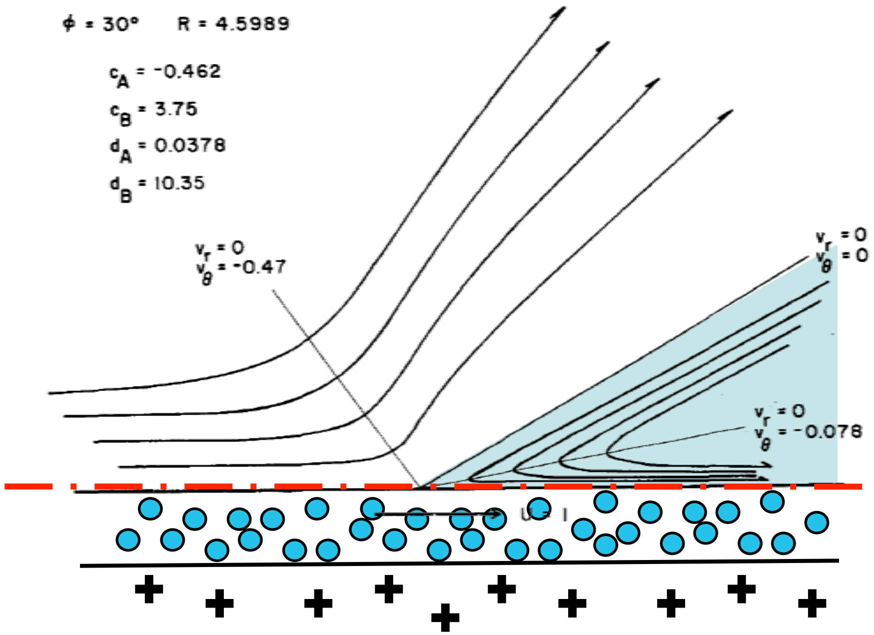

$$f_w \sim \mathrm{Ca} \int_\ell^L \frac{1}{h} dh = \mathrm{Ca} \ln(L/\ell)$$

Hydrodynamic theory

$$p_c = \Delta p = \gamma \kappa$$

Molecular theory

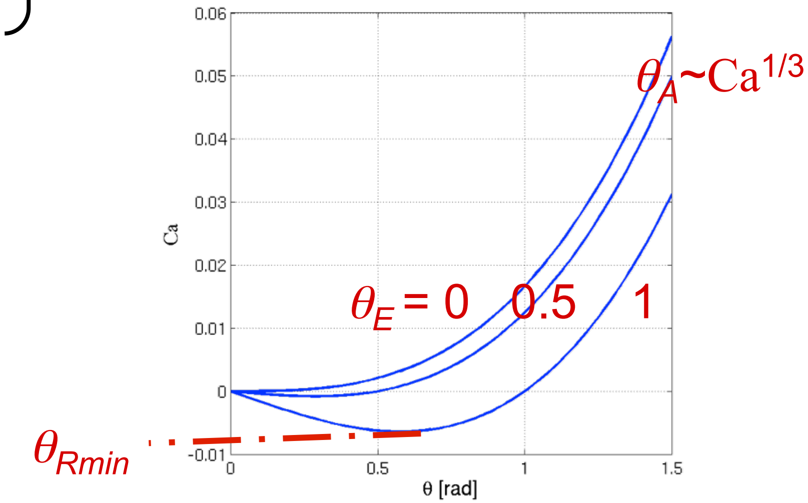

- cut off at molecular length scale
  - hydrodynamic description brakes down
  - avoids infinite friction
- dynamic contact angle, θ_A or θ_R
  - balance btw. viscous and capillary forces
    - e.g. *de Gennes, 1986*

Steady velocity of slug in capillaries

- Bico & Quéré, *J. Coll. Int. Sci.*, 2001
  - liquid: silicon oil (γ = 20.6 mN/m, μ = 16.7 mPa s, ρ = 0.95)
  - vertical glass tube (radius: b = 127 μm; dry and prewetted, film 1.5 μm)

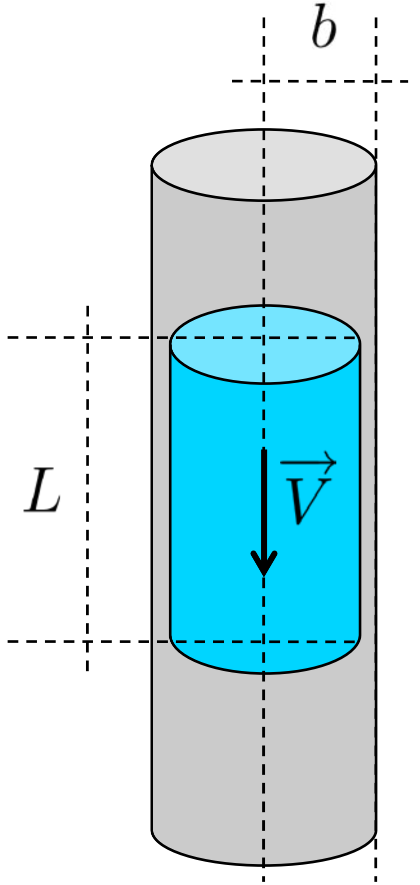

Poiseuille flow $U = \frac{\rho g b^2}{4\mu} \approx 1\ \mathrm{mm/s}$

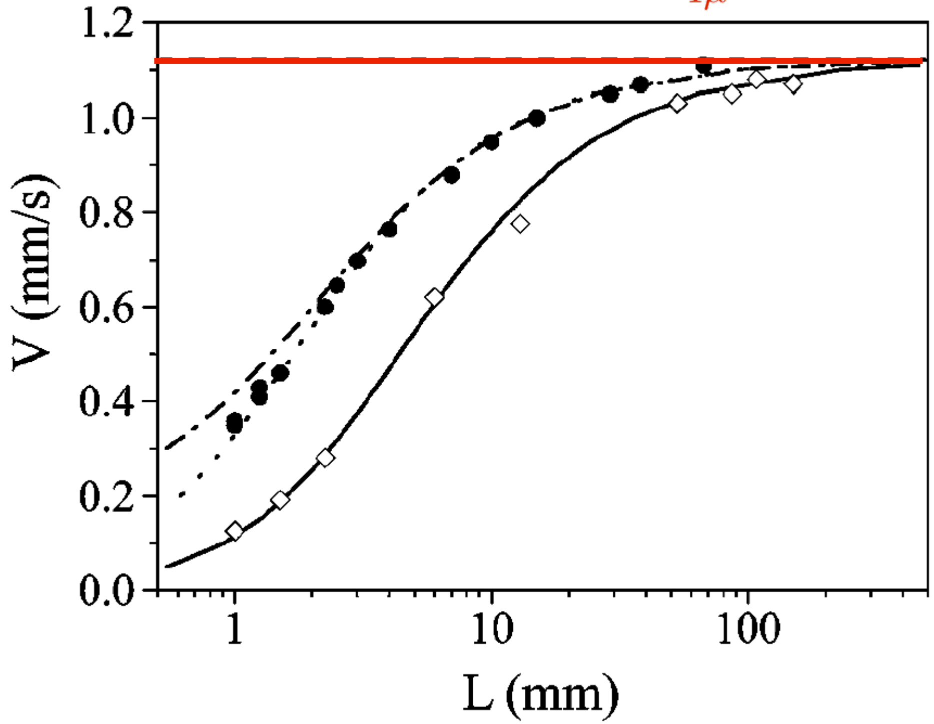

Force resultant: pressure force

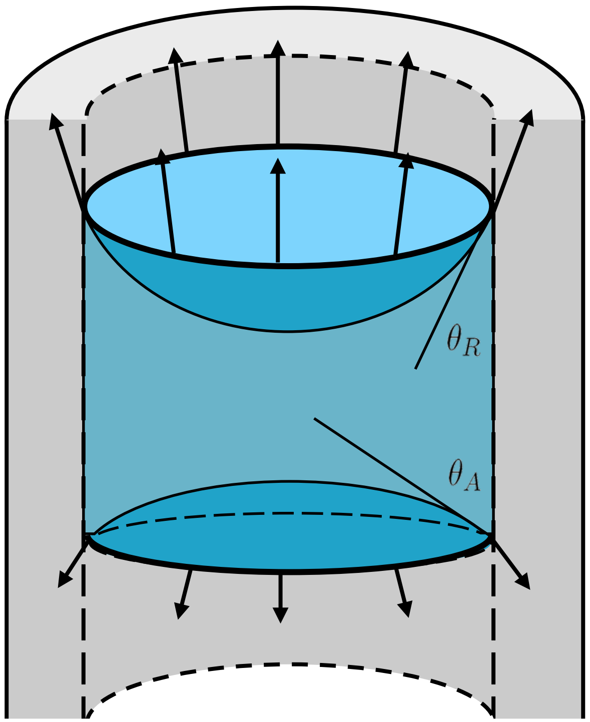

$$\int_S \kappa \, n_j ds = \oint_{\partial S} t_j dl$$

$$\boxed{\int_S p \; n_j \; ds = \gamma \Delta_\theta \oint_{\partial S} dl}$$

capillary drag: $\Delta_\theta = \cos\theta_R - \cos\theta_A$

θ_m

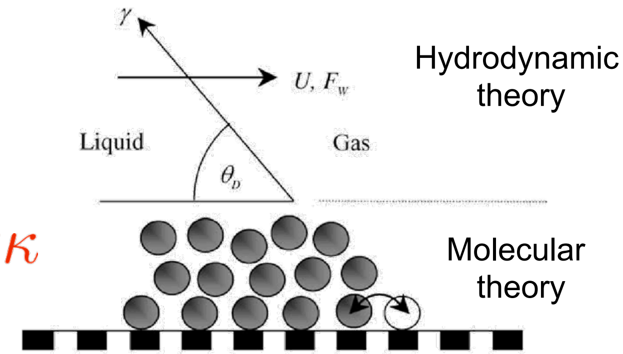

$$\cos\theta_m = \frac{\gamma_{SV} - \gamma_{SL} - G \ \mathrm{sign}(u)}{\gamma}$$

- valid if the hydrodynamic description holds, i.e. $p = \gamma\kappa$
  - capillary force proportional to the curvature
  - not restricted to spherical menisci
- **<u>no additional capillary drag of hydrodynamic origin</u>**

Dimensionless force balance

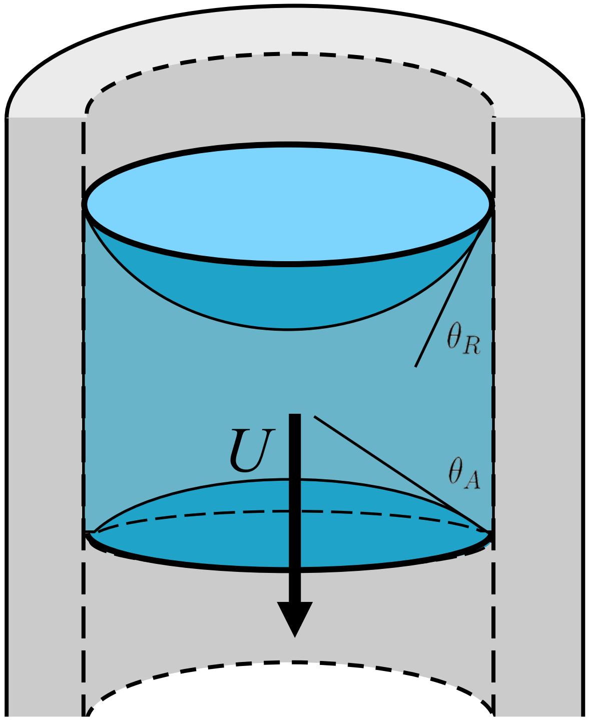

- integrated NS equation in dimensionless form:

$$\boxed{-\epsilon\Delta_\theta - f\,\mathrm{Ca} + \mathrm{Bo} = 0}$$

– capillary number $\mathrm{Ca} = \dfrac{\mu U}{\gamma}$

– Bond number $\mathrm{Bo} = \dfrac{\rho g b^2}{\gamma\,(d-1)}$

– length to radius ratio $\epsilon = \dfrac{b}{L}$

– Capillary drag $\Delta_\theta = \cos\theta_R - \cos\theta_A$

– Shape function

$$f(\theta_A, \theta_R, \mathrm{Ca}, \mathrm{Bo}, \epsilon) = \int_{z'_A}^{z'_R} \left.\frac{\partial u'_z}{\partial r'}\right|_{r'=1} d\zeta > 0$$

(Lunati & Or, *Phys. Fluids*, 2009)

Meniscus behavior in a corner

- description of the transition in the energy-volume space
  - wetting fluid
  - no gravity; slow flow (negligible viscous forces)
  - convex meniscus has higher energy
- at transition viscous forces are not negligible
  - <u>investigation by means of VoF</u>

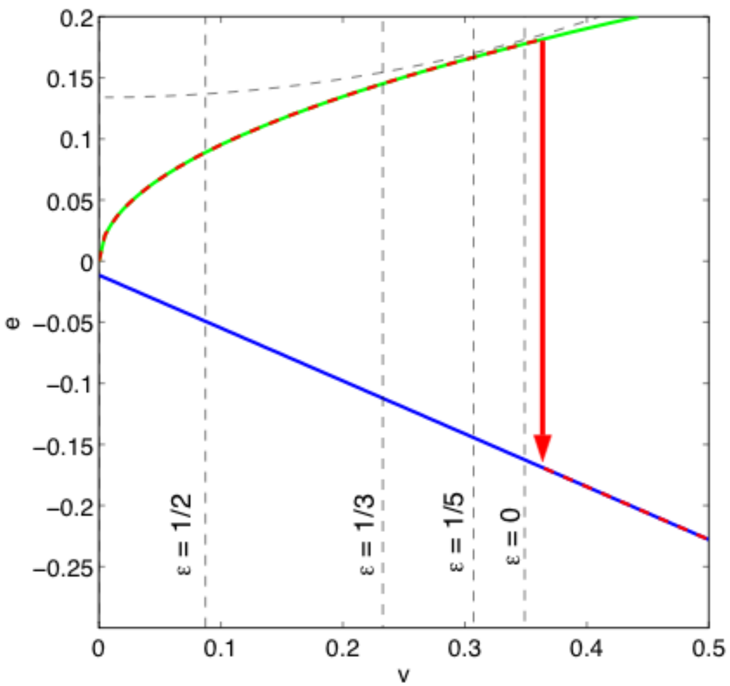

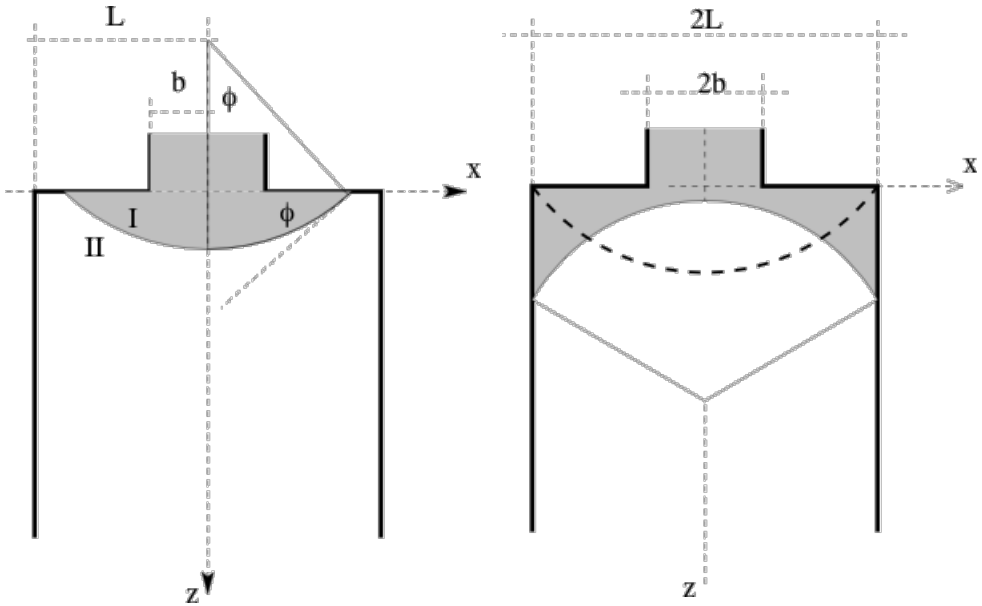

Lunati , 2007 [unpublished]

pressure distribution: contact angle 30°

- contact angle 30°
- Re = U (2b) $\rho/\mu \sim 1$
- Bo = 0
- Ca ~ 10^{-5}
  - water; 2b ~ 1mm; v ~ 1mm/s

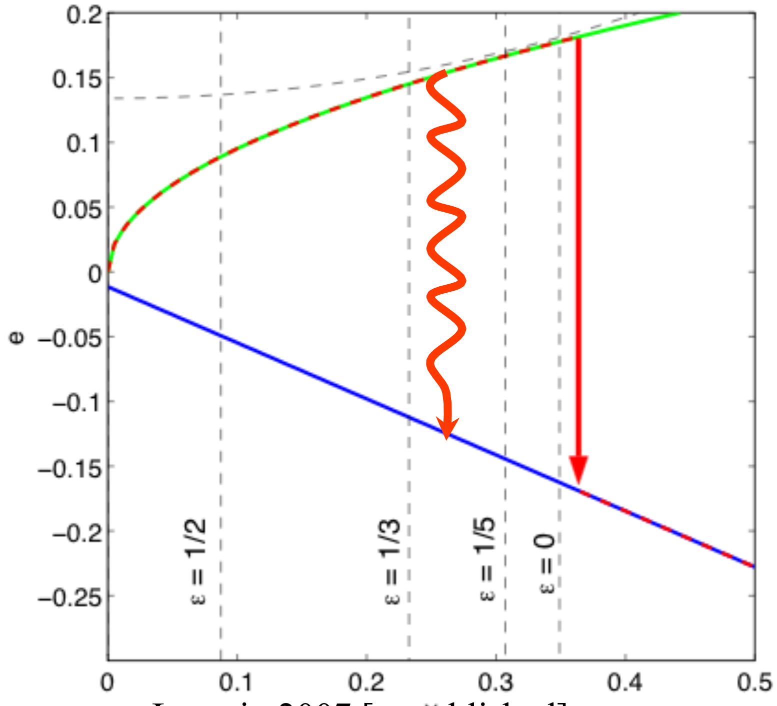

Lunati , 2007 [unpublished]

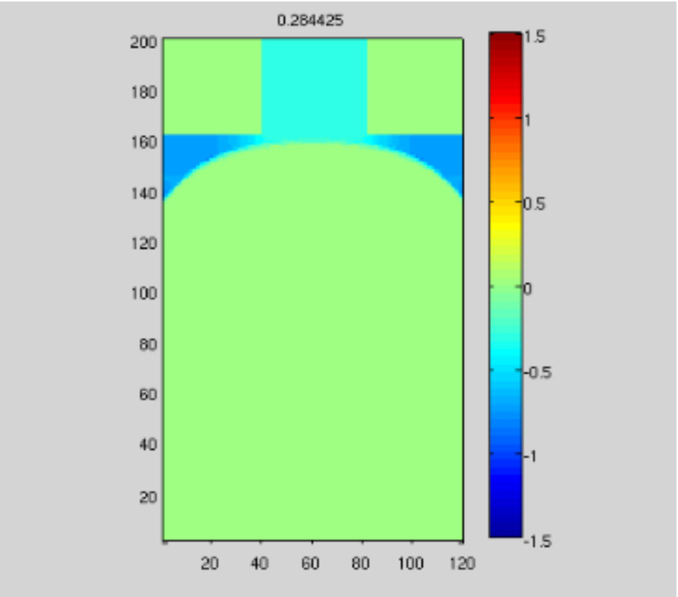

Transition for different injection velocity

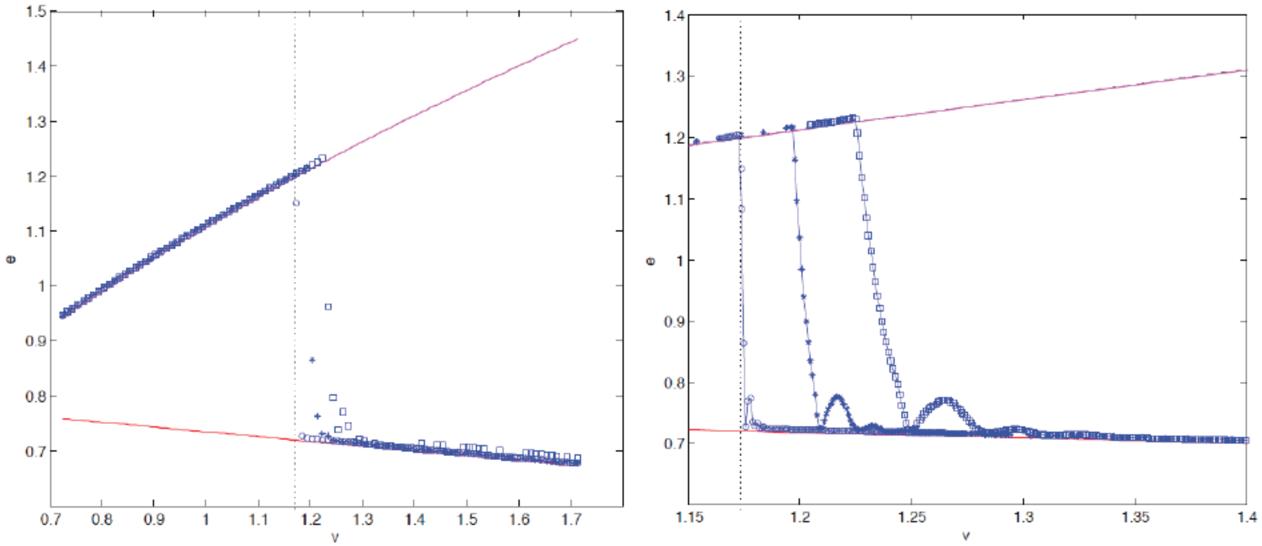

Figure 4. *Surface energy as a function of the injected water volume for a contact angle θ=80°. The inlet velocities are: 10^{-3} m s^{-1} (circles), 5×10^{-3} m s^{-1} (asterisks), and 10^{-2} m s^{-1} (squares), which correspond to $Ca=2\times10^{-5}$, $Ca=10^{-4}$, and $Ca=2\times10^{-4}$, respectively. (a) shows the results of the whole simulation; (b) shows the dynamics of the configuration change in greater detail. The upper, resp. lower, continuous lines is the surface energy evaluated from Eq. 4, resp. Eq. 7; whereas the vertical dotted line indicates the volume for which the static meniscus touches the corner and becomes unstable.*

Table 1 Phase properties used for the numerical simulations

	ρ [kg m^{-3}]	μ [kg m^{-1} s^{-1}]	γ [N m^{-1}]
Water	1000	10^{-3}	5×10^{-2}
Crude oil	500	10^{-2}	

Maniero and Lunati, ECMOR 2010

Oscillations

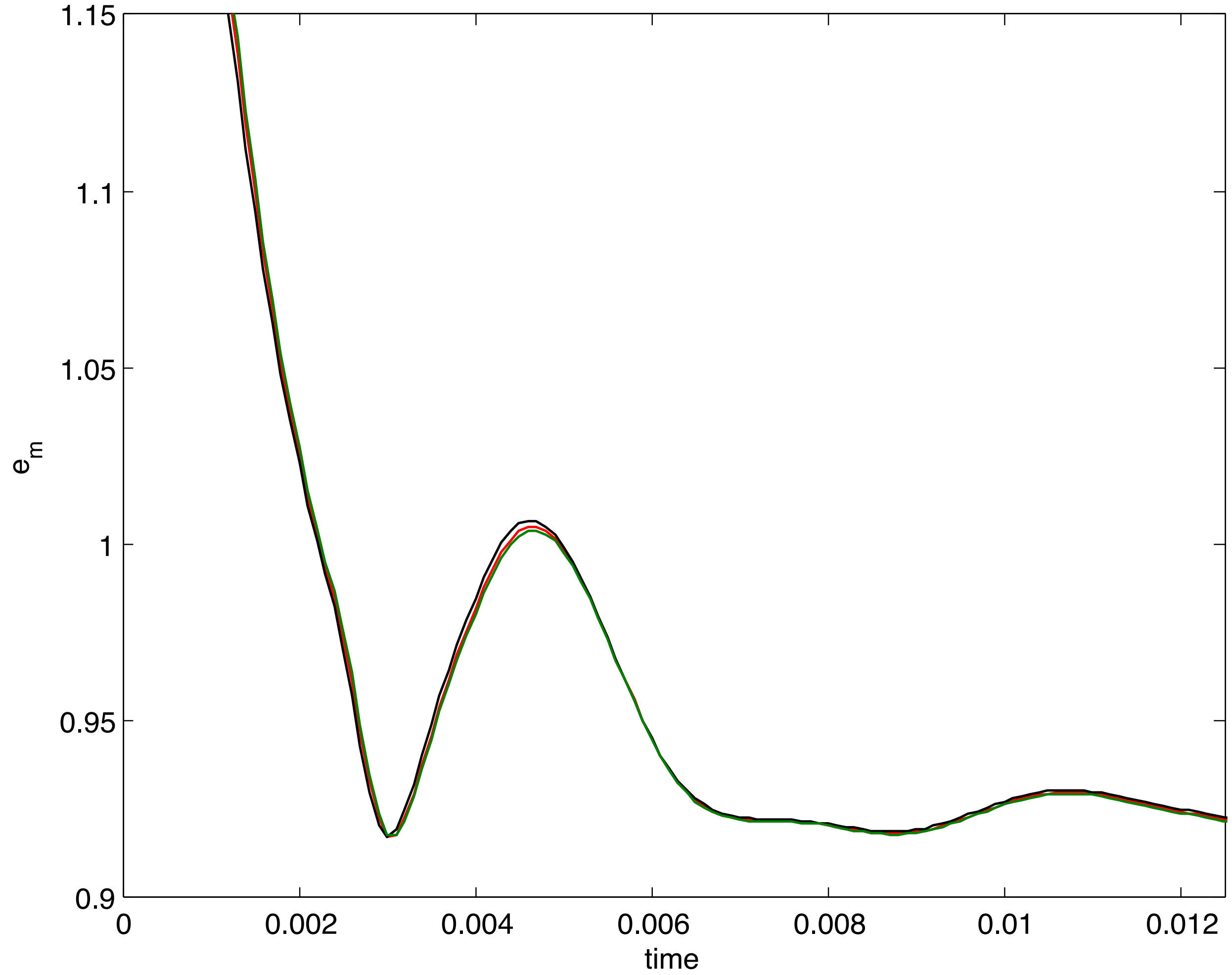

Hysteresis effects (irreversible transition)

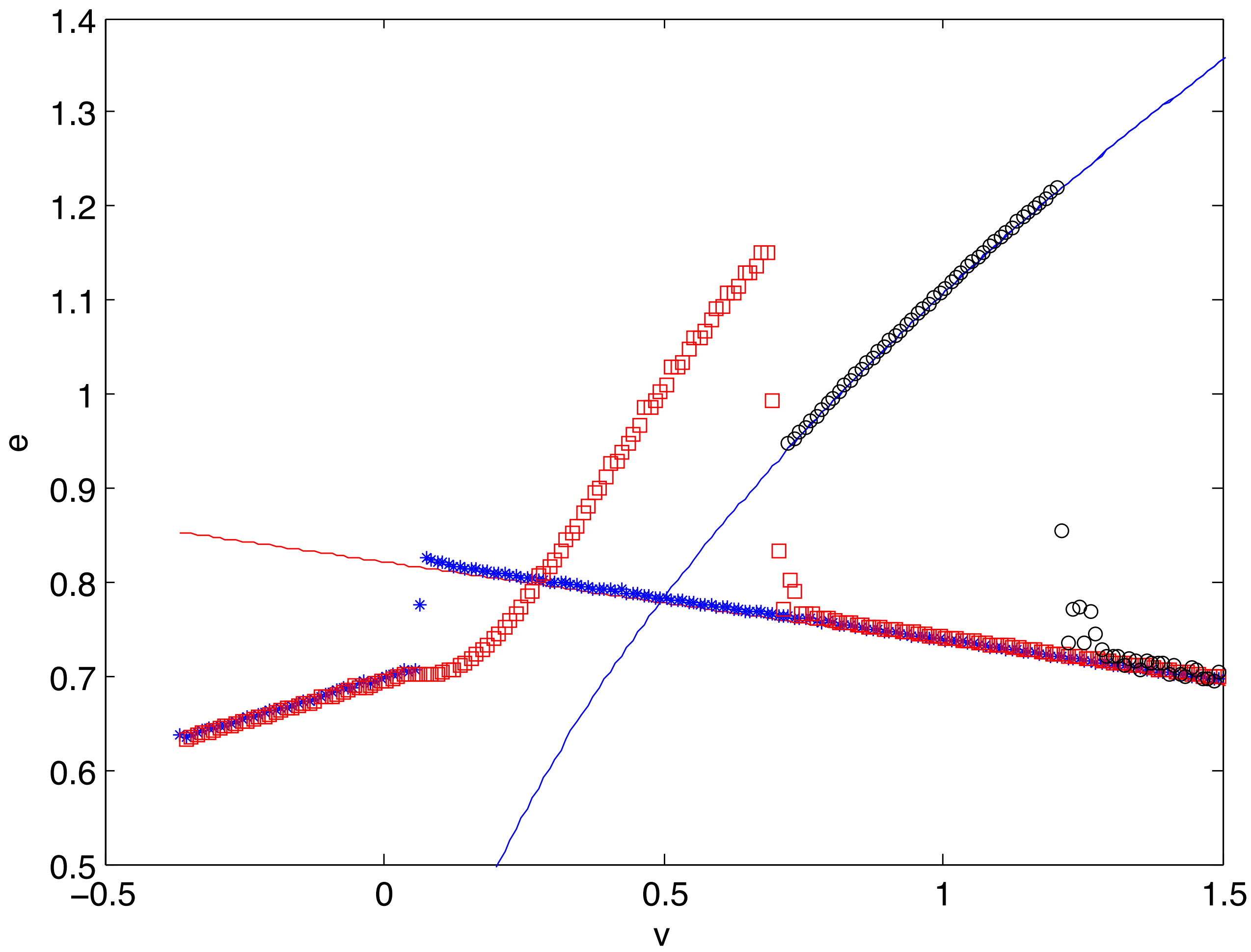

Dewetting – VoF simulation

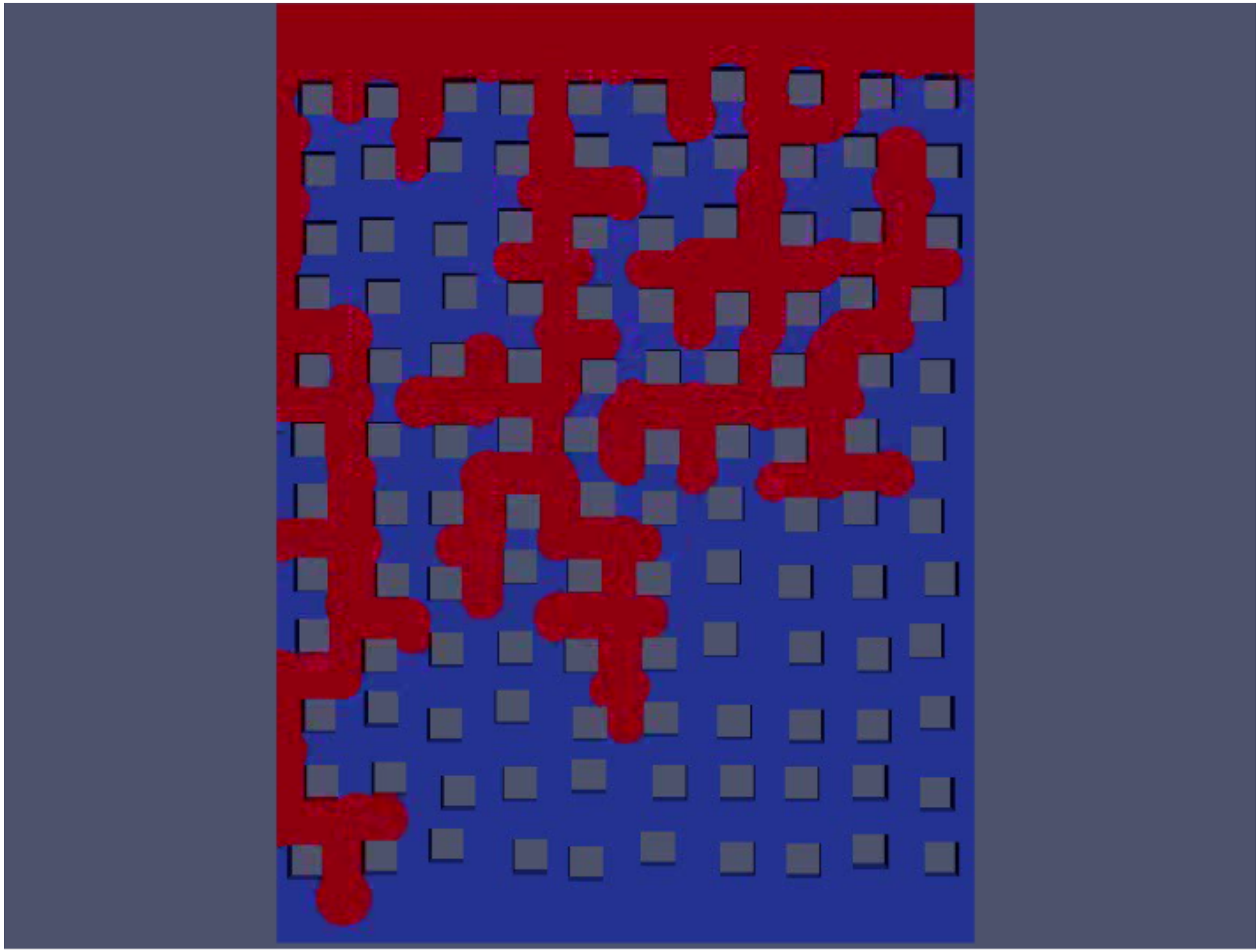

Maniero and Lunati, 2010; [see also Ecmor 2010]